

Power System Planning and Operation using Flexible AC transmission Systems



Smriti Dey

Department of Electrical Engineering
Assam Engineering College
Gauhati University

The thesis is submitted to Gauhati University
As requirement for the degree of

Doctor of Philosophy

Declaration

I hereby declared that the thesis entitled “**Power System Planning and Operation using Flexible AC transmission Systems**” submitted to Gauhati University for the award of the degree of Doctor of Philosophy in the Faculty of Engineering is absolutely based upon my own work under the supervision Dr. D. Hazarika, Professor, Department of Electrical Engineering, Assam Engineering College, Guwahati. I also declared that neither this thesis nor any part of the thesis has been submitted for any degree/diploma or any other academic award any where before.

Dated:

Smriti Dey

Department of Electrical Engineering
Assam Engineering College

Place: Guwahati

Guwahati-781013

Assam

Certificate

This is to certify that the thesis entitled “**Power System Planning and Operation using Flexible AC transmission Systems**” submitted by Ms. **Smriti Dey**, who got her name registered on 11-04-2019 in the Department of Electrical Engineering of Assam Engineering College for the award of the degree of **Doctor of Philosophy in the Faculty of Engineering** is absolutely based upon her own work under my supervision and that neither her thesis nor any part of the thesis has been submitted for any degree/diploma or any other academic award anywhere before.

Date:

Place: Guwahati

Dr. Durlav Hazarika
Research Guide
Electrical Engineering Department
Assam Engineering College
Guwahati -781013

Acknowledgement

I would like to express my deep and sincere gratitude to my supervisor, **Dr. Durlav Hazarika**, Professor, Department of Electrical Engineering, Assam Engineering College for giving me the opportunity to do research and providing invaluable guidance throughout this research. I sincerely thank him for his exemplary guidance and encouragement, without his guidance and persistent help, this project would not have been materialized.

Besides my supervisor, I would like to thank **Prof. Damodar Agarwal**, Head of the Department, Electrical Engineering and all the faculties for their enthusiastic support towards the completion of the project.

My sincere thanks also go to **Prof. Satyajit Bhuyan**, Department of Electrical Engineering for his valuable supports and encouragements during the time of writing the thesis.

I am indebted to my colleagues, friends for their help and moral support all throughout the project.

Finally I would like to thank my Parents, family members for their moral support and encouragement.

Dated:

Place: Guwahati

Smriti Dey

Department of Electrical Engineering
Assam Engineering College
Guwahati-781013
Assam

Abstract

Growth in power consumptions and populations forced the Power system Network (PSN) to operate closer to its operating limit(s) owing to economic and operational factors. Again loss of a heavy generator/ load/ faults in a PSN causes heavy power flows through the transmission lines results in outages of the transmission lines. Therefore creates overloading of nearby lines, voltage deviations, a significant change in phase angles, increased system loss, etc., which may lead to a partial or complete breakdown of the PSN. Thus, it is required to restore the line as early as possible to avoid the line flow limit violation of other lines of a PSN. To reduce these problems the methods of rescheduling of power flow with Series Power Flow Controller (SPFC) and Unified Power Flow Controller (UPFC) are proposed in this work. Mathematical modeling of modified Load Flow (LF) analysis using SPFC and UPFC devices for reducing the Total Real Power Loss (TRPL) and Standing Phase Angle (SPA) difference across the two buses are proposed here. Initially, the Power Loss Sensitivity Factor (PLSF) represented by the change in TRPL to the Change in Power Flow (CPF) for all the lines of a PSN are determined to identify the suitable location of SPFC devices. Then the lines having significant values of PLSF are considered for the introduction of SPFC devices to reduce TRPL. Utilizing the PLSF and their relation to the change in TRPL, the necessary optimal values of CPF for the selected lines are obtained using the Particle Swarm Optimization (PSO) technique. Incorporating the optimal values of CPF for the lines considered to introduce SPFC devices, LF analysis with SPFC is performed to estimate the state variables of SPFC devices. The SPFC devices at the selected transmission lines can reduce the TRPL to 2.5151 p.u. from 3.0851 p.u. also improve the bus voltage profile of the IEEE 118 bus system. Again, to show the economic benefit of installing SPFC at the selected buses of the PSN cost-benefit analysis (CBA) based on the installation cost (IC) of SPFC and the cost-savings due to reduction of TRPL is done.

Again, to reduce SPA across the two buses, the sensitivity relation between change in SPA across two buses of a transmission line, and the CPF through the line having UPFC devices have been formulated. Then the sensitivity relations are used to reschedule the power flow through the line having UPFC device to reduce SPA across the line to be re-connected. Simulations were carried out on IEEE 118 bus system to examine the applicability of the proposed methods for the reduction of TRPL, and SPA across the two buses.

Table of contents

Declaration	i
Certificate	ii
Acknowledgement	iii
Abstract	iv
Table of contents	v
List of figures	viii
List of tables	ix
1 Introduction	1
1.1 Overview of power system	1
1.2 Challenges of Modern Power System	2
1.3 Overview of Flexible AC Transmission Systems	4
1.3.1 Basic types of FACTS Controllers	5
1.3.2 Applications of FACTS technology	6
1.4 Literature Review	7
1.4.1 Heuristic search optimization algorithm	7
1.4.2 Analytical method	9
1.4.3 FACTS devices for improvement of power system performances...	10
1.4.3 Reduction of Standing Phase Angle (SPA)	12
1.5 Motivations towards the Work	13
1.6 Methodologies	14
1.7 Organization of the Thesis	14
2 Load Flow: A tool for analysis of Power system network	16
2.1 Introduction	16
2.2 AC Power Flow equations	17
2.3 Load Flow analysis using Newton Raphson Method	19
2.4 Series Power Flow Controller (SPFC)	22
2.5 Load flow analysis Model using SPFC device for an Interconnected Power system	23
2.6 Unified Power Flow Controller (UPFC)	32

Table of contents

2.7	Load flow analysis using UPFC device for an Interconnected Power system	36
2.8	Conclusions	42
3	Application of Series Power Flow Controller in Reduction of Total Real Power Loss	44
3.1	Introduction	44
3.2	Identification of sensitive lines to introduce SPFC devices	45
3.3	Problem formulation of reduction of TRPL using SPFC device	47
3.4	Particle Swarm Optimization (PSO) technique	48
3.4.1	Implementation of PSO technique for minimization of TRPL	50
3.5	Selection of transmission lines for the reduction of TRPL of a power system and implementation of the LF analysis with SPFC devices in the selected lines	51
3.6	Solution procedure for reduction of TRPL	51
3.7	Identification of sensitive lines and reduction of TRPL using SPFC devices	53
3.7.1	Simulation results of the proposed method	54
3.7.2	Cost analysis for installation of SPFC devices and cost benefit due to reduction of TRPL	60
3.8	Conclusions	63
4	Reduction of Standing Phase Angle using Unified Power Flow Controller	65
4.1	Introduction	65
4.2	Reduction of Standing Phase Angle using UPFC	66
4.2.1	Formulation of Sensitivity Relation between change in SPA and the change in RRPF through the Transmission line	67
4.3	Algorithm for the method of reduction of excessive SPA across the two buses	70
4.4	Simulations and results	72
4.5	Conclusions	84

Table of contents

5	Conclusions and Recommendation for Future Research	86
5.1	Conclusions of the proposed work	86
5.2	Scopes for Future Research	89
	References	90
	Appendix	97
A.1	Single line diagram and bus data and line data IEEE 118 bus system	97
	Research Publications	

List of figures

1.1	Traditional power system	2
1.2	Model of modern electricity market	2
1.3	Classifications of FACTS controller	6
2.1	Three bus network	17
2.2	SPFC connected in the line <i>km</i> of the system	22
2.3	The equivalent circuit diagram of a transmission line with a SPFC device	23
2.4	Basic UPFC Configuration	33
2.5	Phasor representation of UPFC	34
2.6	Configuration of UPFC device containing the SSSC and the SVC	36
2.7	Equivalent circuit of a transmission line with an UPFC device containing the SSSC and SVC	37
3.1	Flowchart for rescheduling of power flow using SPFC device	52
3.2	PLSF for IEEE 118 bus system	55
3.3	Sensitivity factors of the selected lines	56
3.4	Reduction of TRPF with SPFC devices.	59
3.5	Savings due to reduction of TRPL/ year in (\$) for different MFs for the Cost per unit as 4 ₹/kWhr	62
3.6	Savings due to reduction of TRPL/ year in (\$) for different MFs for the Cost per unit 5 ₹/kWhr	62
4.1	Reduction of SPA across the two buses of a disconnected line using UPFC device	71
4.2	Line-tier scheme for incorporating UPFC devices in the transmission lines	74
A.1	Single line diagram of IEEE 118 bus system	97

List of tables

2.1	Types of buses for power flow analysis	18
2.2	Line parameters without and with UPFC device	34
3.1	SFs of the selected lines for the introduction of SPFC devices obtained using BCLF	55
3.2	Power flows in the selected lines before and after the introduction of SPFC device and SPFC parameters (all parameters are mentioned in p.u. and δ_{se} in radian)	58
3.3	Bus voltage and phase angles of IEEE 118 bus system obtained using LF analysis without and with SPFC device in the selected transmission lines (all parameters are mentioned in p.u. and δ in radian)	59
3.4	TRPL in p.u. obtained for IEEE 118 bus system	59
3.5	Calculation of installation cost of the SPFC devices in three lines (with base MVA =100)	61
3.6	Comparison of cost for installation of SPFC and saving due to reduction of TRPL	61
4.1	SPA difference between the two end buses after disconnection	74
4.2	The first load flow analysis results with assigned scheduled power flow as $P_{km}^{sch} = 1.01P_{km}^0$ $Q_{km}^{sch} = 1.01Q_{km}^0$ and $Q_{ksh}^{sch} = 0.05$ for the disconnected line connected between two end buses 26 and 30, 38 and 65, 42 and 49 respectively	76
4.3	UPFC scheduled power flow, variables and sensitivity factors α_{pq} , β_{pq} and γ_{pq} for the lines after reduction of SPA across the buses- (i) bus 26 and bus 30 (ii) bus 38 and bus 65 and (iii) bus 42 and bus 49 due to removal of the lines one at time	78
4.4	First load flow analysis results showing UPFC variables and sensitivity factors α_{pq} , β_{pq} and γ_{pq} for the lines considered for reduction of SPA having assigned scheduled power flow	81

List of tables

	through the UPFC device as 1.01 times of its line flow through the line determined from BCLFA and Q_{ksh}^{sch} is taken as 0.05 pu having excessive SPA across the buses - bus 25 and bus 23	
4.5	UPFC scheduled power flow, variables and sensitivity factors α_{pq} , β_{pq} and γ_{pq} for the lines after reduction of SPA across the buses- bus 25 and bus 23 .	82
4.6	Simulation results of generation rescheduling to reduce reaming SPA across bus 25 and bus 23 after termination of process of SPA reduction by using UPFC device.	83
4.7	Simulation results of generation rescheduling to reduce reaming SPA across bus 25 and bus 23 after termination of process of SPA reduction by using UPFC device.	83
4.8	Simulation results of generation rescheduling to reduce reaming SPA across bus-25 and bus-23, using the method given in reference [3].	84
A-1.1	Generation and load data for IEEE 118 bus system	98
A-1.2	Network transmission line data for IEEE 118 bus system	101
A-1.3	Transformer tap changing data	106
A-1.4	Shunt data of IEEE 118 bus system	106

1

Introduction

1.1 Overview of Power system

The physical structure of a traditional power system network (PSN) mainly consists of generation, transmission, and distribution systems. Figure 1.1 shows the schematic diagram of a PSN. The bulk amount of power generated mainly using thermal power plants. Recently the contribution of renewable energy generation is also having much impact on today's energy generation. The generation voltage is first to step up into a high voltage for transmission and then step down to a lower voltage for distribution and utilization. Initially, the power industry was Vertically Integrated Utility (VTU) where, the same company owns all aspects of generation, transmission, and distribution of electricity to the consumers. It also holds a monopoly on making, controlling, and selling electricity for which it could not provide an efficient performance as competitive firms. Thus, for creating competition among the power sectors, VTUs unbundled their generation, transmission, and distribution sectors which would naturally create competition within each sector. In the competitive electricity market, generation companies (GENCOs), load-serving entities (LSEs) or distribution companies (DISCOs), and traders are major market players, as shown in Figure 1.2. GENCOs, DISCOs, and large consumer trade electricity directly in the competitive wholesale market, small consumers purchase electricity through DISCOs who operate the distribution network and serve the customers within its territory. It improves the economic efficiency in the operation of the interconnected generation and transmission systems by cost savings.

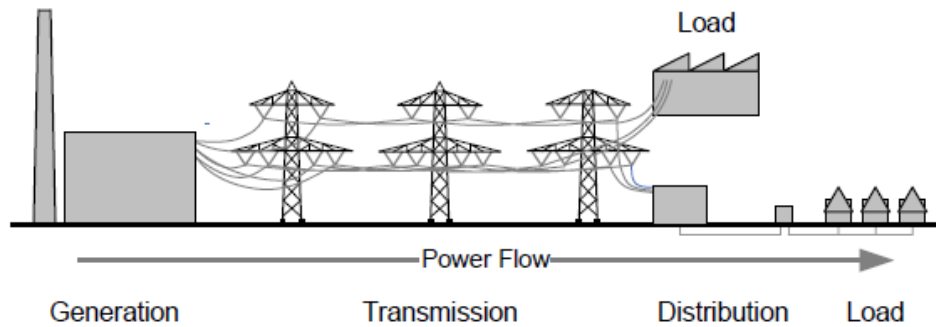


Fig. 1.1 Traditional power system

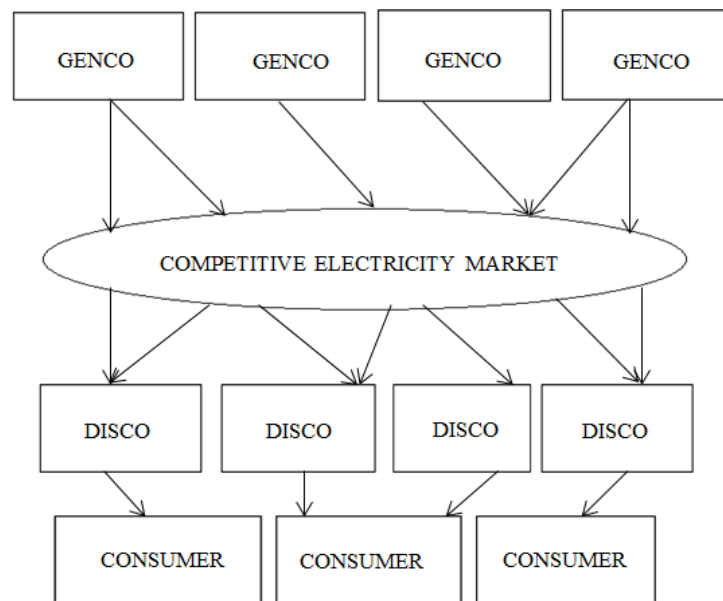


Fig.1.2 Model of modern electricity market [1]

1.2 Challenges of Modern Power System

In the past, transmission systems were composed of a low degree of interconnection, and it was much simple to share the loads among the available generating units. Load on the power system is not constant; it varies from time to time based on consumer demands. Due to the tremendous growth in power consumption and population, a large amount of power needs to be transmitted through the transmission network thus; the existing network has to operate closer to its operating limit(s) owing to economic and operational factors. Therefore generation, as well as transmission network, has to be expanded to meet the load requirement. The increase in load size and operational complexity brought about by widespread

interconnection of transmission systems, some encompassing continental distances, introduced difficulties into the operation and control of PSN. Many challenges have to face by PSN during transmission of power due to various abnormal conditions such as equipment failure, loss of heavy generators, heavy loads, over voltage, or faults on a PSN. Thus, it becomes necessary for many electrical utilities to operate their systems closer to the system operating capacity. It was impractical to determine appropriate operating strategies based only on observation and the experience of the operator. When it comes to an interconnected PSN, the random nature of power demands creates complexity in the operation and control of the power system. If demand on the power system suddenly increases to a very high value it will draw a heavy current from the supply, causes an increase in power loss and overloading of the transmission lines. Due to the increase in power loss in transmission line temperature of the line conductors increases, for which the sag of the conductor increases. This increase in temperature sometimes may lead to thermal limit violation of the conductor. As the thermal limit of the line is the maximum current that can safely transfer through the line thus, there may be an outage of the transmission lines. Again disturbances/faults in PNS bring the system into an emergency condition. Large disturbances in a PSN cause heavy power flow through the transmission lines may lead to outages of the transmission lines, which results in overloading of nearby lines, voltage deviations, a significant change in bus voltage angles, increase in system loss, etc. These may result in a partial or complete blackout of the system if adequate measures are not taken. Thus, it is required to restore the line as early as possible to avoid the line flow limit violation of other lines of a PSN. Abnormal conditions like loss of heavy generators or loads or faults on a PSN causes heavy power flow through the transmission lines, results in a significant change in phase angle difference across the two buses, may affect the stability of a power system if the system is not restored within a shortest possible time.

The power transfer through a conventional AC transmission system is restricted due to several factors such as short circuit current limit, thermal limits, transient stability limit, voltage limit, etc. These limits define the maximum electric power which can be safely transferred from one side of the transmission line network to the other without causing any damage to the electrical equipment and the transmission lines. These limits arise mainly due to the lack of fast response control equipment. Increased power transfer without overloading the transmission lines is possible by bringing changes in the power system layout. However,

this is not feasible, so another way of achieving maximum power transfer capability without any changes in the power system layout is done using variable impedance devices like capacitors and inductors. Using these variable impedance devices a part of the energy is stored as reactive power and returned to the source rather than transferring the whole energy or power from the source to the load thus, the actual amount of the power transferred to the load or the active power is always less than the apparent power or the net power. For ideal power transmission, the active power should be equal to the apparent power, in other words, the power factor (the ratio of active power to apparent power) should be unity. Here, the role of the Flexible AC Transmission System (FACTS) comes. Using FACTS devices it is possible to control and transfer more power without changing the power system layout and keeping the line flow within their respective limits. FACTS devices are used in the power system to enhance line power transfer capacity and increase the controllability of the transmission networks.

1.3 Overview of Flexible AC Transmission Systems (FACTS)

The concept of FACTS technology was first mentioned in Electric Power Research Institute (EPRI) journal in 1986 to control power transmission through the lines and utilize the maximum capacity of the existing transmission lines without compromising the system reliability. The concept of FACTS was first introduced at a luncheon speech during the IEEE PES Summer meeting in July 1987 and a luncheon speech at the 1988 American Power Conference [2]. FACTS is an alternating current transmission system incorporating power electronic based and other static controllers to enhance controllability and increase power transfer capability [3]. Since the FACTS controllers are electronically operated devices, thus the response and execution time of the FACTS devices are fast. FACTS controllers are used in a power system to increase the flexibility of the PSN by enhancing the controllability and power transfer capability of the transmission lines without overloading the transmission lines. It also provides a facility for enhancing the load security of the transmission system, ability to power transfer, prevents cascading outages, and reduces power system oscillations. The power transfer capacity of the line increased by changing various network parameters like circuit current, voltage, impedance, phase angle, etc. Use of different types of FACTS devices in a PSN can increase the voltage during voltage sag, reduce voltage during a light load condition, reduce line reactance, reduce the phase angle difference across the two buses, etc.

1.3.1 Basic types of FACTS Controllers

According to the type of connection, FACTS controllers are classified into four categories shown in Figure 1.3 [3].

a) Series Controllers

Series controller consists of capacitors or reactors which introduce voltage in series with the line. They are variable impedance devices. The main task of series controllers is to reduce the inductivity of the transmission line and supply or consume variable reactive power. Thyristor controlled series capacitor (TCSC), Thyristor switched series capacitor (TSSC), and Static Synchronous Series Compensator (SSSC), etc. are examples of series controllers.

b) Shunt Controllers:

Shunt controllers consist of variable impedance devices like capacitors or reactors and introduce current in series with the line. The injected current is in phase with the line voltage. Static Synchronous Compensator (STATCOM), Thyristor Switched Reactor (TSR), Thyristor Switched Capacitor (TSC), Static VAR Compensator (SVC), etc. are the examples of shunt controllers.

c) Shunt-Series Controllers: These controllers consist of a combination of shunt and series controllers. Unified Power Flow Controller (UPFC), Thyristor controlled Phase Angle Regulators are examples of shunt-series Controllers.

d) Series-Series Controllers: These controllers consist of a combination of series-series controllers providing series compensation and the transfer of real power along the line. An example is Interline Power Flow Controller (IPFC).

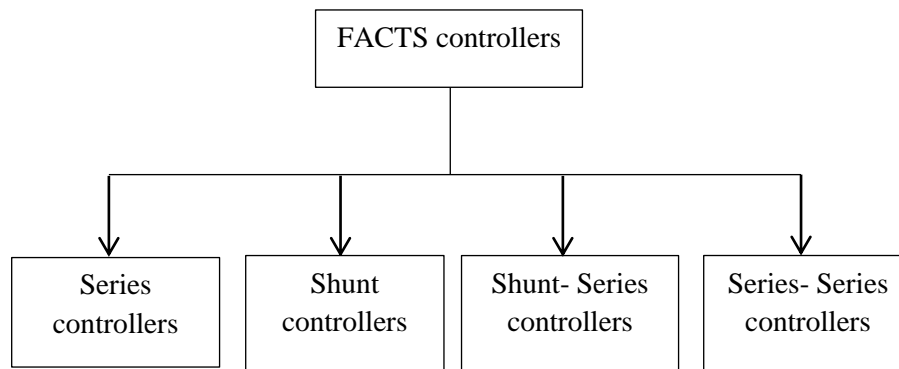


Fig. 1.3 Classification of FACTS controllers

1.3.2 Applications of FACTS Technology

FACTS technology has impacts on all operations of power systems like [3]:

- storage system: converting energy (DC to AC, AC to DC, DC to DC, etc.)
- generation system: damp the power system oscillations created due to power mismatch.
- transmission system: increase power transfer capability of the line.
- distribution system: protect by rapid interruption of circuit current.

There are various applications of FACTS devices in transmission systems including,

- better control of voltage magnitude, phase angle, and line reactance.
- better control of both active and reactive powers.
- power quality improvement and power conditioning.
- reduce reserve margin as it can transfer powers between controlled areas.
- secure power transmission without overloading the lines and improve stability.
- limit the effects of faults or other abnormal conditions to avoid cascading outages.

Power system operation and control are limited by the wearing of the mechanically controlled switches because line loading varies continuously due to frequent variations of load demand, line outages, generation schedules, etc. The use of mechanical switches for controlling series capacitors results in subsynchronous resonance. FACTS technology replaces the mechanically controlled switches and provides flexibility in power system operation and control. It does not consist of a single power electronic device, but the number of power electronic devices along with their controllers constitutes a FACTS device. FACTS controllers can provide control of different parameters of power transmission based on the requirement of the power systems.

Since 1980 several research works going on designing controllers of FACTS technology to meet the various objectives in power systems.

1.4 Literature Review

A large number of researchers and scientists are working on FACTS technology since late 1980. Many research works have been done on various applications of FACTS devices in the operation and planning of a power system. Some of the areas in a power system where FACTS technologies implemented for the improvement of power system performances are listed below:

- improving various electrical parameters of a PSN (voltage, current, impedance, etc.).
- enhancing power system stability.
- optimizing power system parameters.
- finding the optimal location, numbers, and effective FACTS devices.
- improving dynamic performances of a power system.

The benefits of FACTS devices are mainly dependent on the location, type, numbers, and the size of the devices. Again the optimal siting of FACTS devices for meeting some objectives in a power system depends on their capacity, type, numbers, and network operating conditions. Several research works are done to find the suitable locations of various FACTS devices in a PSN for improving the power system conditions. Here two categories of optimal placement of FACTS devices are listed based on the literature available:

1.4.1 Heuristic search optimization algorithm

Using the heuristic search methods the optimum number and location of FACTS devices in a PSN are determined. Among the methods used for the placements of FACTS devices, Genetic Algorithm (GA), Simulated Annealing (SA), Tabu Search (TS), Particle Swarm Optimization (PSO), Evolutionary Algorithm (EA), Bacterial Swarming Algorithm (BSA), Bees Algorithm (BA), etc. are popularly used [4-20]. Use of GA for finding the optimal locations of FACTS devices are presented in [4-8]. The authors of [4-5] proposed simultaneous use of multi types of FACTS devices for improving the operating conditions of a PSN. It was found that the use multi types of FACTS devices shows efficient performance than the individual combination [4-5]. Again loadability of the lines cannot be increased

beyond a certain limit with the use of increasing numbers of FACTS devices for both single and multi-type of FACTS devices [5]. S. R. Najafi et al. propose a method using GA and continuous power flow for determining the maximum numbers of SVCs required to increase the loadability of the line beyond which loadability of the lines cannot be increased further, this may lead to voltage collapse [6]. G. I. Rashed et al. describes a method for maximizing the power system loadability using multiple numbers of TCSC devices using GA and PSO, the PSO technique shows faster response than GA [7]. M. Saravanan et al. used PSO for finding the optimal location of SVC, TCSC, and UPFC to maximize loadability with a minimum installation cost of FACTS devices [8]. PSO optimization tool is used to determine the optimal locations and parameters of UPFC devices to maximize the loadability of the transmission line. Loadability of the system can be improved by increasing the number of UPFC devices upto a certain limit beyond which loadability cannot be increased further as mentioned by S. T. J. Christa and P. Venkatesh [9]. The authors use the UPFC device to control the voltage, active and reactive powers of a PSN and found that the location and parameters of the FACTS device play an important role to enhance the steady-state performance of a power system [10].

S. Gerbex et al. uses five different types of FACTS devices (TCSC, TCVR, TCPSC, SVC, and UPFC) to enhance power system security. The optimal location was determined using three heuristic optimization techniques where TS and GA show faster convergence than SA [11]. E. Ghahremani. et al. proposed the optimal placement of SATCOM devices for minimizing transmission losses and maximizing power transmission using GA [12]. Finding optimal locations of FACTS devices in PSN are done using EA [13-16], BSA [17], group search optimizer with multiple producers (GSOMP) [18], Harmony Search Algorithm (HSA) [19], and BA [20]. The swarm-based probabilistic search technique PSO was introduced by Eberhart and Kennedy in 1995. PSO is used to determine optimal values of control variables to minimize the power system loss are presented in [21-24]. Due to the implicit parallelism property, PSO has less probability to stuck in the local optimum [21]. PSO has quick convergence towards the optimum solution and may have slow convergence when it reaches the minimum solution. R.C. Eberhart et al. [22] have shown that the PSO algorithm is superior to other optimization techniques for its robust nature and efficient computation for finding optimal control parameters. Dynamic PSO shows efficient performance to reduce real power loss in a power system using reactive power control [24]. The authors of [25] show that a

hybrid algorithm like GA-PSO can effectively determine optimal sizing and location of distributed generators for minimizing power losses in a PSN.

Thus from the above discussion, it is clear that

- determining optimal numbers of FACTS devices is necessary for increasing the line loadability of a PSN.
- locations of FACTS devices in a PSN play a significant role to enhance the power system performances.
- PSO technique is superior among other optimization techniques, and also it is computationally efficient for power system optimizations.

1.4.2 Analytical method

The authors of [26] and [27] analyzed the load flow Jacobian matrix singularity to determine the location of FACTS devices in a PSN and found that the weak branches/ nodes are the optimal locations of active and reactive power sources. To find the optimum locations of FACTS devices in a PSN to meet some specific objectives using a sensitivity-based method are presented in [28-31]. S. N. Singh et al. mentioned that the negative values of Performance Index (PI) with respect to TCSC parameters are the potential locations of TCSC devices. Also, the absolute value of high PI with respect to TCSC parameters is the potential location of TCPAR devices for congestion management [28]. The authors of [29] present a method to find the best optimal location of the FACTS device for reducing production cost and device cost. The authors of [30] use the sensitivity of system loading for the placements of UPFC devices to enhance the power system loadability. K. S. Verma et al. proposed a sensitivity of power loss and power flow with respect to control parameters of UPFC to find the best location of UPFC device for uncongested line and for alleviating congestion in the transmission line [31]. Optimal allocation of FACTS devices is determined by considering the cost of installation of different types of FACTS devices presented in [32-34]. It is found that the proper choice and allocation of FACTS devices are necessary to minimize the cost of planning and operation of a power system.

From the above discussion, it is understood that the

- proper choice of type and allocation of FACTS devices are necessary to meet some specific objectives in a power system.
- sensitivity based methods are effective in finding the optimal location of FACTS

devices in a PSN.

1.4.3 FACTS Devices for Improvement of Power system Performances

Applications of FACTS devices in power flow control, maintain bus voltage magnitude being presented in [35-38]. J. Douglas et al. proposes the insertion of FACTS in proper location has a significant impact on the reduction of system loss, the cost of the UPFC device is much higher than other FACTS devices but has the highest power transfer capability [35]. Performance comparison of UPFC, TCSC, and Phase Shifting Transformer is proposed in [36, 37, 40, and 43] based on the improvement of reliability and utilizing maximum power transfer capability of the transmission line. B.Roy et al. show that the UPFC is most efficient than TCSC in reliability improvement. They also mentioned that TCSC can provide fast control of active power flow through lines but for peak load operation use of TCSC increases system risk more than the UPFC [36]. Identification of the optimal location of TCSC and UPFC device that maximizes the real power transfer through the line was proposed by T. Orfanogianni et al. and the authors mentioned that the solution was more difficult in the case of UPFC than TCSC [37]. At least two independent variables are needed to be considered for the UPFC, and it was found that the selection of starting values of control variables have a significant effect on getting global optimum solution [37]. S.K. Srivastava et al. mentioned that the system and equipment constraints must be considered for determining the location, size, and operating mode of UPFC for controlling and maximizing the real power flow in the lines [38]. L. Liu et al. analyses the real, reactive power and voltage balance of UPFC and found that the shunt converter provides control of line reactive power and dc-link capacitor voltage, whereas the series converter provide real power transfer through the line, maintain voltage at the UPFC terminal and avoid excessive voltage at dc-link as well [39]. The optimal power flow control using the UPFC and the performance comparison of UPFC with a phase-shifting transformer is presented by M. Noroozian et al. The authors show that the UPFC can relieve the overload by regulating power flow and minimize system loss without rescheduling the generation [40]. Comparison of various FACTS devices for stability enhancement was proposed in [41, 42, and 43]; found that the performance of UPFC was more effective than the other FACTS devices such as SVC, STATCOM, TCSC, and SSSC. Using multiple FACTS devices thermal burdens of the lines are alleviated where active and reactive power injections were taken as independent variables, and the control parameters of FACTS devices were not

included in the power flow equations therefore, change in the structure and the elements of the Jacobian matrix were not required [44].

M. A. Sayed et al. presents line loss minimization by eliminating loop current using series compensation of UPFC [45]. M. Tripathy et al. proposes a comparison of Bacteria Foraging Algorithm (BFA) and Interior Point Successive Linear Programming (IPSLP) to minimize system loss by determining optimal tap position of OLTC transformer. After optimizing the tap positions, UPFC is introduced in the system. The optimized value of the series injected voltage, the location of UPFC are determined using (BFA) and (IPSLP) [46]. A suitable location of UPFC for congestion management using total real power loss sensitivity factors, which reduces system loss and improves voltage profile proposed by J. Douglas et al. [35]. K.S. Smith et al. proposed a method to regulate the UPFC to improve the dynamic performance of a power system. The series voltage of UPFC responds to the power variations of the transmission line, while the shunt compensation is controlled to maintain the system bus voltage and stabilize the DC link of the UPFC [47]. Minimization of line loss and voltage regulation is achieved by using UPFC by regulating the phase angle of the injected voltage [48-49]. D. Hazarika et al. proposed a method to reduce line overload through rescheduling the power flow for the line with series power flow controllers without considering the impedance of the converter transformer of SPFC devices [50]. FACTS controller is an electronically operated device, thus it has a fast response time and execution time. Among all the FACTS devices, the UPFC is an attractive member of its family, because of its ability to control real and reactive power flow in a transmission line simultaneously or selectively [51].

From the above discussions it is understood that the following types of FACTS devices can effectively participate in power flow control through the transmission lines:

- i) Series power flow controller (SPFC)
- ii) Unified Power Flow Controllers (UPFC)

Among these two devices, UPFC is a very versatile and powerful FACTS device although it is costlier than other FACTS devices.

1.4.4 Reduction of Standing Phase Angle (SPA)

The power system normally operates in a preventive state. Slight overloading is allowed for a small duration of time but, if the disturbance is large, normal operation of the power system gets affected and the system must go for restoration. During restoration, if the SPA difference between two buses is large, then the closing of the circuit breaker may cause equipment damage. Therefore, it is very important to reduce the difference in phase angles between two buses, so that the restoration of the lines becomes easy. Many research works have been done so far in the area of reduction of SPA. A brief description is listed below [52-62].

During the restoration of the EHV/HV network of a PSN, the operator may encounter the problem of excessive SPA across a line to be re-connected. Closing a breaker to reconnect a disconnected line on a large SPA difference causes large power flow through the line. This introduces system oscillation due to the power swing phenomenon. As a result, it may damage the equipment of a power system [52] due to significant limits (voltage and current) violation of the equipment and can lead to the system outage. Therefore, EHV lines are equipped with synchrocheck relays to prevent the breaker closure on SPA greater than the prescribed value for that category of the line. The authors present an algorithm for the reduction of SPA through generation rescheduling and load shedding [54]. Using decoupled load flow model, the SPA reduction technique is presented in [56, 60]. For the SPA reduction, augmentation of the Jacobian matrix is done for the row associated with the reduction in SPA, and a continuation method is applied to achieve an optimal SPA [57]. An approach is presented in [58], where load shedding is incorporated to achieve the desired SPA. Mixed-integer nonlinear programming (MINLP) and alternative Two-Stage Decoupled (TSD) algorithm has been used to restore some un-served load during the process of SPA reduction [58]. The authors use GA to minimize a weighted sum of generation adjustments and load shedding for SPA reduction [59]. Using the Wide Area Monitoring System (WAMS) data, a GA-based approach is presented for the reduction of SPA [60]. Mixed-integer nonlinear programming (MINLP) and alternative Two-Stage Decoupled (TSD) algorithm have been used to restore some unserved load during the process of SPA reduction [61]. An approach for optimal reschedule of generation has been presented for the reduction of SPA [62].

As series power flow controllers are effective for controlling the line power flow. Therefore in this research work initially SPFC device and then the UPFC device is used to reduce system loss and excessive SPA across the two buses of a PSN by controlling the power flow through the transmission lines.

1.5 Motivations towards the Work

Due to the unpredictable nature of the disturbances, PSN faces outages of the equipment such as generators/ transmission lines lead to bus voltage deviations or overloading of the nearby lines or large phase angle difference across the two end buses, etc. Most of the time power system operates in a preventive state. A fault and any abnormal condition bring the system into the emergency condition. If the disturbance is large enough, the system goes into the restorative state. The most likely outcome is either a partial or total outage of the system. So the system has to be re-energized. The process of re-energizing is called restoration. During restoration, if the phase angle difference across the two busses is very large, then the circuit breaker equipped with the synchro-check relay does not allow the system to re-connect the line between the two busses. To maintain the continuity, or avoid system collapse, it is required to re-connect the line as early as possible; otherwise, power flow through another line may violate the limit. Thus, the SPA should be within the specified limit. To overcome this problem power flow control is required to keep the power system parameters within their respective limits. With the use of FACTS devices, it is possible to maintain bus voltage profile, reduce line overload, system loss and improve the overall performance of a PSN by controlling power flow through the transmission lines. Proper initializations of control parameters of FACTS devices are mandatory to ensure the effective performance of FACTS devices. Therefore, the objectives of the work are:

- (i) to develop a mathematical model of using SPFC devices for reducing system loss.
- (ii) to develop a mathematical model using the UPFC device for reducing excessive SPA across the two buses.

1.6 Methodologies

The following methodologies are adopted:

- a) to achieve the reduction of Total Real Power Loss (TRPL) using SPFC devices
 - (i) Determine Power Loss Sensitivity Factors (PLSF) for all the transmission lines of a PSN.
 - (ii) Identify the highly sensitive lines for introducing SPFC devices.
 - (iii) Obtain optimal values change in Real and Reactive Power Flow (RRPF) through the lines with SPFC device using PSO technique and determine modified schedule power flow through the line.
 - (iv) To validate the proposed method, perform the LF analysis with modified schedule power flow and calculate the TRPL of the PSN.

- b) to achieve the reduction of excessive SPA across the two end buses using UPFC devices
 - (i) Sensitivity relation between change in SPA across two end buses of a disconnected transmission line and the change in power flow through the line having UPFC device have been formulated.
 - (ii) The sensitivity relations are used to reschedule the power flow through the line having UPFC device to reduce SPA across the line to be re-connected.
 - (iii) To validate the effectiveness of the proposed method perform the LF analysis using UPFC device with the modified scheduled power flow through the lines with UPFC device.

1.7 Organization of the Thesis

The thesis includes five chapters and a bibliography:

Chapter 1: This chapter provides an introduction of FACTS devices and a brief review of work done on various applications of different types of FACTS devices in a PSN along with the objective of this research work.

Chapter 2: This chapter provides the basic LF analysis using the Newton Raphson method. The detailed modeling of LF analysis using SPFC device including the impedance of

converter transformer of series controllers and also the modeling of LF analysis using UPFC device with three state variables are provided in this chapter.

Chapter 3: This chapter presents a sensitivity analysis to determine the suitable location for placements of SPFC devices in a PSN. SPFC devices introduced in the selected transmission lines for the reduction of TRPL in a PSN by rescheduling the power flow through the transmission lines. Power flow analysis with SPFC device described in chapter-2 is used to examine the performance of SPFC device for the reduction of TRPL of a PSN.

Chapter 4: This chapter provides a formulation of the relationship between the change in SPA across two end buses of a disconnected transmission line and the change in power flow through the line having a UPFC device. Reduction of excessive SPA difference across the two buses of a PSN by rescheduling the power flow through the highly sensitive lines with the UPFC device is presented here. Power flow analysis with the UPFC device described in chapter-2 is used to examine the performance of the UPFC device for the reduction of SPA across the two buses of a disconnected line.

Chapter 5: This chapter presents the summary of the research work in light of its contribution and future scope.

Load Flow: A tool for analysis of Power System Network

2.1 Introduction

Load flow (LF) analysis is a computational tool that involves numerical techniques to determine the operating conditions of a PSN during the steady state condition. Disturbances are unavoidable circumstances in a PSN. Due to the rapid growth in power demands and other abnormal conditions, sometimes PSN has to operate near the maximum operating limits for which expansion of the PSN is necessary. Expansion is possible by upgrading the existing system by adding new generating units, new lines with the existing network for which the power system layout has to be changed. Upgrading existing PSN without changing the power system layout is possible by the use of FACTS devices in the power system that also ensures secure or stable operation of the PSN. LF analysis is an important tool for the planning and operation of a power system. It provides information about the PSN such as the magnitude of bus voltage, the phase angle of bus voltage, power injections, line power flows, and losses in the network.

2.2 AC Power Flow equations

To determine the operating state of a PSN power flow equation has to be solved. This section describes the detailed derivation of power flow equations.

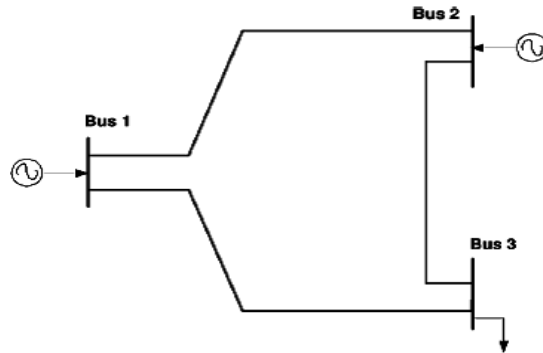


Fig. 2.1 Three bus network

The complex current injections at i^{th} bus for n- bus system is

$$\bar{I}_i = \sum_{j=1}^n \bar{V}_j Y_{ij} \quad (2.1)$$

$$\text{Where, } Y_{ij} = G_{ij} + jB_{ij} \quad (2.2)$$

Let,

$$\left. \begin{aligned} \bar{V}_i &= V_i \angle \delta_i \\ \bar{V}_j &= V_j \angle \delta_j \end{aligned} \right\} \quad (2.3)$$

Complex power injection at i^{th} bus is calculated as:

$$\bar{S}_i = \bar{P}_i + j\bar{Q}_i = \bar{V}_i \bar{I}_i^* \quad (2.4)$$

Using Equations (2.1-2.4) the active and reactive power injections at i^{th} bus is calculated as:

$$P_i = \left[\sum_{j=1}^n V_i V_j (G_{ij} \cos \delta_{ij} + B_{ij} \sin \delta_{ij}) \right] \quad (2.5)$$

$$Q_i = \left[\sum_{j=1}^n V_i V_j (G_{ij} \sin \delta_{ij} - B_{ij} \cos \delta_{ij}) \right] \quad (2.6)$$

where, δ_{ij} = Phase angle difference of voltage between bus- i and bus- j .

Each node/ bus has four variables, i.e., active power (P_i), reactive power (Q_i), voltage magnitude (V_i), and phase angle (δ_i). Thus, for a three bus network, there are twelve variables and six equations. It is not possible to determine these twelve variables from six equations. Therefore the number of unknown variables has to be reduced to six, and this is done by classifying the buses into two types (i) generator bus (PV bus) and (ii) load bus (PQ bus). In

Table 2.1 Types of buses for power flow analysis

Bus type	Quantities specified	Quantities to be obtained
Load bus	P_i, Q_i	$ V_i , \delta_i$
Generator bus	$P_i, V_i $	Q_i, δ_i
Slack bus	$ V_i , \delta_i$	P_i, Q_i

each bus, two known variables and two are unknown. Table 2.1 shows the classifications of buses in a power system according to the known and unknown variables at each bus.

a) PQ or load bus

At this bus, real power injection (P_i), reactive power injection (Q_i) are the specified quantities, and the voltage magnitude ($|V_i|$), phase angles (δ_i) are the quantities to be determined. Most of the buses (about 85% of total buses) in a PSN are load buses.

b) PV bus or Generator bus

When a generator is connected to any bus is called a generator bus or PV bus. At this bus, real power injection (P_i) and voltage magnitude ($|V_i|$) are the specified quantities, and the reactive power injection (Q_i) and phase angles (δ_i) are the quantities to be determined. 15% of the total buses in a PSN are of PV bus. In generating station controlling governor settings, i.e., controlling prime mover input controls active power, and the reactive power is controlled by a voltage regulator which maintains constant voltage at the generator terminals. The bus at which active power injection and voltage magnitude constant is also called the voltage control bus. Tap changing transformers can maintain a fixed voltage at this bus. However, a pure voltage controlled bus has a distinction that it is connected with only voltage controlled equipment like SVCs and not generators. Hence, for voltage controlled bus $P_{Gi} = Q_{Gi} = 0, P_i = -P_{Di}, Q_i = -Q_{Di}, |V_i| = \text{specified quantity}$ and δ_i is unknown quantity.

c) Slack bus/ Swing bus/ Reference bus

The bus with a large capacity of a generator connected where voltage magnitude ($|V_i|$), phase angles (δ_i) are the specified quantities and real power injection (P_i), reactive power injection (Q_i) are the unknown quantities to be obtained called a slack bus. Among the generator buses, one is considered as a slack bus because until the LF solution is complete the losses in the system remain unknown. One of the generator buses is used to supply the losses in the system known as a swing bus. The voltage at the slack bus is assigned as 1.0 p.u. Therefore voltage at the slack bus is taken as reference, and thus its angle is equal to zero. Only one bus is the slack bus in a PSN.

2.3 Load Flow analysis using Newton Raphson Method

Newton Raphson (NR) method is an iterative technique to solve a set of numerical equations for an equal number of unknowns. NR method can be solved using two methods. One uses the rectangular form of the variables while the other uses the polar form of the variables. The polar form of the NR method is a widely used method for solving power flow equations. NR method is preferred over other LF methods because it has a faster response due to quadratic convergence characteristics, the solution is independent of the choice of slack bus, require a fewer number of iterations, and the number of iterations is independent of system size, therefore the system having any size can be easily solved using this method. For solving the power flow equations represented by equations (2.5) and (2.6) bus number 1 is considered as the slack bus. Thus, to relate the change in voltage magnitude and phase angle to the change in real and reactive power injections for the n-bus power system, the LF Jacobian matrix is used. Equation (2.7) represents the relation between change in voltage magnitude and phase angle to change in real and reactive power injections.

$$\begin{bmatrix} \Delta P_2 \\ \vdots \\ \Delta P_k \\ \vdots \\ \Delta P_m \\ \vdots \\ \Delta P_n \\ \Delta Q_2 \\ \vdots \\ \Delta Q_k \\ \vdots \\ \Delta Q_m \\ \vdots \\ \Delta Q_n \end{bmatrix} = \begin{bmatrix} \frac{\partial P_2}{\partial \delta_2} & \dots & \frac{\partial P_2}{\partial \delta_k} & \dots & \frac{\partial P_2}{\partial \delta_m} & \dots & \frac{\partial P_2}{\partial \delta_n} & \frac{\partial P_2}{\partial V_2} & \dots & \frac{\partial P_2}{\partial V_k} & \dots & \frac{\partial P_2}{\partial V_m} & \dots & \frac{\partial P_2}{\partial V_n} \\ \dots & \dots \\ \frac{\partial P_k}{\partial \delta_2} & \dots & \frac{\partial P_k}{\partial \delta_k} & \dots & \frac{\partial P_k}{\partial \delta_m} & \dots & \frac{\partial P_k}{\partial \delta_n} & \frac{\partial P_k}{\partial V_2} & \dots & \frac{\partial P_k}{\partial V_k} & \dots & \frac{\partial P_k}{\partial V_m} & \dots & \frac{\partial P_k}{\partial V_n} \\ \dots & \dots \\ \frac{\partial P_m}{\partial \delta_2} & \dots & \frac{\partial P_m}{\partial \delta_k} & \dots & \frac{\partial P_m}{\partial \delta_m} & \dots & \frac{\partial P_m}{\partial \delta_n} & \frac{\partial P_m}{\partial V_2} & \dots & \frac{\partial P_m}{\partial V_k} & \dots & \frac{\partial P_m}{\partial V_m} & \dots & \frac{\partial P_m}{\partial V_n} \\ \dots & \dots \\ \frac{\partial P_n}{\partial \delta_2} & \dots & \frac{\partial P_n}{\partial \delta_k} & \dots & \frac{\partial P_n}{\partial \delta_m} & \dots & \frac{\partial P_n}{\partial \delta_n} & \frac{\partial P_n}{\partial V_2} & \dots & \frac{\partial P_n}{\partial V_k} & \dots & \frac{\partial P_n}{\partial V_m} & \dots & \frac{\partial P_n}{\partial V_n} \\ \frac{\partial Q_2}{\partial \delta_2} & \dots & \frac{\partial Q_2}{\partial \delta_k} & \dots & \frac{\partial Q_2}{\partial \delta_m} & \dots & \frac{\partial Q_2}{\partial \delta_n} & \frac{\partial Q_2}{\partial V_2} & \dots & \frac{\partial Q_2}{\partial V_k} & \dots & \frac{\partial Q_2}{\partial V_m} & \dots & \frac{\partial Q_2}{\partial V_n} \\ \dots & \dots \\ \frac{\partial Q_k}{\partial \delta_2} & \dots & \frac{\partial Q_k}{\partial \delta_k} & \dots & \frac{\partial Q_k}{\partial \delta_m} & \dots & \frac{\partial Q_k}{\partial \delta_n} & \frac{\partial Q_k}{\partial V_2} & \dots & \frac{\partial Q_k}{\partial V_k} & \dots & \frac{\partial Q_k}{\partial V_m} & \dots & \frac{\partial Q_k}{\partial V_n} \\ \dots & \dots \\ \frac{\partial Q_m}{\partial \delta_2} & \dots & \frac{\partial Q_m}{\partial \delta_k} & \dots & \frac{\partial Q_m}{\partial \delta_m} & \dots & \frac{\partial Q_m}{\partial \delta_n} & \frac{\partial Q_m}{\partial V_2} & \dots & \frac{\partial Q_m}{\partial V_k} & \dots & \frac{\partial Q_m}{\partial V_m} & \dots & \frac{\partial Q_m}{\partial V_n} \\ \dots & \dots \\ \frac{\partial Q_n}{\partial \delta_2} & \dots & \frac{\partial Q_n}{\partial \delta_k} & \dots & \frac{\partial Q_n}{\partial \delta_m} & \dots & \frac{\partial Q_n}{\partial \delta_n} & \frac{\partial Q_n}{\partial V_2} & \dots & \frac{\partial Q_n}{\partial V_k} & \dots & \frac{\partial Q_n}{\partial V_m} & \dots & \frac{\partial Q_n}{\partial V_n} \end{bmatrix} \begin{bmatrix} \Delta \delta_2 \\ \vdots \\ \Delta \delta_k \\ \vdots \\ \Delta \delta_m \\ \vdots \\ \Delta \delta_n \\ \Delta V_2 \\ \vdots \\ \Delta V_k \\ \vdots \\ \Delta V_m \\ \vdots \\ \Delta V_n \end{bmatrix} \quad (2.7)$$

Equation (2.8) represents the compact form of equation (2.7)

$$\begin{bmatrix} \Delta P_i \\ \Delta Q_i \end{bmatrix} = [J] \begin{bmatrix} \Delta \delta_i \\ \Delta V_i \end{bmatrix} \quad (2.8)$$

where,

$$[\Delta \delta_i] = [\Delta \delta_2 \quad \Delta \delta_3 \quad \dots \quad \Delta \delta_n]^T$$

$$[\Delta V_i] = [\Delta V_2 \quad \Delta V_3 \quad \dots \quad \Delta V_n]^T$$

$$[\Delta P_i] = [\Delta P_2 \quad \Delta P_3 \quad \dots \quad \Delta P_n]^T$$

$$[\Delta Q_i] = [\Delta Q_2 \quad \Delta Q_3 \quad \dots \quad \Delta Q_n]^T$$

$$\Delta P_i = P_{Gi} - P_{Di} - P_i$$

$$\Delta Q_i = Q_{Gi} - Q_{Di} - Q_i$$

Equation (2.9-2.16) calculates the elements of Jacobian matrix.

$$\frac{\partial P_i}{\partial \delta_i} = \sum_{\substack{j=1 \\ j \neq i}}^n V_i V_j (-G_{ij} \sin \delta_{ij} + B_{ij} \cos \delta_{ij}) \quad (2.9)$$

$$\frac{\partial P_i}{\partial \delta_j} = V_i V_j (G_{ij} \sin \delta_{ij} - B_{ij} \cos \delta_{ij}) \quad (2.10)$$

$$\frac{\partial P_i}{\partial V_i} = 2G_{ii}V_i + \sum_{\substack{j=1 \\ j \neq i}}^n V_j (G_{ij} \cos \delta_{ij} + B_{ij} \sin \delta_{ij}) \quad (2.11)$$

$$\frac{\partial P_i}{\partial V_j} = V_i (G_{ij} \cos \delta_{ij} + B_{ij} \sin \delta_{ij}) \quad (2.12)$$

$$\frac{\partial Q_i}{\partial \delta_i} = \sum_{\substack{j=1 \\ j \neq i}}^n V_i V_j (G_{ij} \cos \delta_{ij} + B_{ij} \sin \delta_{ij}) \quad (2.13)$$

$$\frac{\partial Q_i}{\partial \delta_j} = -V_i V_j (G_{ij} \cos \delta_{ij} + B_{ij} \sin \delta_{ij}) \quad (2.14)$$

$$\frac{\partial Q_i}{\partial V_i} = -2B_{ii}V_i + \sum_{\substack{j=1 \\ j \neq i}}^n V_j (G_{ij} \sin \delta_{ij} - B_{ij} \cos \delta_{ij}) \quad (2.15)$$

$$\frac{\partial Q_i}{\partial V_j} = V_i (G_{ij} \sin \delta_{ij} - B_{ij} \cos \delta_{ij}) \quad (2.16)$$

For the n-bus power system if n_{PQ} represents the number of load buses and n_{PV} represents the number of generator buses and $n = n_{PQ} + n_{PV} + 1$ then the size of the Jacobian matrix will be $(n + n_{PQ} - 1) \times (n + n_{PQ} - 1)$. For each iteration, the power injections at the buses are calculated to calculate the mismatches (ΔP and ΔQ). The elements of the Jacobian matrix are calculated to determine the corrections values ($\Delta \delta$ and ΔV) using equation (2.7). Equation (2.17) evaluates the updated values of voltage magnitude and phase angles at the buses.

$$\left. \begin{aligned} V_i^{K+1} &= V_i^K + \Delta V_i^K \\ \delta_i^{K+1} &= \delta_i^K + \Delta \delta_i^K \end{aligned} \right\} \quad (2.17)$$

With the updated values of V_i and δ_i equation (2.5-2.7) are solved until all the mismatches are less than specified tolerance value.

2.4 Series Power Flow Controller (SPFC)

Primarily line power flow is limited by the series impedance of the transmission line. Series capacitive compensators were used to modify the line reactive impedance to reduce line voltage drop and change the receiving end voltage of a transmission line, thus change the transmittable power through the line. The FACTS technology allows the introduction of variable series voltage with the line that enables modification in transmittable power through the line and improves the performance of a PSN. A static synchronous series compensator (SSSC) can be used in a transmission line to regulate real and reactive power flow (RRPF) through the transmission line. In this work, an SSSC modeled with a synchronous voltage source having controllable magnitude and phase angle for load flow analysis. Figure 2.2 represents the schematic representation of a transmission line containing an SPFC. The SPFC device is considered to be a synchronous voltage source with controllable magnitude (V_{se}) and phase angle (δ_{se}). The configuration shows that the SPFC device placed between the k^{th} bus of a power system and one end of the transmission line becomes an integral part of the transmission line connected between k^{th} and m^{th} buses of the power system.

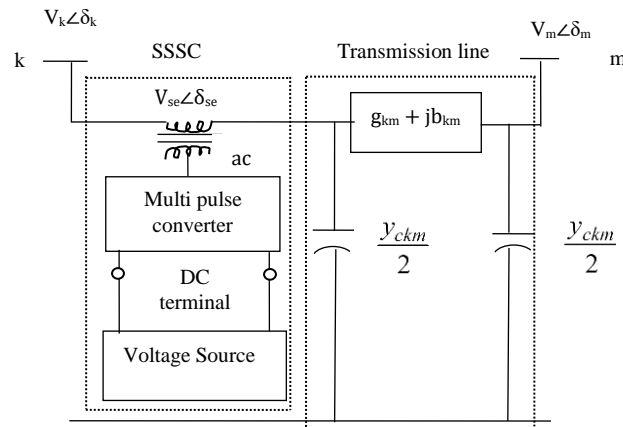


Fig.2.2 SPFC connected in the line km of the system

2.5 Load Flow analysis Model using SPFC device for an Interconnected Power system

The SPFC device used in reference [51] for alleviation of line overload, the SPFC is modeled with a synchronous voltage source with controllable magnitude and phase angles without the impedance of converter transformer. The advantage of the model is that it represents the SPFC device as an integral part of the transmission line. However, the SPFC device is an SSSC, thus it is necessary to include the impedance of SSSC along with the controllable voltage source to evaluate the performance of SPFC realistically. Therefore this work considers the detailed modeling of the SPFC with its impedance when incorporated in a transmission line. The SPFC device is modeled as a synchronous voltage source with controllable magnitude (V_{se}), phase angles (δ_{se}) and series impedance (Z_{se}). The equivalent circuit of a transmission line with an SPFC device containing its controller shown in Figure 2.3 is used to determine RPPF through the transmission line with an SPFC device connected between bus- k and bus- m .

\bar{I}_{km} = current through the line km i.e., from bus k to m .

\bar{I}_{mk} = current through the line mk i.e., from bus m to k .

V_x = voltage at node x .

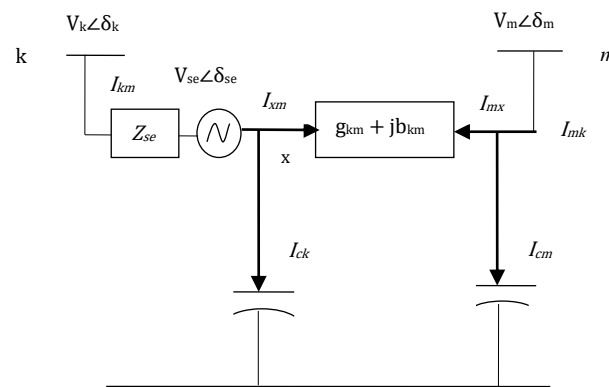


Fig. 2.3 The equivalent circuit diagram of a transmission line with a SPFC device.

The expression for complex power flow in line km is represented as:

$$P_{km} - jQ_{km} = \bar{V}_k^* (\bar{I}_{xm} + \bar{I}_{ck}) \quad (2.18)$$

Now,

$$\bar{I}_{km} = (\bar{V}_k - \bar{V}_{se} - \bar{V}_x) y_{se} \quad (2.19)$$

$$\bar{I}_{km} = \bar{V}_x \frac{y_{ckm}}{2} + (\bar{V}_x - \bar{V}_m) y_{km} \quad (2.20)$$

Using equations (2.19) and (2.20),

$$\begin{aligned} (\bar{V}_k - \bar{V}_{se} - \bar{V}_x) y_{se} &= \bar{V}_x \frac{y_{ckm}}{2} + (\bar{V}_x - \bar{V}_m) y_{km} \\ (\bar{V}_k - \bar{V}_{se}) y_{se} - \bar{V}_x y_{se} &= \bar{V}_x \left[\frac{y_{ckm}}{2} + y_{km} \right] - \bar{V}_m y_{km} \\ \bar{V}_x \left[\frac{y_{ckm}}{2} + y_{km} + y_{se} \right] &= (\bar{V}_k - \bar{V}_{se}) y_{se} + \bar{V}_m y_{km} \\ \bar{V}_x &= \frac{(\bar{V}_k - \bar{V}_{se}) y_{se} + \bar{V}_m y_{km}}{y_T} \\ \bar{V}_x &= (\bar{V}_k - \bar{V}_{se}) y_a + \bar{V}_m y_b \end{aligned} \quad (2.21)$$

where,

$$y_T = \left[\frac{y_{ckm}}{2} + y_{km} + y_{se} \right]$$

$$y_a = \frac{y_{se}}{y_T}$$

$$y_b = \frac{y_{km}}{y_T}$$

Power flow in line km is represented as:

$$\begin{aligned} P_{km} - jQ_{km} &= \bar{V}_k^* \left[\bar{V}_x \frac{y_{ckm}}{2} + (\bar{V}_x - \bar{V}_m) y_{km} \right] \\ &= \bar{V}_k^* \bar{V}_x \left[\frac{y_{ckm}}{2} + y_{km} \right] - \bar{V}_k^* \bar{V}_m y_{km} \end{aligned}$$

Using equation (2.21) in the above equation,

$$P_{km} - jQ_{km} = \bar{V}_k^* \left[(\bar{V}_k - \bar{V}_{se}) y_a + \bar{V}_m y_b \right] \left[\frac{y_{ckm}}{2} + y_{km} \right] - \bar{V}_k^* \bar{V}_m y_{km}$$

$$\begin{aligned}
&= \bar{V}_k^2 \left(y_a \left[\frac{y_{ckm}}{2} + y_{km} \right] \right) - \bar{V}_k^* \bar{V}_{se} \left(y_a \left[\frac{y_{ckm}}{2} + y_{km} \right] \right) + \bar{V}_k^* \bar{V}_m \left(y_b \left[\frac{y_{ckm}}{2} + y_{km} \right] \right) - \bar{V}_k^* \bar{V}_m y_{km} \\
&= \bar{V}_k^2 y_A - \bar{V}_k^* \bar{V}_{se} y_A + \bar{V}_k^* V_m y_B - \bar{V}_k^* \bar{V}_m y_{km} \\
&= V_k^2 y_A \angle \theta_A - V_k V_{se} y_A \angle (\theta_A - \delta_{kse}) + V_k V_m y_B \angle (\theta_B - \delta_{km}) - V_k V_m y_{km} \angle (\theta_{km} - \delta_{km}) \quad (2.22)
\end{aligned}$$

where,

$$\begin{aligned}
y_A &= \left(y_a \left[\frac{y_{ckm}}{2} + y_{km} \right] \right) = g_A + jb_A \\
y_B &= \left(y_b \left[\frac{y_{ckm}}{2} + y_{km} \right] \right) = g_B + jb_B
\end{aligned}$$

Separating real and imaginary parts of equation (2.22) the expressions for RPPF through the line km i.e., from bus- k to bus- m are calculated as:

$$\begin{aligned}
P_{km} &= V_k^2 y_A \cos \theta_A - V_k V_{se} y_A \cos(\theta_A - \delta_{kse}) + V_k V_m y_B \cos(\theta_B - \delta_{km}) - V_k V_m y_{km} \cos(\theta_{km} - \delta_{km}) \\
&= V_k^2 g_A - V_k V_{se} [g_A \cos \delta_{kse} + b_A \sin \delta_{kse}] + V_k V_m [g_B \cos \delta_{km} + b_B \sin \delta_{km}] - V_k V_m [g_{km} \cos \delta_{km} + b_{km} \sin \delta_{km}] \quad (2.23)
\end{aligned}$$

$$-Q_{km} = V_k^2 y_A \sin \theta_A - V_k V_{se} y_A \sin(\theta_A - \delta_{kse}) + V_k V_m y_B \sin(\theta_B - \delta_{km}) - V_k V_m y_{km} \sin(\theta_{km} - \delta_{km})$$

$$Q_{km} = -V_k^2 b_A - V_k V_{se} [g_A \sin \delta_{kse} - b_A \cos \delta_{kse}] + V_k V_m [g_B \sin \delta_{km} - b_B \cos \delta_{km}] - V_k V_m [g_{km} \sin \delta_{km} - b_{km} \cos \delta_{km}] \quad (2.24)$$

where,

$$\delta_{kse} = \delta_k - \delta_{se}$$

$$\delta_{km} = \delta_k - \delta_m$$

$$\theta_{km} = \theta_k - \theta_m$$

Equation (2.25) represents the expression for complex power flow through the line mk i.e., from bus- m to bus- k .

$$P_{mk} - jQ_{mk} = \bar{V}_m^* (\bar{I}_{mx} + \bar{I}_{cm}) \quad (2.25)$$

While calculating the power flow from bus- m to bus- k , from Figure 2.3, the current through SPFC device (I_s) can be written as:

$$\bar{I}_s = (\bar{V}_x + \bar{V}_{se} - \bar{V}_k) y_{se} \quad (2.26)$$

$$\bar{I}_s = (\bar{V}_m - \bar{V}_x) y_{km} - \bar{V}_x \frac{y_{ckm}}{2} \quad (2.27)$$

Using equations (2.26) and (2.27),

$$\begin{aligned}
(\bar{V}_x + \bar{V}_{se} - \bar{V}_k) y_{se} &= (\bar{V}_m - \bar{V}_x) y_{km} - \bar{V}_x \frac{y_{ckm}}{2} \\
\bar{V}_m y_{km} + (\bar{V}_k - \bar{V}_{se}) y_{se} &= \bar{V}_x \left[y_{se} + y_{km} + \frac{y_{ckm}}{2} \right] \\
\bar{V}_x &= \frac{(\bar{V}_k - \bar{V}_{se}) y_{se}}{y_T} + \frac{\bar{V}_m y_{km}}{y_T} \\
\bar{V}_x &= (\bar{V}_k - \bar{V}_{se}) y_a + \bar{V}_m y_b
\end{aligned} \tag{2.28}$$

Equation (2.25) is rewritten as:

$$\begin{aligned}
P_{mk} - jQ_{mk} &= \bar{V}_m^* \left[(\bar{V}_m - \bar{V}_x) y_{km} + \bar{V}_m \frac{y_{ckm}}{2} \right] \\
&= \bar{V}_m^* \left[\bar{V}_m \left(\frac{y_{ckm}}{2} + y_{km} \right) - \bar{V}_x y_{km} \right]
\end{aligned}$$

Using equation (2.28) in the above equation,

$$\begin{aligned}
&= \bar{V}_m^* \left[\bar{V}_m \left(y_{km} + \frac{y_{ckm}}{2} \right) - ((\bar{V}_k - \bar{V}_{se}) y_a + \bar{V}_m y_b) y_{km} \right] \\
&= V_m^2 \left(y_{km} + \frac{y_{ckm}}{2} \right) - \bar{V}_m^* \bar{V}_k y_{km} y_a + \bar{V}_m^* \bar{V}_{se} y_{km} y_a - V_m^2 y_{km} y_b \\
&= V_m^2 \left(y_{km} + \frac{y_{ckm}}{2} \right) - \bar{V}_m^* \bar{V}_k y'_A + \bar{V}_m^* \bar{V}_{se} y'_A - V_m^2 y_{km} y'_B \\
&= V_m^2 \left[y_{km} \angle \theta_{km} + j \frac{y_{ckm}}{2} \right] - V_m V_k y'_A \angle (\theta'_A - \delta_{mk}) + V_m V_{se} y'_A \angle (\theta'_A - \delta_{mse}) - V_m^2 y'_B \angle \theta'_B
\end{aligned} \tag{2.29}$$

where,

$$\begin{aligned}
y'_A &= y_{km} y_a = g'_A + jb'_A \\
y'_B &= y_{km} y_b = g'_B + jb'_B
\end{aligned}$$

Separating real and imaginary parts of equation (2.29) the expressions for RPPF from bus- m to bus- k is calculated as:

$$\begin{aligned}
P_{mk} &= V_m^2 y_{km} \cos \angle \theta_{km} - V_m V_k y'_A \cos \angle (\theta'_A - \delta_{mk}) + V_m V_{se} y'_A \cos \angle (\theta'_A - \delta_{mse}) - V_m^2 y'_B \cos \angle \theta'_B \\
&= V_m^2 (g_{km} - g'_B) - V_k V_m (g'_A \cos \delta_{mk} + b'_A \sin \delta_{mk}) + V_{se} V_m (g'_A \cos \delta_{mse} + b'_A \sin \delta_{mse})
\end{aligned} \tag{2.30}$$

$$\begin{aligned}
Q_{mk} &= -V_m^2 \left(b_{km} + \frac{y_{ckm}}{2} \right) + V_m V_k y'_A \sin \angle(\theta'_A - \delta_{mk}) - V_m V_{se} y'_A \sin \angle(\theta'_A - \delta_{mse}) + V_m^2 y'_B \sin \angle \theta'_B \\
&= -V_m^2 \left(b_{km} + \frac{y_{ckm}}{2} + b'_B \right) - V_k V_m (g'_A \sin \delta_{mk} - b'_A \cos \delta_{mk}) + V_{se} V_m (g'_A \sin \delta_{mse} - b'_A \cos \delta_{mse})
\end{aligned} \tag{2.31}$$

where, $\delta_{mse} = \delta_m - \delta_{se}$ and $\delta_{mk} = \delta_m - \delta_k$

SPFC is considered an integral part of the transmission line. Thus the expression of bus power injections where SPFC is connected will be different from the power injections represented in equations (2.5) and (2.6). Therefore, the expression for P_{km} with SPFC device given by equation (2.23) is added and subtracted by $V_k^2 g_{km}$ to represent the P_{km} through the line with SPFC device so that the expression for line flow without SPFC is also present in it.

$$\begin{aligned}
P_{km} &= V_k^2 g_A - V_k V_{se} [g_A \cos \delta_{kse} + b_A \sin \delta_{kse}] + V_k V_m [g_B \cos \delta_{km} + b_B \sin \delta_{km}] \\
&\quad - V_k V_m [g_{km} \cos \delta_{km} + b_{km} \sin \delta_{km}] + V_k^2 g_{km} - V_k^2 g_{km}
\end{aligned} \tag{2.32}$$

The term $V_k^2 g_{km} - V_k V_m [g_{km} \cos \delta_{km} + b_{km} \sin \delta_{km}]$ represents P_{km} through the line without the SPFC device, and this term is already incorporated in the power injection expression. Therefore, the modified expression of power injection (P_k) with SPFC device is:

$$\begin{aligned}
P_k &= \left[\sum_{j=1}^n V_k V_j (G_{kj} \cos \delta_{kj} + B_{kj} \sin \delta_{kj}) \right] + V_k^2 g_A - V_k V_{se} [g_A \cos \delta_{kse} + b_A \sin \delta_{kse}] \\
&\quad + V_k V_m [g_B \cos \delta_{km} + b_B \sin \delta_{km}] - V_k^2 g_{km}
\end{aligned} \tag{2.33}$$

Similarly, the expression for Q_{km} with SPFC device given in equation (2.24) is added and subtracted by $V_k^2 \left(b_{km} + \frac{y_{ckm}}{2} \right)$ to represent the Q_{km} through the line with SPFC device so that the expression for line flow without SPFC is also present in it.

$$\begin{aligned}
Q_{km} &= -V_k^2 b_A - V_k V_{se} [g_A \sin \delta_{kse} - b_A \cos \delta_{kse}] + V_k V_m [g_B \sin \delta_{km} - b_B \cos \delta_{km}] + V_k^2 \left(b_{km} + \frac{y_{ckm}}{2} \right) \\
&\quad - V_k^2 \left(b_{km} + \frac{y_{ckm}}{2} \right) - V_k V_m [g_{km} \sin \delta_{km} - b_{km} \cos \delta_{km}]
\end{aligned} \tag{2.34}$$

The term $-V_k^2 \left(b_{km} + \frac{y_{ckm}}{2} \right) - V_k V_m [g_{km} \sin \delta_{km} - b_{km} \cos \delta_{km}]$ represents the Q_{km} through the line without SPFC device, and this term is already incorporated in the power injection expression. Therefore, the modified expression for power injection (Q_k) with SPFC device is:

$$Q_k = \left[\sum_{j=1}^n V_k V_j (G_{kj} \sin \delta_{kj} - B_{kj} \cos \delta_{kj}) \right] - V_k^2 b_A - V_k V_{se} [g_A \sin \delta_{kse} - b_A \cos \delta_{kse}] \\ + V_k V_m [g_B \sin \delta_{km} - b_B \cos \delta_{km}] + V_k^2 \left(b_{km} + \frac{y_{ckm}}{2} \right) \quad (2.35)$$

Again, the expression P_{mk} with SPFC device given in equation (2.30) is added and subtracted by $V_k V_m (g_{km} \cos \delta_{mk} + b_{km} \sin \delta_{mk})$ to represent P_{mk} with SPFC device, so that the expression for line flow without SPFC is also present in it.

$$P_{mk} = V_m^2 g_{km} - V_k V_m (g_{km} \cos \delta_{mk} + b_{km} \sin \delta_{mk}) - V_m^2 g'_B - V_k V_m (g'_A \cos \delta_{mk} + b'_A \sin \delta_{mk}) \\ + V_{se} V_m (g'_A \cos \delta_{mse} + b'_A \sin \delta_{mse}) + V_k V_m (g_{km} \cos \delta_{mk} + b_{km} \sin \delta_{mk}) \quad (2.36)$$

The term $V_m^2 g_{km} - V_k V_m (g_{km} \cos \delta_{mk} + b_{km} \sin \delta_{mk})$ represents the P_{mk} through the line without SPFC device, and this term is already incorporated in P_m expression. Therefore, the modified expression for P_m with SPFC device is:

$$P_m = \left[\sum_{j=1}^n V_m V_j (G_{mj} \cos \delta_{mj} + B_{mj} \sin \delta_{mj}) \right] - V_m^2 g'_B - V_k V_m (g'_A \cos \delta_{mk} + b'_A \sin \delta_{mk}) \\ + V_{se} V_m (g'_A \cos \delta_{mse} + b'_A \sin \delta_{mse}) + V_k V_m (g_{km} \cos \delta_{mk} + b_{km} \sin \delta_{mk}) \quad (2.37)$$

Similarly, the expression for Q_{mk} with SPFC device given in equation (2.31) is added and subtracted by $V_k V_m (g_{km} \sin \delta_{mk} - b_{km} \cos \delta_{mk})$ to represent the expression of Q_{mk} with SPFC device, so that the expression for line flow without SPFC is also present in it.

$$Q_{mk} = -V_m^2 \left(b_{km} + \frac{y_{ckm}}{2} \right) - V_m V_k (g_{km} \sin \delta_{mk} - b_{km} \cos \delta_{mk}) - V_m^2 b'_B - V_k V_m (g'_A \sin \delta_{mk} - b'_A \cos \delta_{mk}) \\ + V_s V_m (g'_A \sin \delta_{ms} - b'_A \cos \delta_{ms}) + V_m V_k (g_{km} \sin \delta_{mk} - b_{km} \cos \delta_{mk}) \quad (2.38)$$

The term $-V_m^2 \left(b_{km} + \frac{y_{ckm}}{2} \right) - V_m V_k (g_{km} \sin \delta_{mk} - b_{km} \cos \delta_{mk})$ represents the Q_{mk} without SPFC device, and the term already incorporated in Q_m expression. Therefore, the modified expression for Q_m with SPFC device is:

$$Q_m = \left[\sum_{j=1}^n V_m V_j (G_{mj} \sin(\delta_{mj}) - B_{mj} \cos(\delta_{mj})) \right] - V_m^2 b'_B - V_k V_m (g'_A \sin \delta_{mk} - b'_A \cos \delta_{mk}) + V_{se} V_m (g'_A \sin \delta_{mse} - b'_A \cos \delta_{mse}) + V_m V_k (g_{km} \sin \delta_{mk} - b_{km} \cos \delta_{mk}) \quad (2.39)$$

Using equations (2.32, 2.34, 2.36, and 2.38) for power flow through the line with SPFC device and power injection expressions given in equations (2.33, 2.35, 2.37, and 2.39), the NR LF model with the SPFC device connected in the line km can be represented as:

$$\begin{bmatrix} \frac{\partial P_2}{\partial \delta_2} & \dots & \frac{\partial P_2}{\partial \delta_k} & \dots & \frac{\partial P_2}{\partial \delta_m} & \dots & \frac{\partial P_2}{\partial \delta_n} & \dots & \frac{\partial P_2}{\partial V_2} & \dots & \frac{\partial P_2}{\partial V_k} & \dots & \frac{\partial P_2}{\partial V_m} & \dots & \frac{\partial P_2}{\partial V_n} & 0 & 0 \\ \dots & \dots \\ \frac{\partial P_k}{\partial \delta_2} & \dots & \frac{\partial P_k}{\partial \delta_k} & \dots & \frac{\partial P_k}{\partial \delta_m} & \dots & \frac{\partial P_k}{\partial \delta_n} & \dots & \frac{\partial P_k}{\partial V_2} & \dots & \frac{\partial P_k}{\partial V_k} & \dots & \frac{\partial P_k}{\partial V_m} & \dots & \frac{\partial P_k}{\partial V_n} & \frac{\partial P_k}{\partial \delta_{se}} & \frac{\partial P_k}{\partial V_{se}} \\ \dots & \dots \\ \frac{\partial P_m}{\partial \delta_2} & \dots & \frac{\partial P_m}{\partial \delta_k} & \dots & \frac{\partial P_m}{\partial \delta_m} & \dots & \frac{\partial P_m}{\partial \delta_n} & \dots & \frac{\partial P_m}{\partial V_2} & \dots & \frac{\partial P_m}{\partial V_k} & \dots & \frac{\partial P_m}{\partial V_m} & \dots & \frac{\partial P_m}{\partial V_n} & \frac{\partial P_m}{\partial \delta_{se}} & \frac{\partial P_m}{\partial V_{se}} \\ \dots & \dots \\ \frac{\partial P_n}{\partial \delta_2} & \dots & \frac{\partial P_n}{\partial \delta_k} & \dots & \frac{\partial P_n}{\partial \delta_m} & \dots & \frac{\partial P_n}{\partial \delta_n} & \dots & \frac{\partial P_n}{\partial V_2} & \dots & \frac{\partial P_n}{\partial V_k} & \dots & \frac{\partial P_n}{\partial V_m} & \dots & \frac{\partial P_n}{\partial V_n} & 0 & 0 \\ \frac{\partial Q_2}{\partial \delta_2} & \dots & \frac{\partial Q_2}{\partial \delta_k} & \dots & \frac{\partial Q_2}{\partial \delta_m} & \dots & \frac{\partial Q_2}{\partial \delta_n} & \dots & \frac{\partial Q_2}{\partial V_2} & \dots & \frac{\partial Q_2}{\partial V_k} & \dots & \frac{\partial Q_2}{\partial V_m} & \dots & \frac{\partial Q_2}{\partial V_n} & 0 & 0 \\ \dots & \dots \\ \frac{\partial Q_k}{\partial \delta_2} & \dots & \frac{\partial Q_k}{\partial \delta_k} & \dots & \frac{\partial Q_k}{\partial \delta_m} & \dots & \frac{\partial Q_k}{\partial \delta_n} & \dots & \frac{\partial Q_k}{\partial V_2} & \dots & \frac{\partial Q_k}{\partial V_k} & \dots & \frac{\partial Q_k}{\partial V_m} & \dots & \frac{\partial Q_k}{\partial V_n} & \frac{\partial Q_k}{\partial \delta_{se}} & \frac{\partial Q_k}{\partial V_{se}} \\ \dots & \dots \\ \frac{\partial Q_m}{\partial \delta_2} & \dots & \frac{\partial Q_m}{\partial \delta_k} & \dots & \frac{\partial Q_m}{\partial \delta_m} & \dots & \frac{\partial Q_m}{\partial \delta_n} & \dots & \frac{\partial Q_m}{\partial V_2} & \dots & \frac{\partial Q_m}{\partial V_k} & \dots & \frac{\partial Q_m}{\partial V_m} & \dots & \frac{\partial Q_m}{\partial V_n} & \frac{\partial Q_m}{\partial \delta_{se}} & \frac{\partial Q_m}{\partial V_{se}} \\ \dots & \dots \\ \frac{\partial Q_n}{\partial \delta_2} & \dots & \frac{\partial Q_n}{\partial \delta_k} & \dots & \frac{\partial Q_n}{\partial \delta_m} & \dots & \frac{\partial Q_n}{\partial \delta_n} & \dots & \frac{\partial Q_n}{\partial V_2} & \dots & \frac{\partial Q_n}{\partial V_k} & \dots & \frac{\partial Q_n}{\partial V_m} & \dots & \frac{\partial Q_n}{\partial V_n} & 0 & 0 \\ 0 & \dots & \frac{\partial P_{km}}{\partial \delta_k} & \dots & \frac{\partial P_{km}}{\partial \delta_m} & \dots & 0 & \dots & 0 & \dots & \frac{\partial P_{km}}{\partial V_k} & \dots & \frac{\partial P_{km}}{\partial V_m} & \dots & 0 & \frac{\partial P_{km}}{\partial \delta_{se}} & \frac{\partial P_{km}}{\partial V_{se}} \\ 0 & \dots & \frac{\partial Q_{km}}{\partial \delta_k} & \dots & \frac{\partial Q_{km}}{\partial \delta_m} & \dots & 0 & \dots & 0 & \dots & \frac{\partial Q_{km}}{\partial V_k} & \dots & \frac{\partial Q_{km}}{\partial V_m} & \dots & 0 & \frac{\partial Q_{km}}{\partial \delta_{se}} & \frac{\partial Q_{km}}{\partial V_{se}} \end{bmatrix} \begin{bmatrix} \Delta \delta_2 \\ \dots \\ \Delta \delta_k \\ \dots \\ \Delta \delta_m \\ \dots \\ \Delta \delta_n \\ \Delta V_2 \\ \dots \\ \Delta V_k \\ \dots \\ \Delta V_m \\ \dots \\ \Delta V_n \\ \Delta \delta_{se} \\ \Delta V_{se} \end{bmatrix} = \begin{bmatrix} \Delta P_2 \\ \dots \\ \Delta P_k \\ \dots \\ \Delta P_m \\ \dots \\ \Delta P_n \\ \Delta Q_2 \\ \dots \\ \Delta Q_k \\ \dots \\ \Delta Q_m \\ \dots \\ \Delta Q_n \\ \Delta P_{km} \\ \Delta Q_{km} \end{bmatrix} \quad (2.40)$$

Equation (2.41) represents the compact form of equation (2.40)

$$\begin{bmatrix} \Delta P \\ \Delta Q \\ \Delta P_{km} \\ \Delta Q_{km} \end{bmatrix} = [J_{SPFC}] \begin{bmatrix} \Delta \delta \\ \Delta V \\ \Delta \delta_{se} \\ \Delta V_{se} \end{bmatrix} \quad (2.41)$$

where,

$$\left. \begin{aligned} \Delta P_{km} &= P_{km}^{sch} - P_{km} \\ \Delta Q_{km} &= Q_{km}^{sch} - Q_{km} \end{aligned} \right\}$$

Equations (2.42-2.69) calculates the elements of Jacobian matrix due to the introduction of SPFC device in line km .

$$\begin{aligned} \frac{\partial P_k}{\partial \delta_k} &= \sum_{j=1}^n V_k V_j (-G_{kj} \sin \delta_{kj} + B_{kj} \cos \delta_{kj}) - V_k V_{se} [-g_A \sin \delta_{kse} + b_A \cos \delta_{kse}] \\ &+ V_k V_m [-g_B \sin \delta_{km} + b_B \cos \delta_{km}] \end{aligned} \quad (2.42)$$

$$\begin{aligned} \frac{\partial P_k}{\partial V_k} &= \sum_{j=1}^n V_j (G_{kj} \sin \delta_{kj} + B_{kj} \cos \delta_{kj}) + 2V_k g_A - V_{se} [g_A \cos \delta_{kse} + b_A \sin \delta_{kse}] \\ &+ V_m [g_B \cos \delta_{km} + b_B \sin \delta_{km}] - 2V_k g_{km} \end{aligned} \quad (2.43)$$

$$\begin{aligned} \frac{\partial P_m}{\partial \delta_m} &= \sum_{j=1}^n V_m V_j (-G_{mj} \sin \delta_{mj} + B_{mj} \cos \delta_{mj}) - V_k V_m [-g'_A \sin \delta_{mk} + b'_A \cos \delta_{mk}] \\ &+ V_m V_{se} [-g'_A \sin \delta_{mse} + b'_A \cos \delta_{mse}] + V_m V_k [-g_{km} \sin \delta_{mk} + b_{km} \cos \delta_{mk}] \end{aligned} \quad (2.44)$$

$$\begin{aligned} \frac{\partial P_m}{\partial V_m} &= \sum_{j=1}^n V_j (G_{mj} \cos \delta_{mj} + B_{mj} \sin \delta_{mj}) - 2V_m g'_B - V_k [g'_A \cos \delta_{mk} + b'_A \sin \delta_{mk}] \\ &+ V_{se} [g'_A \cos \delta_{mse} + b'_A \sin \delta_{mse}] + V_k [g_{km} \cos \delta_{mk} + b_{km} \sin \delta_{mk}] \end{aligned} \quad (2.45)$$

$$\frac{\partial Q_k}{\partial \delta_k} = \sum_{j=1}^n V_k V_j (G_{kj} \cos \delta_{kj} + B_{kj} \sin \delta_{kj}) - V_k V_{se} [g_A \cos \delta_{kse} + b_A \sin \delta_{kse}] + V_k V_m [g_B \cos \delta_{km} + b_B \sin \delta_{km}] \quad (2.46)$$

$$\begin{aligned} \frac{\partial Q_k}{\partial V_k} &= \sum_{j=1}^n V_j (G_{kj} \sin \delta_{kj} - B_{kj} \cos \delta_{kj}) - 2V_k b_A - V_{se} [g_A \sin \delta_{kse} - b_A \cos \delta_{kse}] \\ &+ V_m [g_B \sin \delta_{km} - b_B \cos \delta_{km}] + 2V_k \left(b_{km} + \frac{y_{ckm}}{2} \right) \end{aligned} \quad (2.47)$$

$$\begin{aligned} \frac{\partial Q_m}{\partial \delta_m} &= \sum_{j=1}^n V_m V_j (G_{mj} \sin \delta_{mj} + B_{mj} \cos \delta_{mj}) - 2V_m b'_B - V_k V_m [g'_A \cos \delta_{mk} + b'_A \sin \delta_{mk}] \\ &+ V_{se} V_m [g'_A \cos \delta_{mse} + b'_A \sin \delta_{mse}] + V_m V_k [g_{km} \cos \delta_{mk} + b_{km} \sin \delta_{mk}] \end{aligned} \quad (2.48)$$

$$\begin{aligned} \frac{\partial Q_m}{\partial V_m} &= \sum_{j=1}^n V_j (G_{mj} \sin \delta_{mj} - B_{mj} \cos \delta_{mj}) - 2V_m b'_B - V_k [g'_A \sin \delta_{mk} - b'_A \cos \delta_{mk}] \\ &+ V_{se} [g'_A \sin \delta_{mse} - b'_A \cos \delta_{mse}] + V_k [g_{km} \sin \delta_{mk} - b_{km} \cos \delta_{mk}] \end{aligned} \quad (2.49)$$

$$\frac{\partial P_k}{\partial \delta_s} = -V_k V_{se} [g_A \sin \delta_{kse} - b_A \cos \delta_{kse}] \quad (2.50)$$

$$\frac{\partial P_m}{\partial \delta_{se}} = V_m V_{se} [g'_A \sin \delta_{mse} - b'_A \cos \delta_{mse}] \quad (2.51)$$

$$\frac{\partial Q_k}{\partial \delta_{se}} = -V_k V_{se} [-g_A \cos \delta_{kse} - b_A \cos \delta_{kse}] \quad (2.52)$$

$$\frac{\partial Q_m}{\partial \delta_{se}} = V_m V_{se} [g'_A \sin \delta_{mse} - b'_A \cos \delta_{mse}] \quad (2.53)$$

$$\begin{aligned} \frac{\partial P_{km}}{\partial \delta_k} &= -V_k V_{se} (-g_A \sin \delta_{kse} + b_A \cos \delta_{kse}) + V_k V_m (-g_B \sin \delta_{km} + b_B \cos \delta_{km}) \\ &- V_k V_m (-g_{km} \sin \delta_{km} + b_B \cos \delta_{km}) \end{aligned} \quad (2.54)$$

$$\frac{\partial P_{km}}{\partial \delta_m} = V_k V_m (g_B \sin \delta_{km} - b_B \cos \delta_{km}) - V_k V_m (g_{km} \sin \delta_{km} - b_{km} \cos \delta_{km}) \quad (2.55)$$

$$\begin{aligned} \frac{\partial P_{km}}{\partial V_k} &= 2V_k g_A - V_{se} (g_A \cos \delta_{kse} + b_A \sin \delta_{kse}) + V_m (g_B \cos \delta_{km} + b_B \sin \delta_{km}) \\ &- V_m (g_{km} \cos \delta_{km} + b_{km} \sin \delta_{km}) \end{aligned} \quad (2.56)$$

$$\frac{\partial P_{km}}{\partial V_m} = V_k (g_B \cos \delta_{km} + b_B \sin \delta_{km}) - V_k (g_{km} \cos \delta_{km} + b_{km} \sin \delta_{km}) \quad (2.57)$$

$$\frac{\partial P_{km}}{\partial \delta_{se}} = -V_k V_{se} [g_A \sin \delta_{kse} - b_A \cos \delta_{kse}] \quad (2.58)$$

$$\frac{\partial P_{km}}{\partial V_{se}} = -V_k [g_A \cos \delta_{kse} + b_A \sin \delta_{kse}] \quad (2.59)$$

$$\frac{\partial P_k}{\partial V_{se}} = -V_k [g_A \cos \delta_{kse} + b_A \sin \delta_{kse}] \quad (2.60)$$

$$\frac{\partial P_m}{\partial V_{se}} = V_m [g'_A \cos \delta_{mk} + b'_A \sin \delta_{mk}] \quad (2.61)$$

$$\frac{\partial Q_k}{\partial V_{se}} = V_k [g_A \sin \delta_{kse} - b_A \cos \delta_{kse}] \quad (2.62)$$

$$\frac{\partial Q_m}{\partial V_{se}} = V_m [g'_A \sin \delta_{mse} - b'_A \cos \delta_{mse}] \quad (2.63)$$

$$\begin{aligned} \frac{\partial Q_{km}}{\partial \delta_k} &= -V_k V_{se} (g_A \cos \delta_{kse} + b_A \sin \delta_{kse}) + V_k V_m (g_B \cos \delta_{km} + b_B \sin \delta_{km}) \\ &- V_k V_m (g_{km} \cos \delta_{km} + b_{km} \sin \delta_{km}) \end{aligned} \quad (2.64)$$

$$\frac{\partial Q_{km}}{\partial \delta_m} = V_k V_m (-g_B \cos \delta_{km} - b_B \sin \delta_{km}) - V_k V_m (-g_{km} \cos \delta_{km} - b_{km} \sin \delta_{km}) \quad (2.65)$$

$$\frac{\partial Q_{km}}{\partial V_k} = -2V_k b_A - V_m (g_B \sin \delta_{km} - b_B \cos \delta_{km}) - V_m (g_{km} \sin \delta_{km} - b_{km} \cos \delta_{km}) \quad (2.66)$$

$$\frac{\partial Q_{km}}{\partial V_m} = V_k (g_B \sin \delta_{km} - b_B \cos \delta_{km}) - V_k (g_{km} \sin \delta_{km} - b_{km} \cos \delta_{km}) \quad (2.67)$$

$$\frac{\partial Q_{km}}{\partial \delta_{se}} = -V_k V_{se} [-g_A \cos \delta_{kse} - b_A \cos \delta_{kse}] \quad (2.68)$$

$$\frac{\partial Q_{km}}{\partial V_{se}} = V_m [g'_A \sin \delta_{mse} - b'_A \cos \delta_{mse}] \quad (2.69)$$

Equation (2.70) evaluates the updated values of voltage magnitude and phase angles of the SPFC device.

$$\left. \begin{aligned} V_{se}^{K+1} &= V_{se}^K + \Delta V_{se}^K \\ \delta_{se}^{K+1} &= \delta_{se}^K + \Delta \delta_{se}^K \end{aligned} \right\} \quad (2.70)$$

Once the elements of the Jacobian matrix are calculated then correction values are determined. Updated values of V_i , δ_i , V_{se} and δ_{se} are calculated. Equations (2.32-2.39) calculate the power flow through the line and power injections with the SPFC device. The process repeats until the mismatches are less than the specified tolerance value. The limits on the SPFC device are:

$$|V_{se}| \leq 0.2 \quad (2.71)$$

$$-\pi \leq \delta_{se} \leq \pi \quad (2.72)$$

2.6 Unified Power Flow Controller (UPFC)

Gyugyi proposed the concept of UPFC in 1991. UPFC is a type of combined compensator that consists of a static synchronous compensator (STATCOM) and an SSSC connected by a

common dc link that allows bidirectional real power flows between the output terminals of STATCOM and the SSSC [8]. It serves multiple functions in power systems including shunt compensation, series compensation as well as phase shifting. It can control all the parameters related to power flow through the transmission lines like voltage magnitude, phase angle, impedance simultaneously and selectively. Due to this unique specialty of UPFC, the adjective ‘unified’ is used in the name. The RRPF through the line is controlled independently by combining the function of shunt and series compensators of UPFC. The inclusion of UPFC in the transmission lines allows the transmission line to operate near to its thermal limit, thus allows more power transfer through the line.

Conventionally UPFC is a combination of two voltage-source converters. One converter is connected to the power system through a shunt transformer, and the other is connected to the transmission line through a series transformer. DC-link connects the two converters where the capacitor is coupled and allows a bi-directional real power flow between the output terminals of the shunt converter.

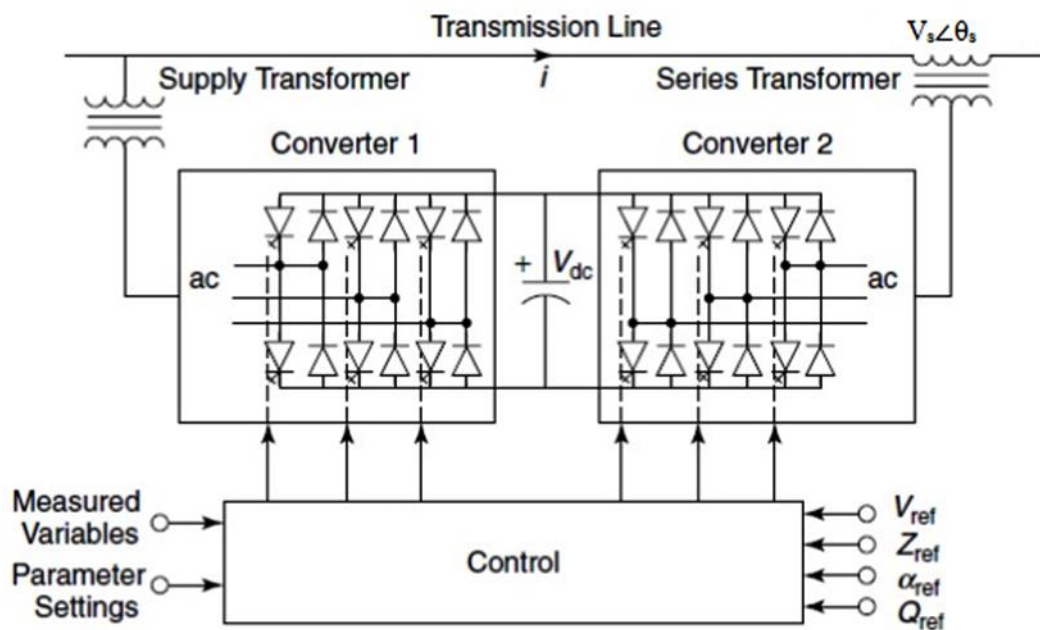


Fig. 2.4 Basic UPFC Configuration [3].

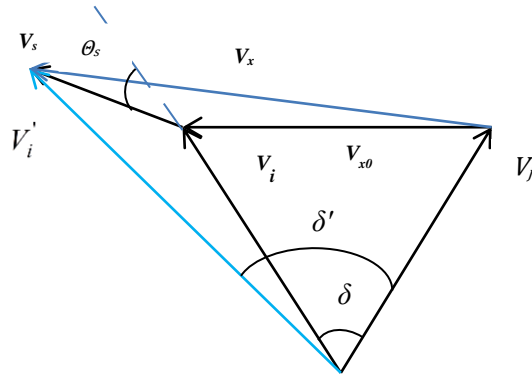


Fig. 2.5 Phasor representation of UPFC

Figure 2.4 shows the basic configuration of the UPFC. The series controller acts as a synchronous voltage source that can inject a controllable voltage in series with the line. The phase angle of the injected voltage is controlled independently of the line current. UPFC can inject controllable magnitude in the range of $(0-V_s^{\max})$ and the phase angle of $(0-360^\circ)$. The function or effect of the UPFC device can be easily explained by the phasor diagram shown in Figure 2.5, where V_s is the voltage at the series terminal of the UPFC device and θ_s is the phase angle of V_s with respect to V_i . From the phasor diagram, it is clear that the change in V_s will change the magnitude of voltage (V_i'), and the phase angle difference (δ') between sending end and receiving end voltage.

Table 2.2 Line Parameters with and without UPFC device

Without UPFC	With UPFC
V_i = Sending end voltage	V_i' = Sending end voltage
V_j = Receiving end voltage	V_x = Voltage drop
V_{x0} = Voltage drop	δ' =Phase angle (SPA) difference
δ =Phase angle (SPA) difference	

a) Shunt converter

The shunt branch of UPFC consists of a DC capacitor, shunt converter and a shunt transformer. It can absorb or generate only reactive power because the output current is in quadrature with the terminal voltage. The function of the shunt branch is to provide the real power demanded by the series converter through the common DC link terminal. Also, it can generate or absorb reactive power independently of the real power and regulates the terminal voltage at the sending end; thus shunt converter regulates the voltage at the input terminals of the UPFC. Again the shunt branch of UPFC provides direct control of the DC capacitor voltage and consequently an indirect regulation of the real power required by the series UPFC branch. The shunt converter provides the amount of real power demanded by the series converter plus the circuit losses. Real power flow from the series converter to shunt converter is possible and in some cases desired, in that case, the series converter would supply the required real power plus the losses to the shunt converter. The shunt converter controls the dc voltage and the bus voltage at the shunt converter transformer.

b) Series converter

The series branch of UPFC consists of a DC Capacitor, series converter, and a series connected transformer. It can act as a voltage source injected in series to the transmission line through the series-connected transformer. The real power can flow from the series converter to the shunt converter and vice versa. Hence, it is possible to introduce positive or negative phase shifts between the voltage at the source and the load. The series injected voltage (V_s) can have any phase shift with respect to the terminal voltage at the source. Therefore, the operating area of the UPFC becomes the circle limited with a radius defined by the maximum magnitude of V_s , i.e., V_s^{\max} . The series converter controls the active and reactive powers flow through the transmission line by adjusting the magnitude and phase angle of the series injected voltage. The series converter directly controls the real power of the line by controlling the magnitude of the series injected voltage. The series converter generates the voltage and phase shift at the fundamental frequency is added in series with the transmission line and directly to the terminal voltage by the series-connected coupling transformer. The transmission line current passes

through the series transformer, and in this process, it exchanges real and reactive power with the series converter.

2.7 Load Flow analysis using UPFC device for an Interconnected Power system

A modified UPFC is considered for the modeling of LF analysis which consists of an SSSC and SVC, SSSC modeled with a controllable series voltage source ($V_s \angle \theta_s$), and SVC modeled as a controllable shunt susceptance (B_{sh}). The UPFC model considered in this research work has only three state variables compared to traditional UPFC with four state variables. As a result, the size of the Jacobian Matrix for LF analysis with this UPFC model is reduced compared to a traditional UPFC model. Further, the motive behind this model is to create a facility for independent control of power flow through the transmission line using the SSSC device and reactive power control at the bus with the SVC device. During LF modeling, the UPFC is considered an integral part of the transmission line. Figure 2.6 shows the configuration of the UPFC device along with a transmission line where the UPFC device containing SSSC and SVC is connected between the k^{th} bus and one end of the transmission line so that the UPFC becomes an integral part of the transmission line connected between k^{th} and m^{th} buses of the power system.

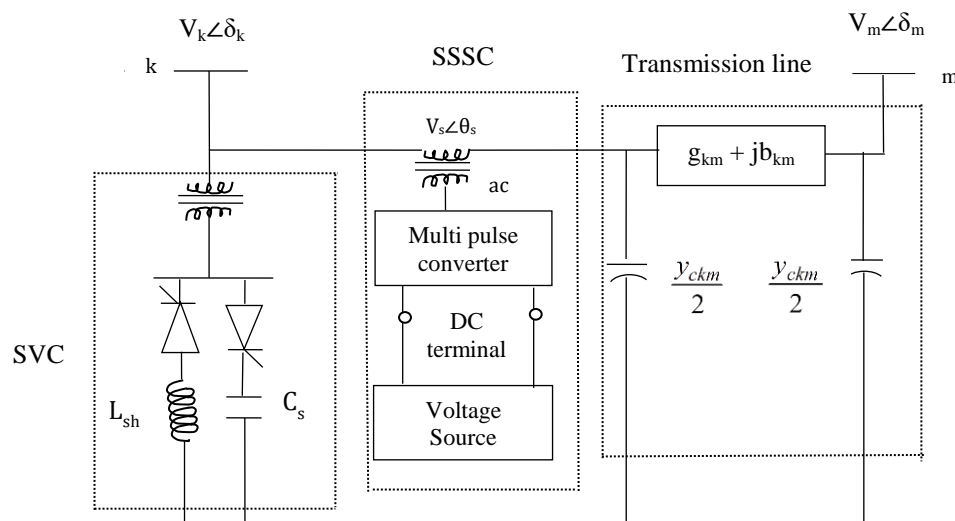


Fig. 2.6 Configuration of UPFC device containing the SSSC and SVC.

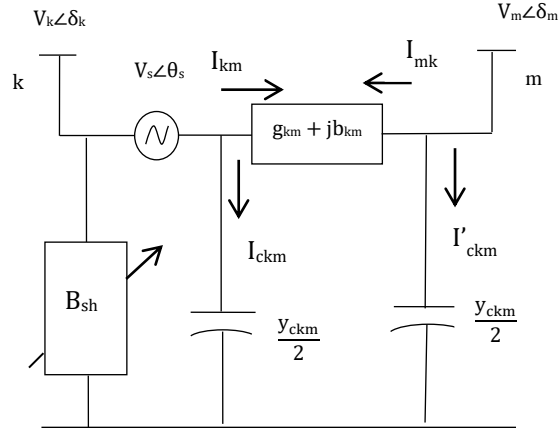


Fig. 2.7 Equivalent circuit of a transmission line with an UPFC device containing the SSSC and SVC.

Figure 2.7 shows the equivalent circuit of a transmission line with an UPFC device containing the SSSC and SVC presented in Figure 2.6. As UPFC is considered as an integral part of the transmission line thus the expression for power injections where UPFC is connected will be different from the power injections represented by equations (2.5) and (2.6). Therefore, with UPFC device implemented in the transmission lines of a PSN depicted in Figure 2.7, the expression for complex power flow from bus- k to bus- m is derived as:

$$\begin{aligned}
 P_{km} + jQ_{km} &= \bar{V}_k (\bar{I}_{km} + \bar{I}_{ckm})^* \\
 &= \bar{V}_k \left([\bar{V}_k - \bar{V}_s - \bar{V}_m] \bar{y}_{km} + [\bar{V}_k - \bar{V}_s] j \frac{y_{ckm}}{2} \right)^* \\
 &= V_k^2 y_{km} \angle -\theta_{km} - V_k V_s y_{km} \angle (\delta_k - \theta_s - \theta_{km}) - V_k V_m y_{km} \angle (\delta_k - \delta_m - \theta_{km}) + V_k^2 \frac{y_{ckm}}{2} \angle -90^\circ \\
 &\quad - V_k V_s \frac{y_{ckm}}{2} \angle (\delta_k - \theta_s - 90^\circ)
 \end{aligned} \tag{2.73}$$

Separating real and imaginary parts of the equation (2.73) P_{km} and Q_{km} is expressed as:

$$\begin{aligned}
 P_{km} &= V_k^2 y_{km} \cos(-\theta_{km}) - V_k V_s y_{km} \cos(\delta_k - \theta_s - \theta_{km}) - V_k V_m y_{km} \cos(\delta_k - \delta_m - \theta_{km}) \\
 &\quad + V_k^2 \frac{y_{ckm}}{2} \cos(-90^\circ) - V_k V_s \frac{y_{ckm}}{2} \cos(\delta_k - \theta_s - 90^\circ)
 \end{aligned} \tag{2.74}$$

$$\begin{aligned}
 Q_{km} &= V_k^2 y_{km} \sin(-\theta_{km}) - V_k V_s y_{km} \sin(\delta_k - \theta_s - \theta_{km}) - V_k V_m y_{km} \sin(\delta_k - \delta_m - \theta_{km}) \\
 &\quad + V_k^2 \frac{y_{ckm}}{2} \sin(-90^\circ) - V_k V_s \frac{y_{ckm}}{2} \sin(\delta_k - \theta_s - 90^\circ)
 \end{aligned} \tag{2.75}$$

Simplifying equation (2.74) the real power flow through the line km is represented as:

$$P_{km} = V_k^2 g_{km} - V_k V_m (g_{km} \cos \delta_{km} + b_{km} \sin \delta_{km}) - V_k V_s \left((g_{km} \cos(\delta_k - \theta_s) + \left(b_{km} + \frac{y_{ckm}}{2} \right) \sin(\delta_k - \theta_s)) \right) \quad (2.76)$$

Simplifying equation (2.75), the reactive power flow through the line km is represented as:

$$Q_{km} = -V_k^2 \left(b_{km} + \frac{y_{ckm}}{2} \right) - V_k V_m (g_{km} \sin \delta_{km} - b_{km} \cos \delta_{km}) - V_k V_s \left(g_{km} \sin(\delta_k - \theta_s) - \left(b_{km} + \frac{y_{ckm}}{2} \right) \cos(\delta_k - \theta_s) \right) \quad (2.77)$$

Again power flow through the shunt branch is represented as:

$$Q_{ksh} = -V_k^2 B_{sh} \quad (2.78)$$

Now, the modified expression for real power and reactive power injection (P_k and Q_k) at the k^{th} bus with UPFC device connected in line ' km ' is represented as:

$$P_k = \left[\sum_{j=1}^n V_k V_j (G_{kj} \cos \delta_{kj} + B_{kj} \sin \delta_{kj}) \right] - V_k V_s \left((g_{km} \cos(\delta_k - \theta_s) + \left(b_{km} + \frac{y_{ckm}}{2} \right) \sin(\delta_k - \theta_s)) \right) \quad (2.79)$$

$$Q_k = \left[\sum_{j=1}^n V_k V_j (G_{kj} \sin \delta_{kj} - B_{kj} \cos \delta_{kj}) \right] - V_k^2 B_{sh} - V_k V_s \left((g_{km} \sin(\delta_k - \theta_s) - \left(b_{km} + \frac{y_{ckm}}{2} \right) \cos(\delta_k - \theta_s)) \right) \quad (2.80)$$

Again the expression for RRPF from bus- m to bus- k is derived as follows.

$$\begin{aligned} P_{mk} + jQ_{mk} &= \bar{V}_m (\bar{I}_{mk} + \bar{I}'_{ckm})^* \\ &= \bar{V}_m \left([\bar{V}_m - (\bar{V}_k - \bar{V}_s)] \bar{y}_{km} + [\bar{V}_m] j \frac{y_{ckm}}{2} \right)^* \\ &= V_m^2 y_{km} \angle -\theta_{km} - V_k V_m y_{km} \angle (\delta_m - \delta_k - \theta_{km}) + V_m V_s y_{km} \angle (\delta_m - \theta_s - \theta_{km}) + V_m^2 \frac{y_{ckm}}{2} \angle -90^\circ \end{aligned} \quad (2.81)$$

Separating real and imaginary parts of equation (2.81), P_{mk} and Q_{mk} can be written as:

$$P_{mk} = V_m^2 y_{km} \cos(-\theta_{km}) - V_k V_m y_{km} \cos(\delta_m - \delta_k - \theta_{km}) + V_m V_s y_{km} \cos(\delta_m - \theta_s - \theta_{km}) + V_m^2 \frac{y_{ckm}}{2} \cos(-90^\circ) \quad (2.82)$$

$$Q_{mk} = V_m^2 y_{km} \sin(-\theta_{km}) - V_k V_m y_{km} \sin(\delta_m - \delta_k - \theta_{km}) + V_m V_s y_{km} \sin(\delta_m - \theta_s - \theta_{km}) + V_m^2 \frac{y_{ckm}}{2} \sin(-90^\circ) \quad (2.83)$$

Simplifying equation (2.82), the real power flow through the line km is represented as:

$$P_{mk} = V_m^2 g_{km} - V_k V_m (g_{km} \cos \delta_{mk} + b_{km} \sin \delta_{mk}) + V_m V_s (g_{km} \cos(\delta_m - \theta_s) + b_{km} \sin(\delta_m - \theta_s)) \quad (2.84)$$

Simplifying equation (2.83), the reactive power flow through the line km is represented as:

$$Q_{mk} = -V_m^2 \left(b_{km} + \frac{y_{ckm}}{2} \right) - V_k V_m (g_{km} \sin \delta_{mk} - b_{km} \cos \delta_{mk}) + V_m V_s (g_{km} \sin(\delta_m - \theta_s) - b_{km} \cos(\delta_m - \theta_s)) \quad (2.85)$$

Now, the modified expression for real power and reactive power injection (P_m and Q_m) at the m^{th} bus with UPFC device connected in line 'km' is represented as:

$$P_m = \left[\sum_{j=1}^n V_m V_j (G_{mj} \cos \delta_{mj} + B_{mj} \sin \delta_{mj}) \right] + V_m V_s (g_{km} \cos(\delta_m - \theta_s) + b_{km} \sin(\delta_m - \theta_s)) \quad (2.86)$$

$$Q_m = \left[\sum_{j=1}^n V_m V_j (G_{mj} \sin \delta_{mj} - B_{mj} \cos \delta_{mj}) \right] + V_m V_s (g_{km} \cos(\delta_m - \theta_s) - b_{km} \sin(\delta_m - \theta_s)) \quad (2.87)$$

With the power flow through the line with a UPFC device and power injection expressions the NR LF model with the UPFC device connected in the line km can be represented as:

$$\begin{bmatrix} \frac{\partial P_2}{\partial \delta_2} & \dots & \frac{\partial P_2}{\partial \delta_k} & \dots & \frac{\partial P_2}{\partial \delta_m} & \dots & \frac{\partial P_2}{\partial \delta_n} & \dots & \frac{\partial P_2}{\partial V_2} & \dots & \frac{\partial P_2}{\partial V_k} & \dots & \frac{\partial P_2}{\partial V_m} & \dots & \frac{\partial P_2}{\partial V_n} & 0 & 0 & 0 \\ \dots & \dots \\ \frac{\partial P_k}{\partial \delta_2} & \dots & \frac{\partial P_k}{\partial \delta_k} & \dots & \frac{\partial P_k}{\partial \delta_m} & \dots & \frac{\partial P_k}{\partial \delta_n} & \dots & \frac{\partial P_k}{\partial V_2} & \dots & \frac{\partial P_k}{\partial V_k} & \dots & \frac{\partial P_k}{\partial V_m} & \dots & \frac{\partial P_k}{\partial V_n} & \frac{\partial P_k}{\partial \theta_s} & \frac{\partial P_k}{\partial V_s} & 0 \\ \dots & \dots \\ \frac{\partial P_m}{\partial \delta_2} & \dots & \frac{\partial P_m}{\partial \delta_k} & \dots & \frac{\partial P_m}{\partial \delta_m} & \dots & \frac{\partial P_m}{\partial \delta_n} & \dots & \frac{\partial P_m}{\partial V_2} & \dots & \frac{\partial P_m}{\partial V_k} & \dots & \frac{\partial P_m}{\partial V_m} & \dots & \frac{\partial P_m}{\partial V_n} & \frac{\partial P_m}{\partial \theta_s} & \frac{\partial P_m}{\partial V_s} & \frac{\partial P_m}{\partial V_{sh}} \\ \dots & \dots \\ \frac{\partial P_n}{\partial \delta_2} & \dots & \frac{\partial P_n}{\partial \delta_k} & \dots & \frac{\partial P_n}{\partial \delta_m} & \dots & \frac{\partial P_n}{\partial \delta_n} & \dots & \frac{\partial P_n}{\partial V_2} & \dots & \frac{\partial P_n}{\partial V_k} & \dots & \frac{\partial P_n}{\partial V_m} & \dots & \frac{\partial P_n}{\partial V_n} & 0 & 0 & 0 \\ \frac{\partial Q_2}{\partial \delta_2} & \dots & \frac{\partial Q_2}{\partial \delta_k} & \dots & \frac{\partial Q_2}{\partial \delta_m} & \dots & \frac{\partial Q_2}{\partial \delta_n} & \dots & \frac{\partial Q_2}{\partial V_2} & \dots & \frac{\partial Q_2}{\partial V_k} & \dots & \frac{\partial Q_2}{\partial V_m} & \dots & \frac{\partial Q_2}{\partial V_n} & 0 & 0 & 0 \\ \dots & \dots \\ \frac{\partial Q_k}{\partial \delta_2} & \dots & \frac{\partial Q_k}{\partial \delta_k} & \dots & \frac{\partial Q_k}{\partial \delta_m} & \dots & \frac{\partial Q_k}{\partial \delta_n} & \dots & \frac{\partial Q_k}{\partial V_2} & \dots & \frac{\partial Q_k}{\partial V_k} & \dots & \frac{\partial Q_k}{\partial V_m} & \dots & \frac{\partial Q_k}{\partial V_n} & \frac{\partial Q_k}{\partial \theta_s} & \frac{\partial Q_k}{\partial V_s} & \frac{\partial Q_k}{\partial V_{sh}} \\ \dots & \dots \\ \frac{\partial Q_m}{\partial \delta_2} & \dots & \frac{\partial Q_m}{\partial \delta_k} & \dots & \frac{\partial Q_m}{\partial \delta_m} & \dots & \frac{\partial Q_m}{\partial \delta_n} & \dots & \frac{\partial Q_m}{\partial V_2} & \dots & \frac{\partial Q_m}{\partial V_k} & \dots & \frac{\partial Q_m}{\partial V_m} & \dots & \frac{\partial Q_m}{\partial V_n} & \frac{\partial Q_m}{\partial \theta_s} & \frac{\partial Q_m}{\partial V_s} & \frac{\partial Q_m}{\partial V_{sh}} \\ \dots & \dots \\ \frac{\partial Q_n}{\partial \delta_2} & \dots & \frac{\partial Q_n}{\partial \delta_k} & \dots & \frac{\partial Q_n}{\partial \delta_m} & \dots & \frac{\partial Q_n}{\partial \delta_n} & \dots & \frac{\partial Q_n}{\partial V_2} & \dots & \frac{\partial Q_n}{\partial V_k} & \dots & \frac{\partial Q_n}{\partial V_m} & \dots & \frac{\partial Q_n}{\partial V_n} & 0 & 0 & 0 \\ \frac{\partial Q_{sh}}{\partial \delta_2} & \dots & \frac{\partial Q_{sh}}{\partial \delta_k} & \dots & \frac{\partial Q_{sh}}{\partial \delta_m} & \dots & \frac{\partial Q_{sh}}{\partial \delta_n} & \dots & \frac{\partial Q_{sh}}{\partial V_2} & \dots & \frac{\partial Q_{sh}}{\partial V_k} & \dots & \frac{\partial Q_{sh}}{\partial V_m} & \dots & \frac{\partial Q_{sh}}{\partial V_n} & 0 & 0 & 0 \\ 0 & \dots & \frac{\partial P_{km}}{\partial \delta_k} & \dots & \frac{\partial P_{km}}{\partial \delta_m} & \dots & 0 & \dots & 0 & \dots & \frac{\partial P_{km}}{\partial V_k} & \dots & \frac{\partial P_{km}}{\partial V_m} & \dots & 0 & \frac{\partial P_{km}}{\partial \theta_s} & \frac{\partial P_{km}}{\partial V_s} & 0 \\ 0 & \dots & \frac{\partial Q_{km}}{\partial \delta_k} & \dots & \frac{\partial Q_{km}}{\partial \delta_m} & \dots & 0 & \dots & 0 & \dots & \frac{\partial Q_{km}}{\partial V_k} & \dots & \frac{\partial Q_{km}}{\partial V_m} & \dots & 0 & \frac{\partial Q_{km}}{\partial \theta_s} & \frac{\partial Q_{km}}{\partial V_s} & 0 \\ 0 & \dots & \frac{\partial Q_{sh}}{\partial V_k} & \dots & 0 & \dots & 0 & 0 & 0 & \frac{\partial Q_{sh}}{\partial B_{sh}} \end{bmatrix} = \begin{bmatrix} \Delta \delta_2 \\ \dots \\ \Delta \delta_k \\ \dots \\ \Delta \delta_m \\ \dots \\ \Delta \delta_n \\ \Delta V_2 \\ \dots \\ \Delta V_k \\ \dots \\ \Delta V_m \\ \dots \\ \Delta V_n \\ \Delta \theta_s \\ \Delta V_s \\ \Delta B_{sh} \end{bmatrix} = \begin{bmatrix} \Delta P_2 \\ \dots \\ \Delta P_k \\ \dots \\ \Delta P_m \\ \dots \\ \Delta P_n \\ \Delta Q_2 \\ \dots \\ \Delta Q_k \\ \dots \\ \Delta Q_m \\ \dots \\ \Delta Q_n \\ \Delta Q_{sh} \end{bmatrix} \quad (2.88)$$

The Jacobian matrix relates the change in system voltages and phase angles along with UPFC state variables to the change in real and reactive power injections of the system along with the change in power flows for the lines with UPFC device.

Equation (2.89) represents the compact form of equation (2.88).

$$\begin{bmatrix} \Delta P \\ \Delta Q \\ \Delta P_{km} \\ \Delta Q_{km} \\ \Delta Q_{ksh} \end{bmatrix} = [J^{UPFC}] \begin{bmatrix} \Delta \delta \\ \Delta V \\ \Delta \theta_s \\ \Delta V_s \\ \Delta B_{sh} \end{bmatrix} \quad (2.89)$$

where,

$$\Delta P_{km} = P_{km}^{sch} - P_{km}$$

$$\Delta Q_{km} = Q_{km}^{sch} - Q_{km}$$

$$\Delta Q_{ksh} = Q_{ksh}^{sch} - Q_{ksh}$$

Equations (2.90-2.117) equates the elements of Jacobian matrix.

$$\frac{\partial P_k}{\partial \delta_k} = \sum_{j=1}^n V_k V_j (-G_{kj} \sin \delta_{kj} + B_{kj} \cos \delta_{kj}) - V_k V_s \left[-g_{km} \sin(\delta_k - \theta_s) + \left(b_{km} + \frac{y_{ckm}}{2} \right) \cos(\delta_k - \theta_s) \right] \quad (2.90)$$

$$\frac{\partial P_k}{\partial V_k} = \sum_{j=1}^n V_j (G_{kj} \cos \delta_{kj} + B_{kj} \sin \delta_{kj}) - V_s \left[g_{km} \cos(\delta_k - \theta_s) + \left(b_{km} + \frac{y_{ckm}}{2} \right) \sin(\delta_k - \theta_s) \right] \quad (2.92)$$

$$\frac{\partial P_m}{\partial \delta_m} = \sum_{j=1}^n V_m V_j (-G_{mj} \sin \delta_{mj} + B_{mj} \cos \delta_{mj}) + V_m V_s [-g_{km} \sin(\delta_m - \theta_s) + b_{km} \cos(\delta_m - \theta_s)] \quad (2.91)$$

$$\frac{\partial P_m}{\partial V_m} = \sum_{j=1}^n V_j (G_{mj} \cos \delta_{mj} + B_{mj} \sin \delta_{mj}) + V_s [g_{km} \cos(\delta_m - \theta_s) + b_{km} \sin(\delta_m - \theta_s)] \quad (2.92)$$

$$\frac{\partial Q_k}{\partial \delta_k} = \sum_{j=1}^n V_k V_j (G_{kj} \cos \delta_{kj} + B_{kj} \sin \delta_{kj}) - V_k V_s \left[g_{km} \cos(\delta_k - \theta_s) + \left(b_{km} + \frac{y_{ckm}}{2} \right) \sin(\delta_k - \theta_s) \right] \quad (2.93)$$

$$\frac{\partial Q_k}{\partial V_k} = \sum_{j=1}^n V_j (G_{kj} \sin \delta_{kj} - B_{kj} \cos \delta_{kj}) - V_s \left[g_{km} \sin(\delta_k - \theta_s) - \left(b_{km} + \frac{y_{ckm}}{2} \right) \cos(\delta_k - \theta_s) \right] \quad (2.94)$$

$$\frac{\partial Q_m}{\partial \delta_m} = \sum_{j=1}^n V_m V_j (G_{mj} \sin \delta_{mj} + B_{mj} \cos \delta_{mj}) + V_m V_s [-g_{km} \sin(\delta_m - \theta_s) + b_{km} \cos(\delta_m - \theta_s)] \quad (2.95)$$

$$\frac{\partial P_m}{\partial V_m} = \sum_{j=1}^n V_j (G_{mj} \sin \delta_{mj} - B_{mj} \cos \delta_{mj}) + V_s [g_{km} \cos(\delta_m - \theta_s) + b_{km} \sin(\delta_m - \theta_s)] \quad (2.96)$$

$$\frac{\partial P_k}{\partial \theta_s} = -V_k V_s \left[g_{km} \sin(\delta_k - \theta_s) - \left(b_{km} + \frac{y_{ckm}}{2} \right) \cos(\delta_k - \theta_s) \right] \quad (2.97)$$

$$\frac{\partial P_m}{\partial \theta_s} = V_m V_s [g_{km} \sin(\delta_m - \theta_s) - b_{km} \cos(\delta_m - \theta_s)] \quad (2.98)$$

$$\frac{\partial Q_k}{\partial \theta_s} = -V_k V_s \left[-g_{km} \cos(\delta_k - \theta_s) - \left(b_{km} + \frac{y_{ckm}}{2} \right) \sin(\delta_k - \theta_s) \right] \quad (2.99)$$

$$\frac{\partial Q_m}{\partial \theta_s} = V_m V_s [g_{km} \sin(\delta_m - \theta_s) - b_{km} \cos(\delta_m - \theta_s)] \quad (2.100)$$

$$\frac{\partial P_{km}}{\partial \delta_k} = -V_k V_m (-g_{km} \sin \delta_{km} + b_{km} \cos \delta_{km}) - V_k V_s \left[-g_{km} \sin(\delta_k - \theta_s) + \left(b_{km} + \frac{y_{ckm}}{2} \right) \cos(\delta_k - \theta_s) \right] \quad (2.101)$$

$$\frac{\partial P_{km}}{\partial \delta_m} = -V_k V_m (g_{km} \sin \delta_{km} - b_{km} \cos \delta_{km}) \quad (2.102)$$

$$\frac{\partial P_{km}}{\partial V_k} = 2V_k g_{km} - V_m (g_{km} \cos \delta_{km} + b_{km} \sin \delta_{km}) - V_s \left[g_{km} \cos(\delta_k - \theta_s) + \left(b_{km} + \frac{y_{ckm}}{2} \right) \sin(\delta_k - \theta_s) \right] \quad (2.103)$$

$$\frac{\partial P_{km}}{\partial V_m} = -V_k [g_{km} \cos \delta_{km} + b_{km} \sin \delta_{km}] \quad (2.104)$$

$$\frac{\partial P_{km}}{\partial \theta_s} = -V_k V_s \left[g_{km} \sin(\delta_k - \theta_s) - \left(b_{km} + \frac{y_{ckm}}{2} \right) \cos(\delta_k - \theta_s) \right] \quad (2.105)$$

$$\frac{\partial P_{km}}{\partial V_s} = -V_k \left[g_{km} \cos(\delta_k - \theta_s) + \left(b_{km} + \frac{y_{ckm}}{2} \right) \sin(\delta_k - \theta_s) \right] \quad (2.106)$$

$$\frac{\partial P_k}{\partial V_s} = -V_k \left[g_{km} \cos(\delta_k - \theta_s) + \left(b_{km} + \frac{y_{ckm}}{2} \right) \sin(\delta_k - \theta_s) \right] \quad (2.107)$$

$$\frac{\partial P_m}{\partial V_s} = V_m [g_{km} \cos(\delta_m - \theta_s) + b_{km} \sin(\delta_m - \theta_s)] \quad (2.108)$$

$$\frac{\partial Q_k}{\partial V_s} = -V_k \left[g_{km} \sin(\delta_k - \theta_s) - \left(b_{km} + \frac{y_{ckm}}{2} \right) \cos(\delta_k - \theta_s) \right] \quad (2.109)$$

$$\frac{\partial Q_m}{\partial V_s} = V_m [g_{km} \cos(\delta_m - \theta_s) + b_{km} \sin(\delta_m - \theta_s)] \quad (2.110)$$

$$\frac{\partial Q_{km}}{\partial \delta_k} = V_k V_m (g_{km} \cos \delta_{km} + b_{km} \sin \delta_{km}) - V_k V_s \left[g_{km} \cos(\delta_k - \theta_s) + \left(b_{km} + \frac{y_{ckm}}{2} \right) \sin(\delta_k - \theta_s) \right] \quad (2.111)$$

$$\frac{\partial Q_{km}}{\partial \delta_m} = -V_k V_m (g_{km} \cos \delta_{km} - b_{km} \sin \delta_{km}) \quad (2.112)$$

$$\frac{\partial Q_{km}}{\partial V_k} = -2V_k \left(b_{km} + \frac{y_{ckm}}{2} \right) + V_m (g_{km} \sin \delta_{km} - b_{km} \cos \delta_{km}) - V_s \left[g_{km} \sin(\delta_k - \theta_s) - \left(b_{km} + \frac{y_{ckm}}{2} \right) \cos(\delta_k - \theta_s) \right] \quad (2.113)$$

$$\frac{\partial Q_{km}}{\partial V_m} = V_k (g_{km} \sin \delta_{km} - b_{km} \cos \delta_{km}) - V_s \left[g_{km} \sin(\delta_k - \theta_s) - \left(b_{km} + \frac{y_{ckm}}{2} \right) \cos(\delta_k - \theta_s) \right] \quad (2.114)$$

$$\frac{\partial Q_{km}}{\partial \theta_s} = V_k V_s \left[g_{km} \cos(\delta_k - \theta_s) - \left(b_{km} + \frac{y_{ckm}}{2} \right) \sin(\delta_k - \theta_s) \right] \quad (2.115)$$

$$\frac{\partial Q_{km}}{\partial V_s} = -V_k \left[g_{km} \sin(\delta_k - \theta_s) - \left(b_{km} + \frac{y_{ckm}}{2} \right) \cos(\delta_k - \theta_s) \right] \quad (2.116)$$

$$\frac{\partial Q_{ksh}}{\partial V_k} = 2V_k B_{sh} \quad (2.117)$$

For n-bus power system with n_{PQ} number of load buses, n_{PV} number of generator buses and with l no of lines with UPFC devices, the size of the Jacobian matrix becomes $(n+n_{PQ}-1+3l) \times (n+n_{PQ}-1+3l)$. At each iteration, the power injections at the buses and line power flows are calculated to determine mismatches ($\Delta P, \Delta Q, \Delta P_{km}, \Delta Q_{km}$ and ΔQ_{ksh}). Elements of Jacobian matrix are calculated to determine the corrections values $\Delta \delta, \Delta V, \Delta \theta_s, \Delta V_s$ and ΔB_{ksh} . Equation (2.118) calculates the updated values of UPFC parameters.

$$\left. \begin{aligned} V_i^{K+1} &= V_i^K + \Delta V_i^K \\ \delta_i^{K+1} &= \delta_i^K + \Delta \delta_i^K \\ V_s^{K+1} &= V_s^K + \Delta V_s^K \\ \theta_s^{K+1} &= \theta_s^K + \Delta \theta_s^K \\ B_{ksh}^{K+1} &= B_{ksh}^K + \Delta B_{ksh}^K \end{aligned} \right\} \quad (2.118)$$

Once the elements of the Jacobian matrix are calculated then the corrections values are determined using equation (2.88). Further updated values of $V_i, \delta_i, V_s, B_{sh}$ and θ_s are calculated until the mismatches are less than the specified tolerance value. The limits on the UPFC device are:

$$|V_s| \leq 0.2 \quad (2.119)$$

$$-\pi \leq \theta_s \leq \pi \quad (2.120)$$

2.8 Conclusions

This chapter provides the detailed theoretical background and the computational process of a power flow analysis using the SPFC and UPFC devices. In the modeling of LF analysis, the SPFC device is considered with a controllable voltage magnitude and phase angle ($V_{se} \angle \delta_{se}$) along with its impedance. The advantage of the model is that it represents the SPFC device as an integral part of the transmission line. As a result, the sensitivity relations between power flows through the SPFC device with any power system control variable (i.e., real and reactive power bus injections) would possess the collective or integrated effect of the SPFC device and transmission line state variables. The use of SPFC to reschedule the power flow through transmission lines helps to reduce system loss. Chapter 3 provides the detailed theoretical background and the computational process of this work.

Similarly, detailed modeling of LF analysis using UPFC device considered with a controllable series voltage source ($V_s \angle \theta_s$) and a controllable shunt susceptance (B_{sh}) is provided here. As such the model allows independent control of power flow through the SSSC and SVC of the UPFC device. The advantage of the model is that it represents the UPFC device as an integral part of the transmission line. This allows the derivation of sensitivity relations among line power flow, reactive power injection at one end of the line and system control variables. The use of UPFC device to reschedule the power flow through the transmission line and the reactive power at one end of the transmission line reduces the excessive SPA problem of the PSN. The detailed theoretical background and the computational process of this research work are provided in chapter 4.

3

Application of Series Power Flow Controller in Reduction of Total Real Power Loss

3.1 Introduction

Due to the tremendous growth in power consumption and population, a large amount of power needs to be transmitted over a long distance through the transmission lines, lead to increased power system loss. To meet the increased load demand the existing network has to operate near the limiting value so, the power system becomes less secure. Thus the generation and transmission network has to be expanded to meet the load requirement. When it comes to an interconnected power system network (PSN), the random nature of power demands creates complexity in controlling or operating the power system. Again due to the occurrence of unavoidable disturbances PSN faces outages of the equipment such as generators/ transmission lines lead to bus voltage deviations or overloading of the nearby lines or large phase angle difference across the two buses, etc. Therefore it is important to control the line power flow. The use of FACTS devices helps to control and transfer more power through the transmission lines without changing the power system layout by keeping the line flow within their respective limits. FACTS devices are used in the power system to enhance line power transfer capacity and increase the controllability of the transmission networks. Controlling power flow

with FACTS devices reduces line overload, reduces system loss, maintains bus voltage profile, and improves overall power system performances. Also, placements of FACTS devices in suitable locations play a significant role in the improvement of power system conditions. Thus in this work, to identify the transmission lines suitable for placements of SPFC devices, a sensitivity relation among the power through lines and TRPL is determined. Highly sensitive lines are selected to introduce SPFC devices for rescheduling the power flow through the transmission lines to reduce the TRPL of a PSN. Further cost-benefit analysis (CBA) based on the installation cost (IC) of SPFC devices and saving due to the reduction of TRPL is presented to show the economic benefit of installing SPFC devices in the selected lines of a PSN.

3.2. Identification of sensitive lines to introduce SPFC devices

To identify the suitable location of SPFC devices a LF analysis is performed for the baseload condition of the system, and utilizing LF results, power loss sensitivity factor (PLSF) values are calculated. Then highly sensitive lines are identified to introduce the SPFC devices for the reduction of TRPL. PLSF is the SF that relates the change in TRPL due to the change in power flow (CPF) through the transmission lines, can be calculated as follows:

Equation (3.1) calculates the TRPL for a power system containing ‘n’ number of buses.

$$P_L = \sum_{i=1}^n P_i \quad (3.1)$$

Therefore, using (3.1) and (2.5) the TRPL can be represented as:

$$P_L = \sum_{i=1}^n \sum_{j=1}^n V_i V_j (G_{ij} \cos \delta_{ij} + B_{ij} \sin \delta_{ij}) \quad (3.2)$$

Considering bus number 1 as the slack bus of the PSN, the change in TRPL in terms of the Jacobian (J) matrix and changes in real and reactive power injection (RRPI) can be expressed as:

$$\Delta P_L = [SFPL] [\Delta P_2 \quad \dots \quad \Delta P_n \quad \Delta Q_2 \quad \dots \quad \Delta Q_n]^T \quad (3.3)$$

where,

$$\left[\frac{\partial P_L}{\partial \delta_2} \quad \dots \quad \frac{\partial P_L}{\partial \delta_n} \quad \frac{\partial P_L}{\partial V_2} \quad \dots \quad \frac{\partial P_L}{\partial V_n} \right] [J]^{-1} = [SFPL]$$

Again, ΔP_{km} in terms of [J], ΔP_i and ΔQ_i for the line km can be expressed as:

$$\Delta P_{km} = [SLF_P] [\Delta P_2 \quad \dots \quad \Delta P_n \quad \Delta Q_2 \quad \dots \quad \Delta Q_n]^T \quad (3.4)$$

where,

$$\left[\frac{\partial P_{km}}{\partial \delta_2} \quad \dots \quad \frac{\partial P_{km}}{\partial \delta_n} \quad \frac{\partial P_{km}}{\partial V_2} \quad \dots \quad \frac{\partial P_{km}}{\partial V_n} \right] [J]^{-1} = [SLF_P]$$

Multiply both sides of (3.4) by $[SLF_P]^T$

$$[SLF_P]^T \Delta P_{km} = [SLF_P] [SLF_P]^T [\Delta P_2 \quad \dots \quad \Delta P_n \quad \Delta Q_2 \quad \dots \quad \Delta Q_n]^T \quad (3.5)$$

Divide (3.3) by (3.5),

$$\begin{aligned} \frac{\Delta P_L}{[SLF_P]^T \Delta P_{km}} &= \frac{[SFPL]}{[SLF_P] [SLF_P]^T} \\ \Rightarrow \frac{\Delta P_L}{\Delta P_{km}} &= \frac{[SFPL] [SLF_P]^T}{[SLF_P] [SLF_P]^T} \end{aligned} \quad (3.6)$$

Using (3.6), SF_{Pkm} can be represented as:

$$SF_{Pkm} = \frac{\partial P_L}{\partial P_{km}} = \frac{[SFPL] [SLF_P]^T}{[SLF_P] [SLF_P]^T} \quad (3.7)$$

Similarly, ΔQ_{km} in terms of [J] and RRPI can be represented as:

$$\Delta Q_{km} = [SLF_Q] [\Delta P_2 \quad \dots \quad \Delta P_n \quad \Delta Q_2 \quad \dots \quad \Delta Q_n]^T \quad (3.8)$$

where,

$$\left[\frac{\partial Q_{km}}{\partial \delta_2} \quad \dots \quad \frac{\partial Q_{km}}{\partial \delta_n} \quad \frac{\partial Q_{km}}{\partial V_2} \quad \dots \quad \frac{\partial Q_{km}}{\partial V_n} \right] [J]^{-1} = [SLF_Q]$$

Multiply both sides of (3.8) by $[SLF_Q]^T$

$$[SLF_Q]^T \Delta Q_{km} = [SLF_Q] [SLF_Q]^T [\Delta P_2 \quad \dots \quad \Delta P_n \quad \Delta Q_2 \quad \dots \quad \Delta Q_n]^T \quad (3.9)$$

Divide (3.3) by (3.9)

$$\begin{aligned} \frac{\Delta P_L}{[SLF_Q]^T \Delta Q_{km}} &= \frac{[SFPL]}{[SLF_Q] [SLF_Q]^T} \\ \Rightarrow \frac{\Delta P_L}{\Delta Q_{km}} &= \frac{[SFPL] [SLF_Q]^T}{[SLF_Q] [SLF_Q]^T} \end{aligned} \quad (3.10)$$

Therefore, SF_{Qkm} can be represented as:

$$SF_{Qkm} = \frac{\partial P_L}{\partial Q_{km}} = \frac{[SFPL] [SLF_Q]^T}{[SLF_Q] [SLF_Q]^T} \quad (3.11)$$

Using (3.7) and (3.11), the PLSF value for the line km is calculated as:

$$PLSF_{km} = \sqrt{SF_{Pkm}^2 + SF_{Qkm}^2} \quad (3.12)$$

Equation (3.12) calculates the PLSF values for all lines of a PSN. PLSF values are ranked to select the lines for the introduction of the SPFC device to reduce TRPL. The lines possessing a significant value of PLSF in the PLSF rank list are chosen to introduce the SPFC device. Sensitivity factors (SF) and their relation to the change in TRPL are used to represent an objective function for applying particle swarm optimization (PSO) technique to estimate the necessary optimal values CPF in the lines considered for the introduction of SPFC devices. Incorporating the optimal values of CPF through the transmission lines obtained using PSO, LF analysis with SPFC is performed to estimate the state variables (v_s) and (δ_s) of the SPFC device and determine TRPL.

3.3 Problem formulation of reduction of TRPL using SPFC device

The objective of the proposed work is to reduce the TRPL of a PSN by rescheduling the line flow of the selected transmission lines using SPFC devices also analyze the IC of the SPFC device, and saving due to reduction of TRPL. The selection of transmission lines to introduce SPFC devices has been made based on the rank of PLSF. To reduce the TRPL it is necessary to maximize the difference between TRPL obtained before and after the introduction of the SPFC devices in selected transmission lines. Therefore, the objective function for maximization in terms of the difference between TRPL obtained before and after the introduction of SPFC devices with power system operating constraints is:

$$\int_{MAX} P_L = P_L^{BCLF} - P_L^{SPFC} \quad (3.13)$$

where,

P_L^{BCLF} is the TRPL obtained from base case load flow (BCLF) analysis without SPFC device.

P_L^{SPFC} is the TRPL obtained using LF analysis with SPFC devices in the selected sensitive lines.

The operating constraints of the network are:

a) Equality constraints:

- Power balance equations are:

$$\left. \begin{aligned} P_i - \left[\sum_{j=1}^n |V_i| |V_j| (G_{ij} \cos(\delta_{ij}) + B_{ij} \sin(\delta_{ij})) \right] &= 0 \\ Q_i - \left[\sum_{j=1}^n |V_i| |V_j| (G_{ij} \sin(\delta_{ij}) - B_{ij} \cos(\delta_{ij})) \right] &= 0 \end{aligned} \right\} \quad (3.14)$$

b) Inequality constraints:

- Constraints on PSN are:

$$\left. \begin{aligned} P_i^{\min} &\leq P_i \leq P_i^{\max} \\ V_i^{\min} &\leq V_i \leq V_i^{\max} \\ \delta_i^{\min} &\leq \delta_i \leq \delta_i^{\max} \end{aligned} \right\} \quad (3.15)$$

- Constraints on SPFC device are:

$$\left. \begin{aligned} |V_{se}| &\leq V_{se}^{\max} \\ \delta_{se}^{\min} &\leq \delta_{se} \leq \delta_{se}^{\max} \end{aligned} \right\} \quad (3.16)$$

3.4 Particle Swarm Optimization (PSO) Technique

PSO is a swarm-based search technique where the potential individuals or particles fly through the search space and follow the current optimum particles. Potential particles make the decision based on their own and other particles' experiences. The particles change or update the velocity and positions after each generation based on previous best positions of their own and neighbors'. If the velocity and position of i^{th} particle in j - dimensional search space is $V_{ij} = [V_{i1}, V_{i2}, \dots, V_{ij}]$, and $P_{ij} = [P_{i1}, P_{i2}, \dots, P_{ij}]$ respectively; where, $i=1, 2, \dots, Np$, and Np is the population size. Then, the particle changes their velocity and position in j - dimensional search space are determined using equations (3.17) and (3.18) [21].

$$V_{ij}^{itr+1} = I_w \times V_{ij}^{itr} + W_1 \times R_1 \times (P_{best_{ij}} - P_{ij}^{itr}) + W_2 \times R_2 \times (G_{best_{ij}} - P_{ij}^{itr}) \quad (3.17)$$

$$P_{ij}^{(itr+1)} = P_{ij}^{(itr)} + V_{ij}^{(itr)} \quad (3.18)$$

where,

I_w = Inertia weight.

W_1 = weighting factor (constant) related to P_{best} .

W_2 = weighting factor (constant) related to G_{best} .

R_1 and R_2 is the random numbers varies from 0 to 1.

$P_{best_{ij}}$ and $G_{best_{ij}}$ is the personal best and global best of the particle i .

Proper selection of ' I_w ' provides the balance between local and global search which results in less iteration required to get an optimal solution. Thus, a higher initial value of I_w and lower final values of I_w is selected to apply the PSO technique. It provides the particle with higher global search ability at the beginning and higher local search ability at the end of the run result in faster convergence.

$$I_w = I_{w_{\max}} - \frac{I_{w_{\max}} - I_{w_{\min}}}{itr_{\max}} \times itr \quad (3.19)$$

where,

$I_{w_{\max}}$ = initial weight (random numbers).

$I_{w_{\min}}$ = final weight (random numbers).

itr = iteration count.

3.4.1 Implementation of PSO technique for minimization of TRPL

The objective function for implementation of PSO for reduction TRPL is:

$$J_{PSO} = \xi P_L^{BCLF} + \Delta P_L \quad (3.20)$$

ξ is the factor, represents the targeted percentage of loss to be reduced with respect to the TRPL determined from the BCLF results. ΔP_L is the change in system loss due to the change in power flow through the selected lines containing SPFC devices. The value of ΔP_L has to be negative to reduce the TRPL of the power system. Therefore, ΔP_L is considered as a positive term in the objective function configured for PSO.

Using the calculus of variation, ΔP_L due to CPF through the line km can be represented as:

$$\Delta P_L = \left[\frac{\partial P_L}{\partial P_{km}} \Delta P_{km} + \frac{\partial P_L}{\partial Q_{km}} \Delta Q_{km} \right] \quad (3.21)$$

Now, using SFs due to the change in real and reactive power flow (RRPF) represented in equations (3.7) and (3.11) ΔP_L can be calculated as:

$$\Delta P_L = SF_{P_{km}} \Delta P_{km} + SF_{Q_{km}} \Delta Q_{km} \quad (3.22)$$

Therefore, for M number of lines, equation (3.22) can be expressed as:

$$\Delta P_L = \sum_{l=1}^M SF_{P_l} \Delta P_l + SF_{Q_l} \Delta Q_l \quad (3.23)$$

where, ' l ' represent the line number, connected between two buses.

The limits of the change in RRPf for the lines are selected and using the PSO optimal values of ΔP_l and ΔQ_l of the selected lines is obtained. Thus, the schedule values of RRPf of the line are calculated as:

$$\left. \begin{aligned} P_l^{sch} &= P_l + \Delta P_l \\ Q_l^{sch} &= Q_l + \Delta Q_l \end{aligned} \right\} \quad (3.24)$$

• Algorithms for the implementation of PSO technique for the minimization of objective function are as follows:

1. Initially LF analysis is performed for the baseload condition is to obtain P_L^{BCLF} without the SPFC device.
2. Calculate $\xi = \frac{\xi^{\max} + \xi^{\min}}{2}$.
3. Initialize PSO parameters such as population size, inertia weight (I_w) and weighting factors (W_1, W_2), etc.
4. Set the upper and lower limits for the control variables i.e., change in RRPf (ΔP_{kn} and ΔQ_{kn}) for the selected lines.
5. Set iteration count (itr) and the tolerance value.
6. Generate the initial parameters of (ΔP_{kn} and ΔQ_{kn}) randomly.
7. Calculate the objective function using equation (3.20).
8. Select $Gbest_{ij}$ and position $Pbest_{ij}$ corresponding to minimum objective function.
9. Update velocity (V_{ij}) and position (P_{ij}) using equations (3.17) and (3.18).
10. If the tolerance value is less than the specified tolerance value then stop and show results.
11. Otherwise update iteration and go to step (6), and repeat till the maximum iteration count is reached.

3.5 Selection of transmission lines for the reduction of TRPL of a power system and implementation of the LF analysis with SPFC devices in the selected lines

Initially, LF analysis without the SPFC device is performed on IEEE 118 bus system to determine the initial operating condition of the system. Using those LF results, SF relation for change in TRPL (ΔP_L) with the changes in RRPf (ΔP_l) and (ΔQ_l) are determined using equations (3.7) and (3.11). Equation (3.12) calculates the PLSF value of the transmission lines using the value of SF_{P_l} and SF_{Q_l} . To identify/select transmission lines to introduce the SPFC devices to reduce the TRPL PLSF values are utilized. The necessary change in RRPf through the selected transmission lines is determined using the PSO optimization technique based on the objective function given in equation (3.20). The required change in RRPf obtained with the PSO technique are used to reschedule the power flow through the selected lines. Then the LF analysis model containing the SPFC device described in chapter 2 is used to validate the operating state of the power system.

3.6 Solution procedure for reduction of TRPL

The solution process starts with a BCLF analysis of a power system to determine its initial operating condition and TRPL of the system. Using the BCLF results, PLSFs for the lines are calculated and ranked according to the degree of their sensitivity values to select the lines. To introduce the SPFC device for reducing the TRPL, the lines that possess significant values of PLSF in the PLSF rank list are selected. It is necessary to adjust the value of ξ given in the objective function of PSO to determine the changes in RRPf (ΔP_l and ΔQ_l) through the lines with the SPFC device. The reduction of TRPL is possible to a certain percentage of P_L^{BCLF} . Therefore, an iterative search technique has to be adopted with assigned limits of ξ . To assign the value of ξ in the objective function of PSO using the upper limit (ξ^{\max}) and lower limit (ξ^{\min}) of ξ the bisection method is applied. With the assigned value of ξ , the optimal values of ΔP_l and ΔQ_l through the lines with the SPFC device are determined using the PSO technique. The modified values of scheduled power flow are determined using equation (3.24).

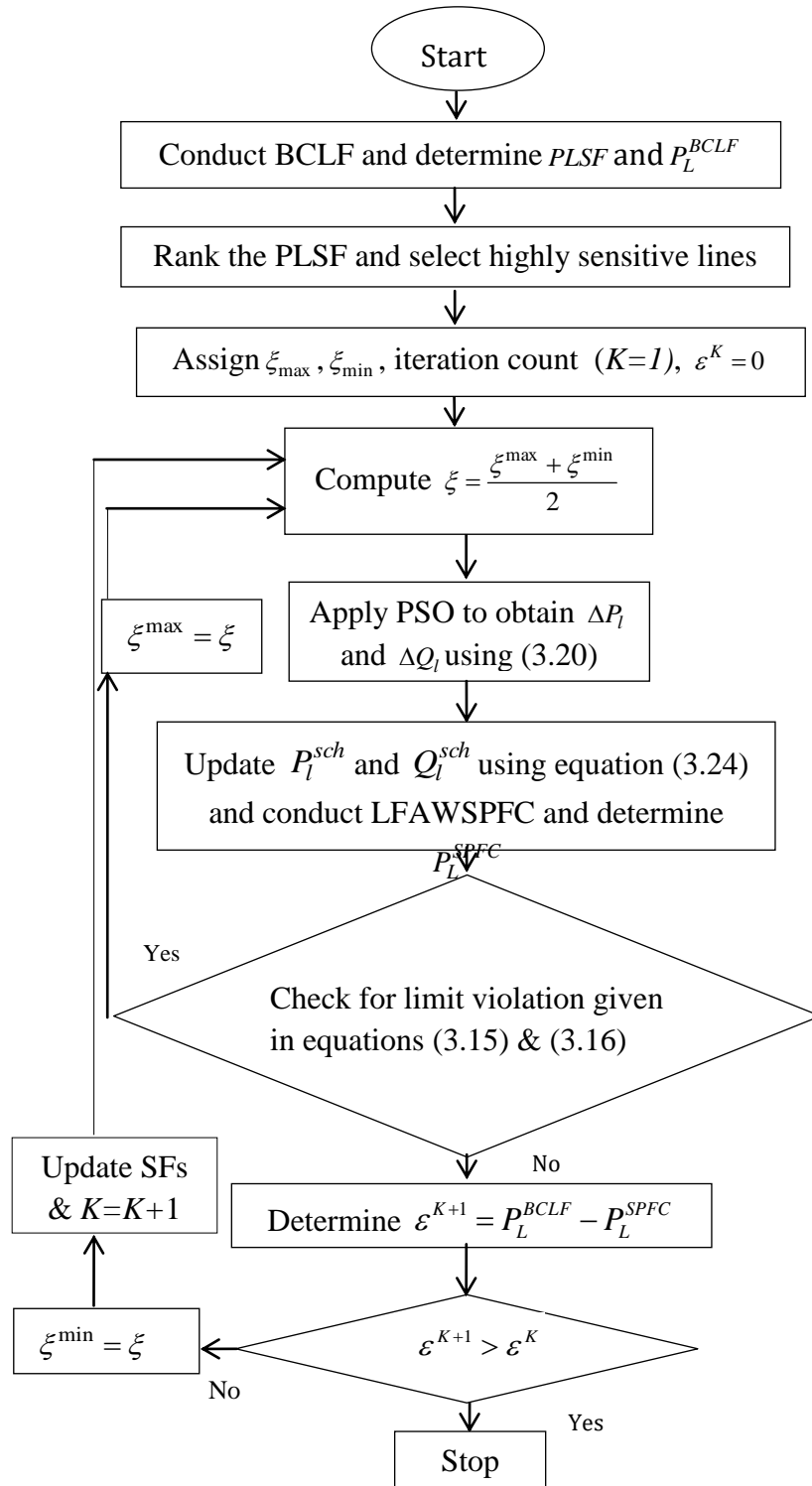


Fig. 3.1 Flowchart for rescheduling of power flow using SPFC device.

At this point, a LF analysis with the SPFC device is performed to validate the proposed method. Therefore, to examine the possible operating limit violation of SPFC parameters and other power system operating constraints LF analysis with SPFC (LFAWSPFC) is carried out.

In case any violation is detected, and then ξ^{\max} is set to the value of ξ assigned in the objective function of PSO, i.e., with the current assigned value of ξ and the reduction of TRPL is not possible due to limit violations of power system operating constraints. If no limit violation is detected, then ξ^{\min} is set with the assigned value of ξ in the objective function of PSO, i.e., with the current value of ξ , reduction of TRPL is achieved, and a further reduction in TRPL is possible. It is worth mentioning that the CPF through lines with the SPFC device would affect the power balance of the system, and to maintain the power balance, the power flow through other transmission lines would change. The CPF through other transmission lines which are less sensitive to the CPF would also influence the TRPL of the system. At one point of time, TRPL may increase for further modification of scheduled power flow through the line with SPFC. This condition is checked during the iterative process. The term $\varepsilon^{K+1} = P_L^{BCLF} - P_L^{SPFC}$ is introduced in the flow chart, where ε^{K+1} represents the reduction in TRPL achieved at $(K+1)^{\text{th}}$ iteration. The iterative process has to be carried out till $\varepsilon^{K+1} > \varepsilon^K$, where, ε^K represents the reduction in TRPL achieved at K^{th} iteration. The logic used for the termination of the iterative process confirms the satisfaction of the objective function shown in equation (3.13). Figure 3.1 shows the flow chart of the solution procedure adopted to reduce the TRPL.

3.7 Identification of sensitive lines and reduction of TRPL using SPFC devices

PLSF values obtained using initial LF results without the SPFC devices are utilized to identify the transmission lines suitable for the inclusion of SPFC devices. PLSF relates the change in TRPL (ΔP_L) with the changes in RRPf through the transmission line of a power system. It is worth mentioning here that the significantly sensitive transmission line(s) with higher values of PLSF are to be selected for the introduction of SPFC devices while reducing the TRPL of a power system. The maximum value of PLSF is used to determine the threshold value of PLSF, and the transmission lines possessing PLSF values above the threshold value of PLSF are considered for the introduction of SPFC devices. Equation (3.25) evaluates the threshold value of PLSF.

$$PLSF^{THOLD} = \eta PLSF^{\max} \quad (3.25)$$

The value of η has to be decided in such a way that only the significantly sensitive transmission lines participate in the process of reduction of TRPL using SPFC devices.

3.7.1 Simulation results of the proposed method

To examine the validity and applicability of the proposed approach to reduce the TRPL of a power system using the SPFC devices IEEE 118 bus system is considered. At first, LF analysis at the baseload of the IEEE 118 bus system is carried out without the SPFC device. Figure 3.2 shows the PLSF values obtained for transmission lines using the initial LF results for IEEE 118 bus system. To reduce the TRPL of a power system it is necessary to install optimum numbers of SPFC devices at the potential locations of the IEEE 118 bus system because an insignificant PLSF value would change the TRPL negligibly due to the change in RPPF in the lines. To select the line(s) for the SPFC devices only significant sensitive lines are to be considered. The maximum PLSF ($PLSF^{\max}$) value is used as a reference to select the other lines to participate in the process of reduction of TRPL using the SPFC device. The lines having $PLSF^{THOLD} \geq \eta PLSF^{\max}$, considered for the reduction of system loss, where η is the percentage value to be selected to ensure the participation of highly sensitive lines in the process of TRPL reduction using SPFC devices. It is advisable to select the value of η in such a way that only the sensitive lines have to participate in the process. Therefore, the lines having the PLSF value more than 30% of the maximum value of the PLSF are considered to participate in the process of reduction of TRPL using SPFC devices. From Figure 3.2 it is seen that the line no 111, 41, 112 have significantly large values of PLSF than the other lines of the system. Therefore, these lines are considered for the introduction of the SPFC device. As line no 111 is connected between slack bus and PV bus and line no 41 connected between two PV buses so, it is not possible to change the power flow through these lines as they are radially connected without any parallel path to accommodate the CPF in the lines. Therefore, these lines will not participate in the process of reduction of TRPL using SPFC devices. Line no 112 is considered for rescheduling the power flow with the SPFC device to reduce the TRPL of the system. It is found that a significant reduction of TRPL was possible by rescheduling the power flow through line 112 but, for the demonstration purpose, multiple numbers of SPFC devices at line numbers 112 and 116 and 120 are considered here for rescheduling the power flow to reduce TRPL of the system. As line 39 is connected between two PV buses thus, it will

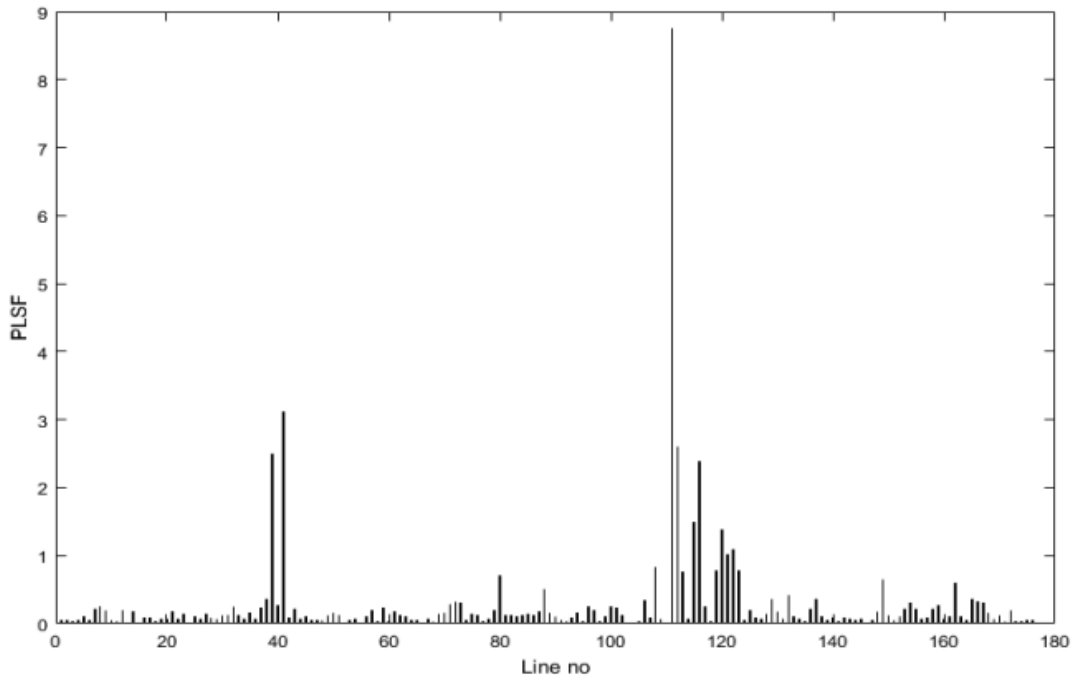


Fig. 3.2 PLSF for IEEE 118 bus system.

not participate in the reduction of TRPL. Table 3.1 shows the SP_{km} and SQ_{km} values of the selected lines to introduce SPFC devices. Figure 3.3 shows the SP_{km} and SQ_{km} for the line no 112, 116 and 120, and it is observed that the line 112 and 116 have a positive value of SF and 120 has negative SF. As the change in RRPf through the transmission lines has been related to the change in TRPL of the power system thus the changes in RRPf in lines are considered as control variables for applying the PSO technique. The objective function of PSO has to minimize the difference between zP_L^{BCLF} and ΔP_L due to the changes in P_l and Q_l (for $l= 1.. M$). The ΔP_L is estimated using equation (3.23) for the selected three lines with SPFC devices.

Table 3.1 SFs of the selected lines for the introduction of SPFC devices obtained using BCLF results

Line No(l)	Line connected between		Sensitivity Factor	
	Bus- k	Bus- m	$SF_{P_{km}}$	$SF_{Q_{km}}$
112	69	75	0.2917	2.5859
116	70	75	0.3138	2.3577
120	75	77	-0.1036	-1.3723

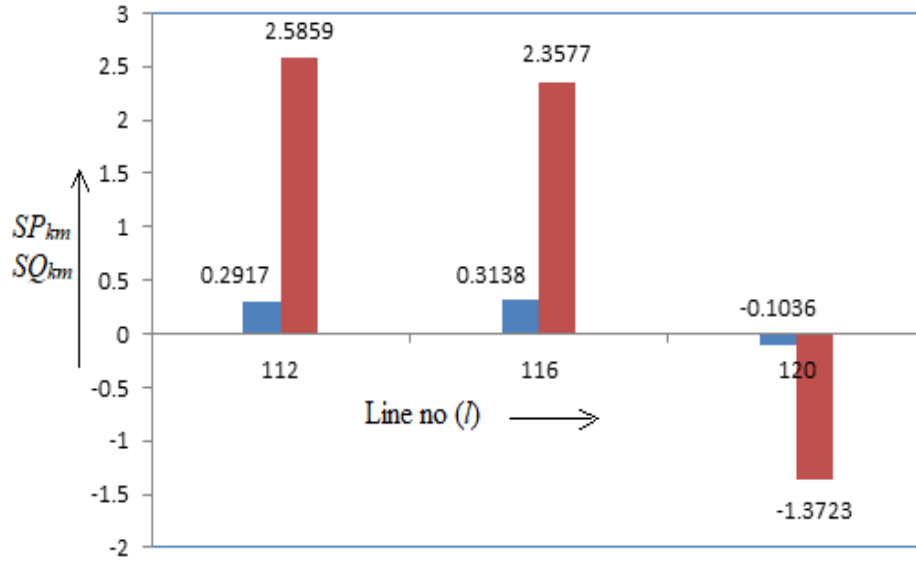


Fig. 3.3 Sensitivity factors of the selected lines.

While finding optimal values of ΔP_l and ΔQ_l for the selected lines using PSO, the CPF limits are taken as -0.2 p.u. to +0.2 p.u. The limits are restricted to narrow values so that the estimated values of ΔP_l and ΔQ_l remain relatively low during the iteration process of the bisection method. It helps to avoid large changes in ΔP_l and ΔQ_l in a single step of the bisection method as the insignificantly low value of SFs for the line would lead to estimation of large value of ΔP_l and ΔQ_l . Due to the large values of ΔP_l and ΔQ_l , changes in scheduled RRPf through the line with SPFC will be more. Thus, LF analysis with SPFC may not converge or may violate the operating limits of the SPFC parameters. For each iteration step of the bisection method, ΔP_l and ΔQ_l (for $l=1, \dots, M$) is determined using PSO to calculate the modified scheduled power through the line with the SPFC device using (3.24). LFAWSPFC is carried out with the modified schedule power flow by SPFC at lines 112, 116, and 120. For the bisection method, limits for ξ are assigned as $\xi^{\max} = 0.2$ (i.e., 20%) and $\xi^{\min} = 0.0$. The maximum reduction of TRPL is targeted as the 20% of P_L^{BCLF} . Table (3.2-3.4) represents the final results obtained after the termination of the iterative process. The RRPf obtained for initial LF analysis and LF analysis with SPFC devices are given in Table 3.2. The proposed method can control both RRPf through the lines results in the reduction of TRPL presented in Table 3.2. Table 3.2 represents the voltage magnitudes and phase angles of the three SPFC devices connected at the transmission lines 112, 116, and 120. The results show that all the

SPFC parameters are within their respective limits. Again it has been observed that the introduction of SPFC in the three lines of the system can improve the bus voltage profile of the IEEE 118 bus system. Table 3.3 shows the improvement of bus voltages of the test system using SPFC at the selected transmission lines. Table 3.4 shows the TRPL obtained with and without SPFC devices. Thus, the proposed method of LF analysis with SPFC devices can reduce the TRPL to 2.5151 p.u. from 3.0851 p.u. i.e., 0.57 p.u. reduction of TRPL is achieved as shown in Figure 3.4 with the final value of ξ at 0.18475 at the end of the termination of the iterative process. The value of ξ appeared as 0.2 (i.e., 20%, the maximum targeted % reduction of TRPL), the bisection iterative process has to be repeated with a higher value of ξ^{\max} , as there is room for further reduction of TRPL of the system. The values of ξ_{\max} and ξ_{\min} are to be chosen in such a way that it should not overestimate P_i^{sch} and Q_i^{sch} because it may lead to overloading of the lines with SPFC and further causes numerical instability of LF analysis and create convergence problem. Again, an immediate large CPF at lines with SPFC would result in substantial changes in power flow through the transmission lines of the power system to maintain the power balance, which may again increase the TRPL. In this work, the assigned range for targeted percentage loss to be reduced is considered as (0-20) %. It is settled down to 18% corresponding to minimum TRPL.

Table 3.3 Bus voltage and phase angles obtained using LF analysis without and with SPFC device in the selected transmission lines (all parameters are mentioned in p.u. and δ in radian)

Bus No (i)	Bus type	Bus voltage and phase angles			
		Without SPFC device		With SPFC device	
		$ V $	δ	$ V $	δ
69	Slack	1.035	0	1.035	0
75	PQ	0.863	-0.2868	0.9004	-0.3041
70	PV	0.984	-0.2488	0.984	-0.2404
77	PV	1.006	-0.1422	1.006	-0.1317

Table 3.4 TRPL in p.u. obtained for IEEE 118 bus system

TRPL from BCLF	TRPL from LFAWSPFC	Reduction of TRPL
3.0851	2.5151	0.57

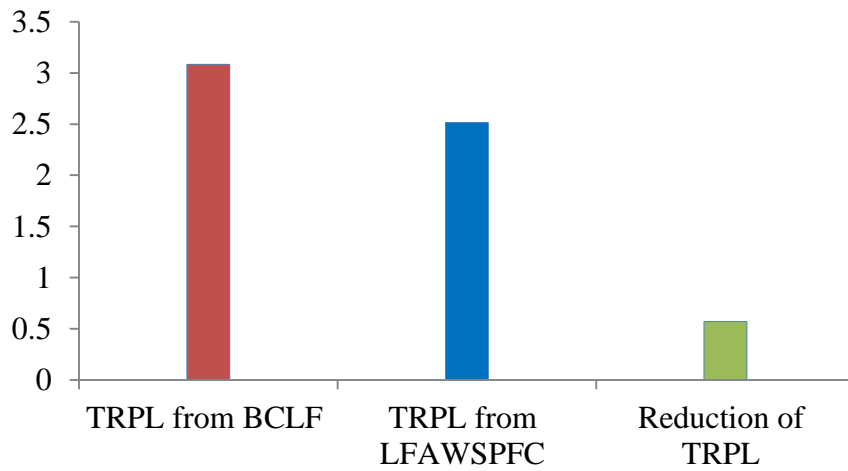


Fig. 3.4 Reduction of TRPF with SPFC devices.

3.7.2 Cost analysis for installation of SPFC devices and cost benefit due to reduction of TRPL

CBA based on the IC of SPFC device and the reduction of system loss is done to show the economic benefit of installing SPFC devices in the selected transmission lines of the standard IEEE 118 bus system. The IC of the SPFC device is quite significant, and it varies according to the installation capacity of the device. Equation (3.25) represents the IC of the SPFC device [32].

$$C = 0.0003R_p^2 - 0.2691R_p + 188.22 \quad (3.25)$$

where,

C is the IC of the SPFC device.

R_p is the range of operation of the SPFC device in MVar [32].

Therefore, the value of R_p would be the difference in MVar flow for a line with and without the SPFC device and can be represented as:

$$R_p = \left\| \left| Q_{km}^{With\ SPFC} \right| - \left| Q_{km}^{Without\ SPFC} \right| \right\| \quad (3.26)$$

Equation (3.25) shows that the IC of a SPFC has a fixed term and two other variable terms dependent on the installation capacity of the device. The overall IC [32] for a SPFC is represented as:

$$IC = C * R_p * 1000 \text{ in } \$ \quad (3.27)$$

Calculation of IC for SPFC devices to reduce TRPL of the test system is shown in Table 3.5. The cost of energy generation in India varies from ₹4/kWhr - ₹5/kWhr throughout the day. Therefore, to compare the IC of SPFC devices and cost of saving due to reduction of TRPL, the cost of energy is considered in US\$. The reduction in TRPL using SPFC devices in the selected sensitive lines of the IEEE 118 bus for the baseload has been found as 0.57 p.u. (=57 MW). However, it would vary according to the loading condition of the system at different hours of the day. As such, average reduction of TRPL for a year can be represented as:

Average reduction of TRPL/ year

$$= MF * \text{Reduction of system loss in MW at the baseload} * 1000 * 8760 \text{ (kWhr)} \quad (3.28)$$

Table 3.5 Calculation of IC of the SPFC devices in three lines
(with base MVA =100)

Line no	R_{pl}	Installation Cost of the SPFC devices ($IC_l = C_l * R_{pl} * 1000$) in \$	Over all installation cost ($IC = IC_{112} + IC_{116} + IC_{120}$) in \$
112	87.11	$167.06 * 87.11 * 1000 = 14,552,597$	
116	91.44	$166.12 * 91.44 * 1000 = 15,190,013$	32,614,569
120	15.6	$184.10 * 15.6 * 1000 = 2,871,960$	

Table 3.6 Comparison of cost for installation of SPFC and saving due to reduction of TRPL

Total IC three SPFC devices (\$)	Cost/unit (\$/kWhr) (Assuming 1 \$ = ₹ 73.35)	MF	Saving due to reduction of TRPL/ year
		0.5	13,481,640
		0.6	16,177,968
		0.7	18,874,296
	4	0.8	21,570,624
		0.9	24,266,952
		1.0	26,963,280
32,614,569		0.5	16,976,880
		0.6	20,372,256
		0.7	23,767,632
	5	0.8	27,163,008
		0.9	30,558,384
		1.0	33,953,760

Therefore, cost of saving due to reduction of TRPL for IEEE 118 bus system can be represented as:

$$\text{Cost of savings} = \text{Average reduction of system loss/ year} * \text{cost/unit (in \$)} \quad (3.29)$$

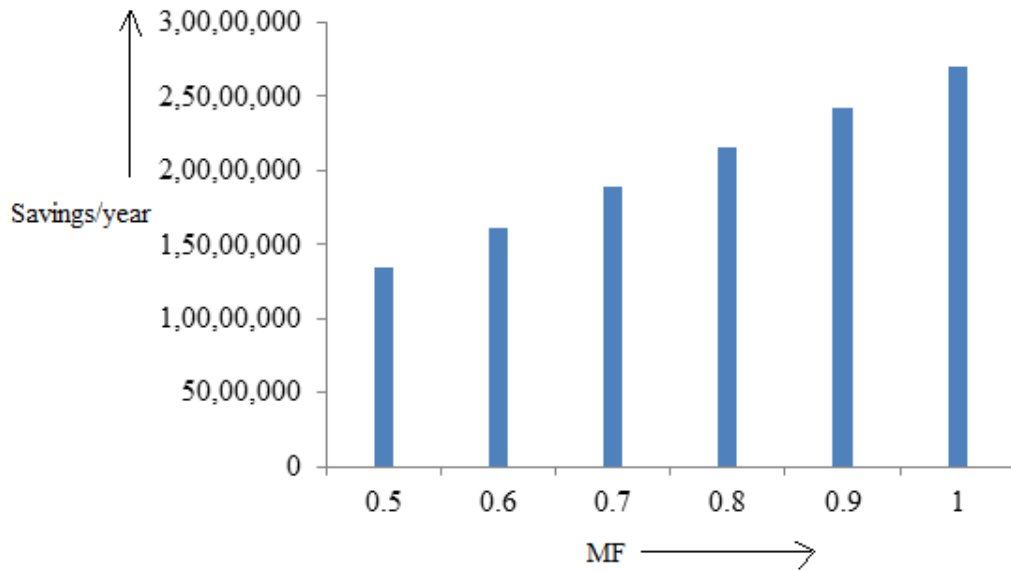


Fig. 3.5 Savings due to reduction of TRPL/ year in (\$) for different MFs for the Cost per unit as 4₹/kWhr.

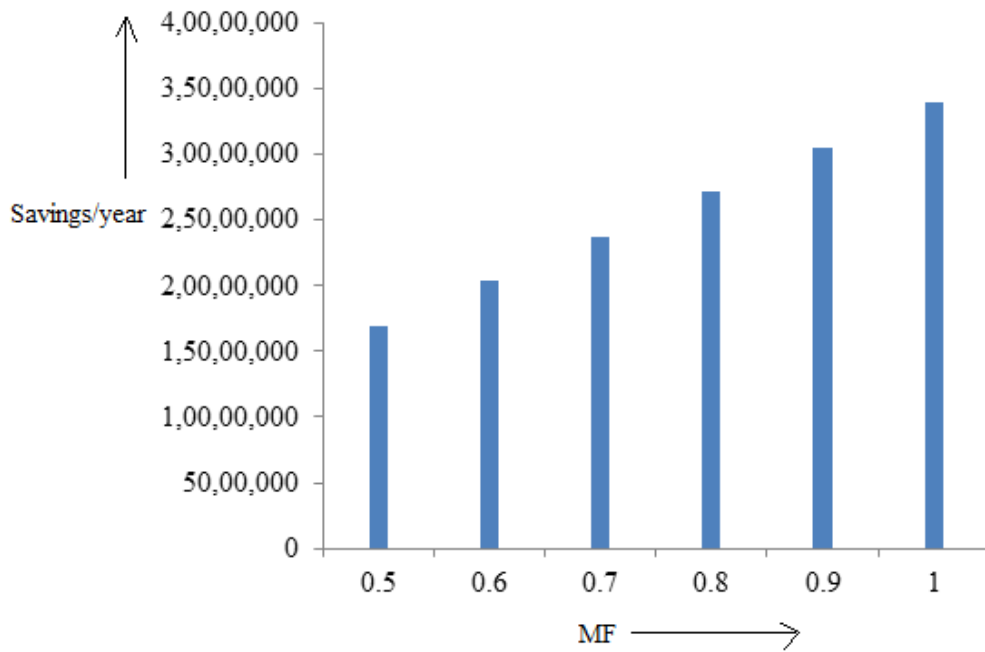


Fig. 3.6 Savings due to reduction of TRPL/ in (\$) for different MFs for the Cost per unit 5₹/kWhr.

Figures 3.5 and 3.6 represent the cost savings due to the reduction of TRPL per year in \$ for different MFs with the cost price of ₹4/kWhr and ₹5 /kWhr respectively. Table 3.6 shows that the cost of savings due to reduction in TRPL with two different costs per unit and MF is significant. It shows with MF=1, and the cost of the power unit as ₹5/kWhr would recover the IC of the three SPFCs within a year. However, the reduction in TRPL would vary according to the load variation through a day therefore; MF may be less or more than one depending upon the loading condition of the power system.

To present a scenario for recovery of the IC of three SPFC devices, MF is taken as 0.7. For this value, the savings per year for the IEEE 118 bus system would be \$18,874,296 or \$23,767,632/ year for the unit cost of ₹4/kWhr or ₹5/kWhr respectively. Even for this scenario, the recovery of the IC of three SPFCs could be attained within 1 and $\frac{3}{4}$ years, 1 and $\frac{5}{12}$ years for two different costs per unit. Beyond this period, they will offer cost benefit due to the reduction of TRPL of the system. In addition to this, the SPFC devices would provide other applications, such as power transfer enhancement, alleviation of line overload in nearby overloaded lines, improvement of bus voltage profile, etc.

3.8 Conclusions

In this research work, a method for the reduction of TRPL by CPF through the lines with SPFC devices is proposed. To identify the suitable location of the SPFC devices a LF analysis is performed for the baseload condition of the system, and utilizing LF results, PLSF values are calculated. Lines with significant values of PLSFs are considered for the introduction of SPFC devices. Power flows through these lines are rescheduled to reduce the TRPL of a power system. Using the PSO technique the optimal changes in RPPF are obtained to reduce the TRPL. To verify the effectiveness of the proposed method LF analysis is performed in standard IEEE 118 bus. It has been observed that the rescheduling of power flow through the sensitive lines using SPFC devices involving the PSO technique could reduce the TRPL of the system from 3.0851 p.u to 2.5151 p.u.

Further, it has been observed from the CBA of the SPFC devices that the IC of the SPFC devices would be recovered within 1 and $\frac{3}{4}$ years, even with MF=0.7 and cost of the unit as

₹4/kWhr. Further, they would also create a facility for other applications such as power transfer enhancement, alleviation of line overload in nearby overloaded lines, improvement of bus voltage profile, etc.

Table 3.2 Power flows in the selected lines before and after the introduction of SPFC device and SPFC parameters (all parameters are mentioned in p.u. and δ_{se} in radian)

Line No	Line connected between buses		Line flow without SPFC device		Schedule line flow with SPFC device		Change in line flow		SPFC Parameters	
	$Bus-k$	$Bus-m$	P_{km}	Q_{km}	P_{km}	Q_{km}	ΔP_{km}	ΔQ_{km}	V_{se}	δ_{se}
112	69	75	2.3912	0.8314	2.0972	1.7025	-0.294	0.8711	0.1569	2.4806
116	70	75	0.4452	0.6786	0.3173	1.593	-0.1279	0.9144	0.1825	2.4267
120	75	77	-0.7317	-0.3891	-0.5324	0.2331	-0.1993	-0.156	0.1226	3.1374

4

Application of Unified Power Flow Controller for Reduction of Standing Phage Angle

4.1 Introduction

The phase angle associated with the bus voltage of an AC Power System Network (PSN) under real and reactive power balanced conditions is referred to as the Standing Phage Angle (SPA) of the bus. The occurrence of unavoidable disturbances in PSN may lead to outages of generators or transmission lines. This creates overloading in the nearby lines, voltage deviations, and changes in bus voltage angles, which may result in a partial or complete blackout of the system. Due to these, it is necessary to restore the power system to a normal condition within the shortest possible time. The restoration process of the power system must be done by taking restoration time as a prime concern but it should include prioritization of repairing, balancing between supply and demand without violating network constraints, and creating fewer transients effects. During the restoration of extra high voltage or high voltage lines of a PSN, the operator may experience the problem of excessive SPA difference between the two buses of a PSN for the line to be re-connected. If a circuit breaker is closed to reconnect a line during a large SPA difference, then it results in a large power flow through the line. Due to this system dynamics change and power oscillation occurs due to the power swing

phenomenon. This may damage the equipment connected to the power system [52] due to significant limits (voltage and current) violation of the equipment and can further lead to the system outage. Thus, it is necessary to reduce the SPA difference between the two buses of the system for the line to be re-connected.

4.2 Reduction of Standing Phase Angle across the two buses using UPFC device

For restoration of transmission lines, SPA across the two buses should be small enough to avoid large power transfer through the lines. The reduction of excessive SPA across the two buses of a PSN by rescheduling the Real and Reactive Power Flow (RRPF) through the line with the UPFC device is reported in this chapter. Reduction of SPA in a power system is an emergency process to re-energize the EHV line having excessive SPA across the two end buses of the line. Therefore, it is economically not advisable or worth installing the UPFC device especially for the reduction of SPA in a power system. However, the UPFC devices readily available in a power system can be used to reduce excessive SPA in a power system. UPFC device is normally used to influence a limited area in the vicinity of a large PSN [51]. A modified UPFC is considered for the modeling of LF analysis which consists of the SSSC and SVC. SSSC is modeled with a controllable series voltage source and SVC is modeled as a controllable shunt susceptance. The UPFC has considered in this research work has only three state variables, as compared to that of traditional UPFC with four state variables, as a result, the size of the Jacobian Matrix [J] for LF analysis with this UPFC model is less compared to a traditional UPFC model. Further, the motive behind this model is to create a facility for independent control of power flow through the transmission line using the SSSC and reactive power control at the bus with the SVC. Again, during LF modeling, this UPFC is considered an integral part of a transmission line, wherever, it is installed. As a result, the sensitivity relations between power flows through the series controller with any power system control variable would possess the collective or integrated effect of UPFC device and transmission line state variables. In the proposed work excessive SPA difference between the two buses is created by disconnecting the lines having power flow greater than 1.8 p.u. For the reduction of SPA across the two buses with the use of UPFC device sensitivity relation between change in SPA across two end buses of a disconnected transmission line and the change in power flow

through the line having UPFC device have been formulated. The sensitivity relations are used to reschedule the power flow through the line having UPFC device to reduce SPA across the line to be re-connected.

4.2.1 Formulation of Sensitivity Relation between change in SPA and the change in RRPF through the Transmission line

To show the effect of change in RRPF through the transmission line on the SPA difference, it is necessary to develop the relationships between change in SPA and the changes in RRPF through the transmission line. The expression for change in SPA for the p^{th} and q^{th} buses of an interconnected PSN is derived using NR LF model with an UPFC device connected between k^{th} and m^{th} buses of the system explained in sections 2.7. Using NR LF with UPFC device at k^{th} bus of the transmission line connected between k^{th} and m^{th} buses of a PSN represented in equation (2.88), the change in phase angle at p^{th} bus can be represented as:

$$\Delta\delta_p = \left[\sum_{i=2}^n f_{pi} \Delta P_i + \sum_{i=n+2}^{2n} f'_{pi} \Delta Q_i \right] + \alpha_p \Delta P_{km} + \beta_p \Delta Q_{km} + \gamma_p \Delta Q_{ksh} \quad (4.1)$$

where, f_{pi} , f'_{pi} , α_p , β_p and γ_p are the p^{th} row elements of the inversion of $[J^{UPFC}]$. These are the SFs which relates ΔP , ΔQ , ΔP_{km} , ΔQ_{km} and ΔQ_{ksh} with the system variables.

Similarly, using NR LF with UPFC device at k^{th} bus of the transmission line connected between k^{th} and m^{th} buses of a PSN represented in (2.88), the change in phase angle at q^{th} bus can be represented as:

$$\Delta\delta_q = \left[\sum_{i=2}^n f_{qi} \Delta P_i + \sum_{i=n+2}^{2n} f'_{qi} \Delta Q_i \right] + \alpha_q \Delta P_{km} + \beta_q \Delta Q_{km} + \gamma_q \Delta Q_{ksh} \quad (4.2)$$

where, f_{qi} , f'_{qi} , α_q , β_q and γ_q are the q^{th} row elements of the inversion of $[J^{UPFC}]$. These are the SFs which relates ΔP , ΔQ , ΔP_{km} , ΔQ_{km} and ΔQ_{ksh} with the system variables.

Using equations (4.1) and (4.2), the expression for change in SPA difference across p^{th} and q^{th} buses is presented as:

$$\Delta\delta_p - \Delta\delta_q = \left[\sum_{i=2}^n (f_{pi} - f_{qi}) \Delta P_i + \sum_{i=n+2}^{2n} (f'_{pi} - f'_{qi}) \Delta Q_i \right] + (\alpha_p - \alpha_q) \Delta P_{km} + (\beta_p - \beta_q) \Delta Q_{km} + (\gamma_p - \gamma_q) \Delta Q_{ksh} \quad (4.3)$$

$$\Delta\delta_{pq} = \left[\sum_{i=2}^n f_{pqi} \Delta P_i + \sum_{i=n+2}^{2n} f'_{pqi} \Delta Q_i \right] + \alpha_{pq} \Delta P_{km} + \beta_{pq} \Delta Q_{km} + \gamma_{pq} \Delta Q_{ksh} \quad (4.4)$$

If SPA value across the two buses of the disconnected line exceeds the prescribed limit (δ_{pq}^{pre}) of the transmission line, to reconnect the disconnected line, it is necessary to reduce the SPA difference less than the δ_{pq}^{pre} value. The desired value of change in SPA across the bus- p and bus- q (δ_{pq}^{des}) in terms of prescribed value of change in SPA across the bus- p and bus- q (positive value, i.e., 20° , 40° and 60° , according to the category of transmission lines) is represented as:

$$\Delta\delta_{pq}^{des} = \begin{cases} \delta_{pq}^{pre} - \delta_{pq} & \text{if } \delta_{pq} > 0 \\ -\delta_{pq}^{pre} - \delta_{pq} & \text{if } \delta_{pq} < 0 \end{cases} \quad (4.5)$$

In this proposed work of reduction of SPA between the two buses of the disconnected line (pq) without changing power injection at the buses is achieved by regulating the power flow through the line km connected between bus- k and bus- m containing UPFC device. Thus, by considering the change in Real and Reactive Power Injection (RRPI) at the other buses of a PSN except the bus where UPFC shunt branch is connected is considered (ΔP_i and ΔQ_i) as zero in equation (2.88), the desired change in SPA across the bus- p and bus- q in terms of the change in RRPF flow through the line km containing a UPFC device is represented as:

$$\Delta\delta_{pq}^{des} = \begin{bmatrix} \alpha_{pq} & \beta_{pq} & \gamma_{pq} \end{bmatrix} \begin{bmatrix} \Delta P_{km} \\ \Delta Q_{km} \\ \Delta Q_{ksh} \end{bmatrix} \quad (4.6)$$

To obtain the required change in RRPF flow through the line km containing UPFC device in terms of desired change in SPA across the disconnected line connected between two bus- p and bus- q , both sides of equation (4.6) is multiplied by $\begin{bmatrix} \alpha_{pq} & \beta_{pq} & \gamma_{pq} \end{bmatrix}^T$.

$$\begin{bmatrix} \Delta P_{km} \\ \Delta Q_{km} \\ \Delta Q_{ksh} \end{bmatrix} = \frac{1}{\alpha_{pq}^2 + \beta_{pq}^2 + \gamma_{pq}^2} \begin{bmatrix} \alpha_{pq} \\ \beta_{pq} \\ \gamma_{pq} \end{bmatrix} \Delta\delta_{pq}^{des} \quad (4.7)$$

Thus, the change in RRPF flow through the line km (ΔP_{km} , ΔQ_{km}) and the change in reactive power through the shunt branch (ΔQ_{ksh}) are represented as:

$$\left. \begin{aligned} \Delta P_{km} &= \frac{\alpha_{pq}}{\alpha_{pq}^2 + \beta_{pq}^2 + \gamma_{pq}^2} \Delta \delta_{pq}^{des} \\ \Delta Q_{km} &= \frac{\beta_{pq}}{\alpha_{pq}^2 + \beta_{pq}^2 + \gamma_{pq}^2} \Delta \delta_{pq}^{des} \\ \Delta Q_{ksh} &= \frac{\gamma_{pq}}{\alpha_{pq}^2 + \beta_{pq}^2 + \gamma_{pq}^2} \Delta \delta_{pq}^{des} \end{aligned} \right\} \quad (4.8)$$

Using the values of change in RRPf flow obtained with equation (4.8) and the pre-modified power flows, the modified scheduled RRPf through the line km and reactive power flow through the shunt branch ($P_{km}^{sch_m}$, $Q_{km}^{sch_m}$ and $Q_{ksh}^{sch_m}$) is calculated as:

$$\left. \begin{aligned} P_{km}^{sch_m} &= P_{km}^{sch_{pm}} + \sigma \Delta P_{km} \\ Q_{km}^{sch_m} &= Q_{km}^{sch_{pm}} + \sigma \Delta Q_{km} \\ Q_{ksh}^{sch_m} &= Q_{ksh}^{sch_{pm}} + \sigma \Delta Q_{ksh} \end{aligned} \right\} \quad (4.9)$$

During simulation of LF analysis with UPFC device it has been found that the voltage magnitude of series controller of an UPFC plays decisive role in the operation related planning of an UPFC device. Therefore, proper selection of the initial value of series parameters (V_s and θ_s) of UPFC device is necessary to ensure the convergence of LF analysis with UPFC device. As the estimated values of UPFC series parameters are dependent on schedule power flows through the line, thus, over estimation of modified scheduled power flow through the series controller of the UPFC device may result in violation of voltage magnitude and phase angle of series controller (V_s and θ_s). Thus, to avoid this limit violation a normalization factor σ is introduced while estimating the modified scheduled power flow through the line with UPFC device using equation (4.9). The factor σ normalizes the effect of over estimation of modified line flows. Because, overestimation of modified schedule power flow may cause numerical instability of LF analysis using UPFC device. Also the estimated values of modified power flows through the line must satisfy the maximum power transfer capacity of the line (S_{km}^{\max}) i.e.,

$$\sqrt{\left[\left(P_{km}^{sch_m} \right)^2 + \left(Q_{km}^{sch_m} \right)^2 \right]} \leq S_{km}^{\max} \quad (4.10)$$

$$Q_{ksh}^{sch_m} \leq S_{ksh}^{\max} \quad (4.11)$$

While reducing the SPA of the disconnected line connected between bus- p and bus- q , SFs of the line containing UPFC device must be enough sensitive that it should be able to keep the line flows within their respective limits given in equations (4.10-4.11). During reduction of

excessive SPA by rescheduling of RRPf through the line with UPFC device if the line flow limit violation occurs then reduction of SPA difference between the buses of the disconnected line is not possible by rescheduling the power flow through the line containing UPFC device. Along with the line flow limit the UPFC parameters have to be within their respective limits given in (2.119) and (2.120).

4.3 Algorithm for the method of reduction of excessive SPA across the two buses

LF Jacobian matrix provides linear relationship among change in bus voltage magnitude and phase angle to the change in CPI. As SFs (α_{pq} , β_{pq} and γ_{pq}) are determined using LF Jacobian matrix given in equation (2.88) thus, it also provides linear relationships between the change in RRPf flow (ΔP_{km} , ΔQ_{km} and ΔQ_{ksh}) of the line containing UPFC device and the change in SPA ($\Delta \delta_{pq}$). Modified schedule power flow ($P_{km}^{sch_m}$, $Q_{km}^{sch_m}$ and $Q_{ksh}^{sch_m}$) determined using equation (4.9) may not guarantee the exact value of change in SPA ($\Delta \delta_{pq}^{des}$). So an iterative technique which involves LF analysis using UPFC device is used to verify the SPA (δ_{pq}) by rescheduling the power flows through the line containing UPFC device. With the LF analysis using UPFC device, if the desired value of SPA is not achieved then $\Delta \delta_{pq}^{des}$ is calculated using equation (4.5). The modified scheduled power flow are determined at current operating condition and the iterative procedure is to be repeated until the value of $|\Delta \delta_{pq}^{des}|$ is less than $\varepsilon = 0.001$. Rescheduling of power flow through the line will change the line loading thus; the iterative procedure has to be terminated if either of the two conditions is reached:

- (i) line flow limit violate and
- (ii) operating limits of UPFC parameters violate.

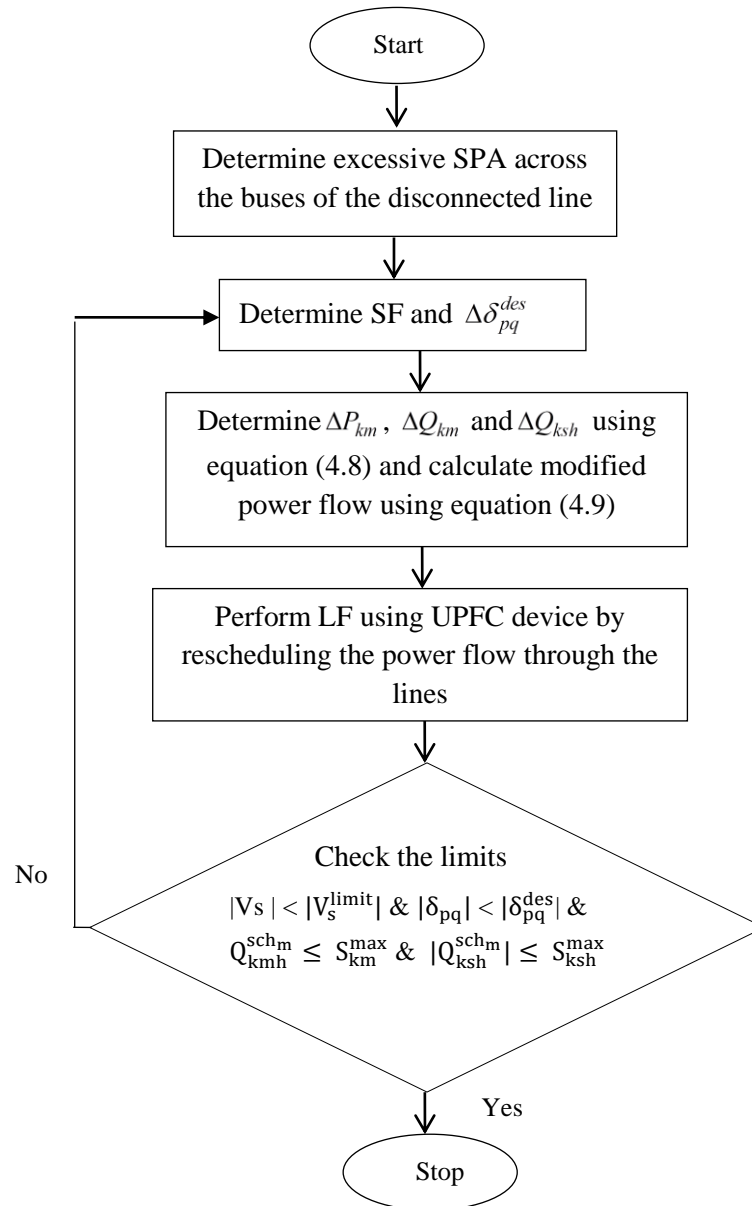


Fig. 4.1 Reduction of SPA across two buses of a disconnected transmission line using UPFC device.

To restore the disconnected line pq , the reduction of SPA is done by rescheduling the power flow through the line with UPFC device and the detail procedure is depicted with the help of flowchart given in Figure 4.1.

4.4 Simulations and results

In the proposed work of reduction of excessive SPA across the two buses of the disconnected transmission line, UPFC device is used to reschedule the RRPF. To examine the effectiveness of the proposed method, the analysis is performed on standard IEEE 118 bus. Initially a LF analysis with baseload is performed to obtain the initial operating conditions and power flows through the transmission lines of 118 bus system. As the convergence of LF analysis using UPFC device depends on the selection of initial values of UPFC parameters i.e., V_s and θ_s . Therefore, proper selection of the initial value of V_s and θ_s are necessary. For this purpose, the calculation of initial value of V_s and θ_s are done based on the scheduled values of RRPF through the line with UPFC device is shown below:

$$P_{km}^{sch} - V_k^2 g_{km} + V_k V_m (g_{km} \cos(\delta_{km}) + b_{km} \sin(\delta_{km})) = -V_k V_s \left((g_{km} \cos(\delta_k - \theta_s) + \left(b_{km} + \frac{y_{ckm}}{2}\right) \sin(\delta_k - \theta_s)) \right) \quad (4.14)$$

$$Q_{km}^{sch} + V_k^2 \left(b_{km} + \frac{y_{ckm}}{2}\right) + V_k V_m (g_{km} \sin(\delta_{km}) - b_{km} \cos(\delta_{km})) = -V_k V_s \left(g_{km} \sin(\delta_k - \theta_s) - \left(b_{km} + \frac{y_{ckm}}{2}\right) \cos(\delta_k - \theta_s) \right) \quad (4.15)$$

Let,

$$A = -V_k V_s \left((g_{km} \cos(\delta_k - \theta_s) + \left(b_{km} + \frac{y_{ckm}}{2}\right) \sin(\delta_k - \theta_s)) \right) \quad (4.16)$$

$$B = -V_k V_s \left(g_{km} \sin(\delta_k - \theta_s) - \left(b_{km} + \frac{y_{ckm}}{2}\right) \cos(\delta_k - \theta_s) \right) \quad (4.17)$$

Divide equation (4.16) by (4.17)

$$\begin{aligned} \frac{A}{B} &= \frac{\left((g_{km} \cos(\delta_k - \theta_s) + \left(b_{km} + \frac{y_{ckm}}{2}\right) \sin(\delta_k - \theta_s)) \right)}{\left(g_{km} \sin(\delta_k - \theta_s) - \left(b_{km} + \frac{y_{ckm}}{2}\right) \cos(\delta_k - \theta_s) \right)} \\ \Rightarrow \frac{A}{B} \left(g_{km} \sin(\delta_k - \theta_s) - \left(b_{km} + \frac{y_{ckm}}{2}\right) \cos(\delta_k - \theta_s) \right) &= \left(g_{km} \cos(\delta_k - \theta_s) + \left(b_{km} + \frac{y_{ckm}}{2}\right) \sin(\delta_k - \theta_s) \right) \\ \Rightarrow \tan(\delta_k - \theta_s) &= \frac{\left(g_{km} + \frac{A}{B} \left(b_{km} + \frac{y_{ckm}}{2}\right) \right)}{\left(\frac{A}{B} g_{km} - \left(b_{km} + \frac{y_{ckm}}{2}\right) \right)} \end{aligned}$$

$$\Rightarrow \theta_s = \delta_k - \tan^{-1} \left(\frac{g_{km} + \frac{A}{B} \left(b_{km} + \frac{y_{ckm}}{2} \right)}{\frac{A}{B} g_{km} - \left(b_{km} + \frac{y_{ckm}}{2} \right)} \right) \quad (4.18)$$

Using the expression of phase angle (θ_s) obtained from (4.18), the initial value of magnitude of series controller voltage V_s is calculated from (4.16) and it is represented as:

$$V_s = \frac{A}{-V_k \left(g_{km} \cos(\delta_k - \theta_s) + \left(b_{km} + \frac{y_{ckm}}{2} \right) \sin(\delta_k - \theta_s) \right)} \quad (4.19)$$

The large SPA difference between the two buses is created by disconnecting the transmission lines one at a time with power flow more than 1.8 p.u. While removing the line one at a time of 118 bus system, it has been found that the SPA difference between the two buses after disconnection of lines through which power transfers is more than 1.8 p.u. remains below 40° . Therefore, SPA value more than 30° were considered to investigate the use of UPFC devices for reducing SPA difference between the two end buses of a disconnected lines. SPA across the two end buses of the disconnected lines of 118 bus system is presented in Table 4.1. From the economic point of view, it is not advisable or worth to install UPFC device only for SPA reduction in PSN. Therefore, to reduce excessive SPA difference between the two end buses of a PSN readily available UPFC devices in the vicinity can be used. If a UPFC device is installed in a transmission line it must influence the power flow through the other lines in the vicinity of a large PSN [17]. Thus, in this research work of reduction of SPA across the two end buses of the disconnected lines, it is decided to select the line having significant values of SFs α_{pq} , β_{pq} and γ_{pq} for introduction of UPFC devices around the vicinity of the disconnected lines. For simplicity line-tier scheme shown in Figure 4.2 is considered for introducing UPFC devices to investigate the effectiveness of the use of UPFC devices for the reduction of SPA across the two end buses of the disconnected lines.

Table 4.1 SPA difference between the two end buses after disconnection

Line connected between		Power flow before removal of the line	SPA value after removal of the line
Bus-p	Bus-q		
26	30	2.14501- j 0.3951	35.2594
38	65	1.6735 - j 0.8149	-30.4312
42	49	-1.2609 - j 0.0011	-38.5252

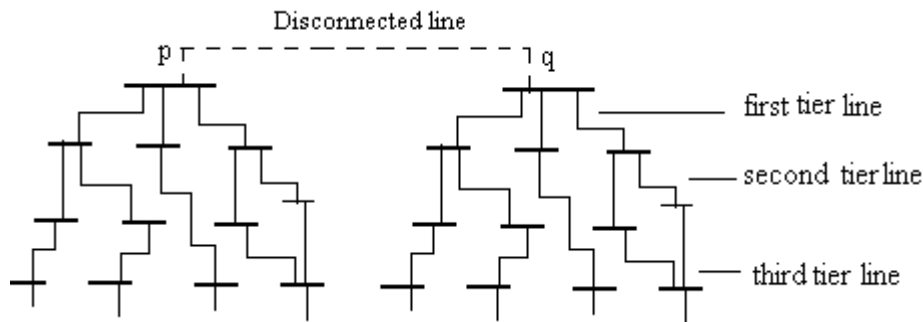


Fig. 4.2 Line-tier scheme for incorporating UPFC devices in the transmission lines.

Figure 4.2 shows the different tier levels such as first tier, second tier and third tier lines connected on the bus- p and bus- q of the disconnected line pq . To incorporate UPFC devices, the lines in the three tier level are considered to reduce excessive SPA across the bus- p and bus- q of the disconnected line pq . The lines were removed to create large SPA difference across the two buses and the LF analysis is performed to estimate the SPA values across the two buses are presented in Table 4.1. To determine the line numbers for incorporating UPFC devices search process based on ‘line to bus connectivity’ are used in the tier system extended up to three tier level. LF using UPFC is performed by considering one line at a time with the scheduled power flow (P_{kn}^{sch} and Q_{kn}^{sch}) as 1.01 times of power flow through the line obtained from initial LF and Q_{ksh}^{sch} is taken as 0.05 p.u. The lines having significant values α_{pq} , β_{pq} and γ_{pq} with an UPFC device under three tier scheme were selected for reduction of SPA across the two end buses (bus- p and bus- q) of the disconnected lines pq . SF of the selected lines (α_{pq} , β_{pq} and γ_{pq}), state variables of UPFC and the lines having excessive SPA across the buses- (i) bus

26 and bus 30 and (ii) bus 38 and bus 65 and (iii) bus 42 and bus 49 due to removal of the lines one at time are shown in Table-4.2. UPFC is implemented in the line km considering the scheduled power flow though as 1.01 times of power flow through these lines obtained from initial LF and Q_{ksh}^{sch} is taken as 0.05 p.u. It can be observed from the Table 4.2 that when the power flow through the line km is rescheduled with the introduction of the UPFC devices, SPA across the disconnected line gets modified from the SPA difference obtained using initial LF analysis. When the line connected between bus-26 and bus-30 was removed, the SPA across the bus-26 and bus-30 obtained using initial LF analysis was 35.2594° but rescheduling of power flow through the line connected between bus-25 and bus-23 has reduced the SPA across the bus-26 and bus-30 to 34.98214° . The desired value of SPA across the two buses is considered as 20° and the allowable limit for series controller voltage is considered as 0.2 pu. As the of voltage of series controller is highly sensitive to the change in power flow through that line therefore, it is necessary to assign the value of σ between 0.05 to 0.1 to avoid large change in schedule value of power flow through the line km calculated by using equation (4.9). The simulation results for IEEE 118 bus system are presented in Table 4.2 and Table 4.3.

The final results obtained by rescheduling the power flow through the line having UPFC device are presented in Table 4.3. It is found that there is a significant reduction in SPA value across the disconnected line but due to the limit imposed on series controller voltage magnitude it could not be reduced to the desired value of SPA i.e., 20° . From Table 4.3 it can be seen that when power flow is rescheduled through the selected lines of IEEE 118 bus system using UPFC device, the SPA across the disconnected line connected between bus-26 and bus-30 is reduced from 35.2594° to 25.8356° again the SPA across the disconnected line connected between bus-38 and bus-65 is reduced from -30.4312° to -21.7816° and the SPA across the disconnected line connected between bus-42 and bus-49 is reduced from 38.5252° to -27.1562° . However, the line under three tier levels is also effective in reduction of SPA across the two end buses. Therefore, any line with UPFC device having significant values of SFs (α_{pq} , β_{pq} and γ_{pq}) can be selected for reduction of excessive SPA across the two end buses by rescheduling the power flow through the lines. Thus, SFs provide a basis for selecting the lines with UPFC device for reduction of excessive SPA. SFs value varies from first iteration to final iteration presented in Table-4.2 and Table-4.3 and the method is explained in the above algorithm. For creating large SPA ($>40^\circ$) for 118 bus system across the two end buses of a disconnected line, reference [54] is used, transmission line connected across buses 25 and 23, 25 and 27 were disconnected for creating large SPA across bus-25 and bus-23. Table-4.4 shows the first LF results considering scheduled power flow through the line km for different tier levels as 1.01 times of the power flow through these lines obtained from initial LF and Q_{ksh}^{sch} is taken as 0.05 p.u.

Reduction of SPA across the bus-25 and bus-23, keeping voltage magnitude of series controller of UPFC within maximum limit of 0.2 p.u. are represented in Table-4.5. Here, the desired value of SPA is considered as 20° but due to the voltage constrain of series controller of UPFC device the SPA across bus-25 and bus-23 could not be reached to the desired value by rescheduling the power flow through the line with UPFC device. Therefore, to reduce SPA value further it is necessary to use generation rescheduling or load shedding. To apply generation rescheduling for further reduction of SPA value across the bus-25 and bus-23, the reduced value of SPA across the bus-25 and bus-23 achieved by rescheduling the power flow through the line with UPFC connected between bus-30 and bus-26 appeared in the second tier are considered as reference as maximum reduction was possible with this line. Now, for remaining reduction ($\Delta\delta_{pq}^{des} = 20^\circ - 35.8711^\circ = -15.8711^\circ$) of SPA across the bus-25 and bus-23, generation rescheduling is applied by modifying the generation using the procedure give in [54]. It has been found that the generator located at bus-25 or bus-26 can reduce SPA to the desired value. The results are presented in Table-4.6 and Table 4.7.

Table 4.6 Simulation results of generation rescheduling to reduce remaining SPA across bus-25 and bus-23 after termination of process of SPA reduction by using UPFC device.

Bus number	Generation before SPA reduction	SPA before generation rescheduling	Generation after SPA reduction	SPA after generation rescheduling
26	3.1390 p.u.	35.8711°	2.0805 p.u.	20.0153°

Table 4.7 Simulation results of generation rescheduling to reduce remaining SPA across bus-25 and bus-23 after termination of process of SPA reduction by using UPFC device.

Bus number	Generation before SPA reduction	SPA before generation rescheduling	Generation after SPA reduction	SPA after generation rescheduling
25	1.850 p.u.	35.8711°	0.8927 p.u.	20.0042°

Table 4.8 Simulation results of generation rescheduling to reduce remaining SPA across bus-25 and bus-23, using the method given in reference [54].

Bus number	Generation before SPA reduction	SPA before generation rescheduling	Generation after SPA reduction	SPA after generation rescheduling
25	1.8500 p.u.	48.1037°	0.6107 p.u.	20.0034°
26	3.1390 p.u.		1.1475 p.u.	

Again, using the method of reduction of SPA presented in [54], the SPA across bus-25 and bus-23 is reduced by generation rescheduling at the sensitive buses. It is observed that to bring the SPA value at the desired value of 20° from 48.1037° minimum two generating units located at bus-25 and bus-26 are required and the results are presented in Table-4.8. To achieve desired value of SPA total generation rescheduling required is $((1.85+3.139) - (0.6107+1.1475))= 3.2308$ p.u [54], but with the combined use of UPFC device and rescheduling of generation using generator at bus-26 would be $(3.1390-2.0805)= 1.0585$ p.u., similarly, rescheduling of generation using generator at bus-25 would be $(1.8500-0.8927) = 0.9573$ p.u. Thus, it can be conclude that the combined method required less amount of generation rescheduling than only generation rescheduling using generating units and load shedding which result in less ramping time for generation rescheduling. This allows faster restoration of the transmission line. Use of UPFC for SPA deduction along with generation rescheduling and load shedding would help in avoiding/reducing load shedding, in case load shedding becomes necessary to reduce SPA to the desired value.

4.5 Conclusions

In this method of reduction of excessive SPA across the two busses, a sensitivity-based method is adopted to reduce the SPA difference below the prescribed value for the category of the line to be restored/ re-connected. Sensitivity relation between change in SPA across two end buses of transmission line and the change in power flows through the line having UPFC device have been formulated for this purpose. The sensitivity relations are used to reschedule the power flow through the line having UPFC device to reduce SPA across the line to be re-connected. The sensitivity factors of the line containing the UPFC device have to be sensitive enough to

keep the scheduled power flow and the state variables of the UPFC device within the operating limits. It has been found that the voltage magnitude of the series controller of the UPFC plays a decisive role in the operation-related planning of the UPFC device. Simulation results for IEEE 118 bus system indicated that SPA reduction across the buses of a disconnected line is sensitive to the voltage magnitude of the series controller of the UPFC device. The voltage limit on the series controller of UPFC plays a significant role in the reduction of SPA across the buses of a disconnected line. It may not be possible to reduce excessive SPA across the buses of a disconnected line to the desired value using rescheduling of power flow through the UPFC device. Therefore, in case of violation of the operating limit of a UPFC device, it is possible to achieve only a partial reduction of SPA across the buses of the line to be re-energized. Under such circumstances, for the reduction of the remaining SPA value across buses of a line, a method like generation rescheduling or load shedding can be adopted. Such a combined process would ensure less amount of generation rescheduling or load shedding compared to the method that applies only generation rescheduling or load shedding to reduce excessive SPA across the buses of a disconnected line and may help in avoiding load shedding or reducing the magnitude of load to be shaded during the restoration of a transmission line having SPA problem.

Table 4.2 The first load flow analysis results with assigned scheduled power flow as $P_{km}^{sch} = 1.01P_{km}^0$ $Q_{km}^{sch} = 1.01Q_{km}^0$ and $Q_{ksh}^{sch} = 0.05$ for the disconnected line connected between two end buses 26 and 30, 38 and 65, 42 and 49.

Disconnected line and SPA across the two end buses determined by BCLF	Two end bus number of line considered for introducing UPFC		Tier level	Line flow through the line considered for SPA reduction determine by BCLF	Power flow result of the UPFC device, where the UPFC power flow is assigned as $P_{km}^{sch} = 1.01P_{km}^0$, $Q_{km}^{sch} = 1.01Q_{km}^0$ and $Q_{ksh}^{sch} = 0.05$			SPA value across the two end buses of the disconnected line after introducing the UPFC device in the line connected between bus- k and bus- m
	k	m			P_{km}^0	$P_{km}^{sch} = 1.01P_{km}^0$	V_s in pu	
SPA value across the two end buses 26 and 30 of disconnected line $= \delta_{pq}$ $= 35.2594^\circ$	30	17	1	0.9940	1.0041	0.0051	0.1231	35.0585°
				1.0064	1.0164	1.1251	0.0014	
				0.0500	-0.0494	0.0003		
	25	23	2	2.9430	2.9724	-0.0108	-0.3013	34.9821°
				0.4556	0.4601	1.5500	0.0117	
				0.0500	-0.0453	0.0000		
32	113	3	0.6040	0.6101	0.0028	-0.1143	35.2312°	
			-0.2978	-0.2978	-2.0648	-0.0012		
			0.0500	-0.0540	0.0024			
SPA value across	37	38	1	-1.4756	-1.4904	0.0293	0.2361	-29.5412°

the two end buses				0.8134	0.8215	-1.7794	-0.0834	
38 and 65 of					0.0500	0.0512	-0.0063	
disconnected line	8	9	3	-4.8323	-4.8807	-0.0216	-0.2615	-30.1223°
= $\delta_{pq} = -30.4312^\circ$				-0.7707	-0.7784	1.6273	0.0303	
					0.0500	-0.0488	0.0065	
	49	42	3	1.9704	1.9901	-0.0180	0.6646	-30.0345°
				0.2113	0.2134	0.9836	0.3373	
					0.0500	-0.0490	0.0000	
SPA value across	38	37	1	3.6223	3.6585	-0.0204	0.3016	-37.3256°
the two end buses				-0.2268	-0.2290	1.0870	0.1008	
42 and 49 of					0.0500	-0.0530	0.0519	
disconnected line	8	9	3	-4.8326	-4.8809	-0.0219	-0.0987	-38.4036°
= $\delta_{pq} = -38.5252^\circ$				-0.7472	-0.7546	1.8078	0.0100	
					0.0500	-0.0487	0.0012	
	34	43	3	-0.1944	-0.1963	-0.0018	-0.1771	-38.4768°
				0.1625	0.1641	-1.5442	0.0117	
					0.0500	-0.0516	0.0000	

Table 4.3 UPFC scheduled power flow, variables and sensitivity factors α_{pq} , β_{pq} and γ_{pq} for the lines after reduction of SPA across the buses- (i) bus-26 and bus-30 (ii) bus-38 and bus-65 and (iii) bus-42 and bus-49 due to removal of the lines one at time

Disconnected line and SPA across the two end buses determined by BCLF	SPA value across the two end buses of the disconnected line after introducing the UPFC device in the line connected between k and m buses.	Two end bus number of line considered for introducing UPFC		Tier level	UPFC scheduled power flow, variables and sensitivity factors α_{pq} , β_{pq} and γ_{pq}			SPA value after reduction δ_{pq}
		k	m		P_{km} in pu	V_s in pu	α_{pq}	
					Q_{km} in pu	θ_s in radian	β_{pq}	
SPA value across the two end buses 26 and 30 of disconnected line = δ_{pq} = 35.2594°	35.0585°	30	17	1	-0.2336	0.2020	0.1282	25.9291°
					0.9608	1.3476	0.0015	
					0.0433	-0.0426	-0.0048	
	34.9821°	25	23	2	3.5304	-0.2139	-0.3014	25.8356°
					0.4401	1.5221	0.0117	
					0.0294	-0.0267	0.0000	
	35.2312°	32	113	3	1.0985	0.2085	-0.1139	30.1162°
					-0.2938	-1.8914	0.0024	

SPA value across the two end buses 38 and 65 of disconnected line = δ_{pq} = -30.4312°	-29.5412°	37	38	1	0.0541	-0.0589	-0.0000	
					-0.9798	0.2089	0.2760	-21.7816°
					0.6238	-1.8406	-0.1326	
					-0.1488	0.1524	-0.0063	
	-30.1223°	8	9	3	-5.4557	-0.2062	-0.1903	-22.1584°
					-0.8058	1.9055	0.0058	
SPA value across the two end buses 42 and 49 of disconnected line = δ_{pq} = -38.5252°	-30.0345°	49	42	3	0.0960	-0.0953	0.0067	
					2.1996	-0.2202	0.4212	-22.1161°
					0.3081	0.9481	0.1599	
					0.1457	-0.1429	0.0000	
	-37.32567°	38	37	1	4.0470	0.2007	0.1946	-27.1562°
					-0.1105	-1.9860	0.0407	
SPA value across the two end buses 42 and 49 of disconnected line = δ_{pq} = -38.5252°	-38.4036°	8	9	3	0.1606	-0.1773	0.0405	
					-5.5076	-0.2183	-0.1013	-33.6721°
					-0.7913	2.0532	0.0109	
					0.0866	-0.0855	0.0013	
	-38.4768°	34	43	3	-0.4978	-0.2376	-0.1949	-33.5344°
					0.1338	-2.0767	0.0047	
				0.0619	-0.0639	-0.0000		

Table 4.4 First load flow analysis results showing UPFC variables and sensitivity factors α_{pq} , β_{pq} and γ_{pq} for the lines considered for reduction of SPA having assigned scheduled power flow through the UPFC device as 1.01 times of its line flow through the line determined from BCLF and Q_{ksh}^{sch} is taken as 0.05 p.u. having excessive SPA across the bus-25 and bus-23

Disconnected line and SPA across the two end buses determined by BCLFA	Two end bus number of line considered for introducing UPFC		Tier level	Line flow through the line considered for SPA reduction determine by BCLFA	power flow result of the UPFC device, where the UPFC power flow is assigned as $P_{km}^{sch} = 1.01P_{km}^0$, $Q_{km}^{sch} = 1.01Q_{km}^0$ and $Q_{ksh}^{sch}=0.05$				SPA value across the two end buses of the disconnected line after introducing the UPFC device in the line connected between k and m buses.			
	k	m			P_{km}^0	Q_{km}^0	$P_{km}^{sch} = 1.01P_{km}^0$	$Q_{km}^{sch} = 1.01Q_{km}^0$		$Q_{ksh}^{sch}=0.05$	V_s in pu	α_{pq}
							θ_s in radian	B_{sh} in pu		β_{pq}	γ_{pq}	
SPA value across the two end buses 25 and 23 of disconnected line = $\delta_{pq} = 48.1037^\circ$	32	23	1	-0.2332	-0.2355	-0.0019	-0.2814	48.1662°				
				-0.1297	-0.1310	-1.2833	0.0141					
				0.0500	-0.0543	0.0005						
= $\delta_{pq} = 48.1037^\circ$	26	25	1	1.8529	1.8714	-0.0512	0.5615	47.6293°				
				0.9827	0.9925	2.0406	0.0026					
				0.0500	-0.0453	0.0000						
= $\delta_{pq} = 48.1037^\circ$	30	26	2	-4.7889	-4.8368	-0.034069	-0.7468	50.0249°				
				0.7681	0.7681	2.092793	0.4556					
				0.0500	-0.051509	0.1007						

Table 4.5 UPFC scheduled power flow, variables and sensitivity factors α_{pq} , β_{pq} and γ_{pq} for the lines after reduction of SPA across the bus-25 and bus-23

Disconnected line and SPA across the two end buses determined by BCLF	SPA value across the two end buses of the disconnected line after introducing the UPFC device in the line connected between bus- k and bus- m	Two end bus number of line considered for introducing UPFC		Tier level	UPFC scheduled power flow, variables and sensitivity factors α_{pq} , β_{pq} and γ_{pq}			SPA value after reduction δ_{pq}
		k	m		P_{km} in pu	V_s in pu	α_{pq}	
SPA value across the two end buses 25 and 23 of disconnected line $= \delta_{pq} = 48.1037^\circ$	48.1662°	32	23	1	0.1163	0.2004	-0.2566	42.1987°
					-0.1602	-1.9690	0.0423	
					0.0197	-0.0216	0.0013	
	47.6293°	26	25	1	1.6746	-0.2234	0.5752	36.0573°
					0.9937	1.9019	0.0123	
					0.0512	-0.0464	-0.0000	
	50.0249°	30	26	2	-4.6474	-0.2005	-0.7457	35.8711°
					0.6495	-1.2378	0.4547	
					-0.0522	0.0534	0.1005	

Conclusions and Recommendation for Future Research

5.1 Conclusions of the proposed work

Due to the growth in power consumptions and populations, a huge amount of power needs to be transmitted through the transmission lines thus the existing network has to operate closer to its limiting value. Again disturbances/faults in PNS bring the system into an emergency condition. Large disturbance in a power system may lead to outages of the generators or transmission lines that result in overloading of nearby lines, voltage deviations, and large changes in bus voltage angles. Due to these, it is necessary to restore the PSN to a normal condition within the shortest possible time. Abnormal conditions like loss of heavy generators/ loads, or fault on a PSN cause heavy power flow through the transmission lines results in significant change in phase angle difference across the two buses as a result stability problems may arise if the system is not restored within the shortest possible time. During the restoration of transmission lines if the phase angle difference between the two buses is huge then the circuit breaker equipped with the synchrocheck relay does not allow the system to re-connect the line across the two buses. Again to avoid the line flow limit violation of other lines of the PSN it is required to reconnect the line as early as possible. In

order to avoid these problems, this thesis presents line power flow control with SPFC and UPFC devices.

To evaluate the performance of SPFC realistically the impedance of SSSC along with controllable voltage source is considered when it is incorporated in the transmission lines. The advantage of this LF model is that the sensitivity relations between power flows through the SPFC device with any power system control variables would possess the collective or integrated effect of SPFC device and transmission line state variables. Similarly, modeling of LF analysis with UPFC device allows derivation of sensitivity relations among line power flow, reactive power injection at one end of the line, and system control variables would possess the collective or integrated effect of UPFC device and transmission line state variables. Mathematical modeling of LF analysis with SPFC and UPFC devices are configured to investigate the use of SPFC and UPFC devices for the reduction of TRPL and the excessive SPA across the two buses of the disconnected lines of IEEE 118 bus system.

The reduction of TRPL is done by rescheduling the power flow through the lines using the SPFC devices. The lines having a large value of PLSF i.e., a large value of change in TRPL due to change in RRRF through the lines are considered for rescheduling of power flow. The optimized value of TRPL is achieved using equation (3.13) by rescheduling the power flow through the selected lines using SPFC devices. The TRPL obtained with the proposed method is 2.5151 p.u. Thus $(3.0851 - 2.5151 =) 0.57$ p.u. loss reduction is achieved with the proposed method of rescheduling of power flows through the selected transmission lines of the IEEE 118 bus system. In addition to this, the use of SPFC devices in the selected lines also improves the bus voltage profile of the system. Further, the use of SPFC devices would also create a facility for other applications such as power transfer enhancement, alleviation of line overload in nearby overloaded lines, etc. The cost analysis related to the installation of SPFC devices and saving due to reduction of TRPL is also reported in section 3.6.2. It is found that the IC of the SPFC devices would be recovered within 1 and $\frac{3}{4}$ years, even with MF=0.7 and cost of unit as ₹4/kWhr.

Chapter 2 represents LF modeling with UPFC device, the UPFC device is modeled with only three state variables so that the size of the Jacobian matrix is reduced. SFs (α_{pq} , β_{pq} and γ_{pq}) are determined using the LF Jacobian matrix which provides a linear relationship between the change in SPA across two end buses of a disconnected transmission line and

the change in power flow through the line (ΔP_{kn} , ΔQ_{kn} and ΔQ_{ksh}) having UPFC device. As modified schedule power flow may not ensure the exact change in SPA across the disconnected line pq thus, to verify the SPA (δ_{pq}) obtained by rescheduling the power flow with the line having UPFC device a LF analysis with UPFC is performed. The SFs of the line containing the UPFC device have to be sensitive enough to keep the scheduled power flow and the state variables of the UPFC device within the operating limits. It has been found that the voltage magnitude of the series controller of the UPFC device plays a decisive role in the operation of a UPFC device. Simulation results for IEEE 118 bus system indicated that the SPA reduction across the buses of a disconnected line is sensitive to the voltage magnitude of the series controller of the UPFC device. During simulation violation of operating limit of UPFC device was detected therefore, only a partial reduction of SPA was possible with the use of UPFC devices and the remaining SPA across the buses of the line to be re-energized are achieved using generation rescheduling. This combined process of rescheduling of line power flow with UPFC device and generation rescheduling ensures less amount of generation rescheduling than the method that applies only generation rescheduling or load shedding to reduce the excessive SPA across the two end buses of the line to be re-energized.

5.2 Conclusions

During simulation, it is observed that the rescheduling of RRPf with the use of SPFC devices at line number 112 of the IEEE 118 bus system was able to reduce a considerable amount of TRPL of the system as the line have a PLSF value of more than 30% of the maximum value of the PLSF. Even though line numbers 111 and 41 have higher values of PLSF than line number 112 but as they are radially connected without any parallel path to accommodate the change in power flow in the lines thus could not participate in the process reduction of TRPL of the IEEE 118 bus system. In addition to the reduction of TRPL placements of SPFC devices also provides improvement of bus voltage profile of IEEE 118 bus system.

To achieve the desired value of SPA (20.0153°) with only generation rescheduling, the total generation rescheduling required was 3.2308 p.u. $((1.85+3.139) - (0.6107+1.1475))$ [54]. With the combined use of UPFC device and rescheduling of generation using the generator at

bus-26 is $(3.1390-2.0805) = 1.0585$ p.u. Similarly, rescheduling of generation for the generator at bus-25 is $(1.8500-0.8927) = 0.9573$ p.u. So the total generation rescheduling required with the combined method is 2.0158 p.u. Thus, it can be concluded that the combined method required less amount of generation rescheduling than only generation rescheduling using generating units and load shedding. This allows faster restoration of the transmission line. Use of UPFC for SPA deduction along with generation rescheduling and load shedding would help in avoiding/reducing load shedding, in case load shedding becomes necessary to reduce SPA to the desired value.

5.3 Scopes for Future Research

Following are the future scopes of the research work:

- For identifying the locations of SPFC device only real power loss in the transmission line is considered in the proposed work. In addition to real power loss, power transfer capability, stability can also be considered to identify the locations of SPFC devices.
- These FACTS devices can also be utilized to improve the voltage stability of a PSN.
- Investment cost of UPFC devices can be done to justify the use of UPFC device for reduction of SPA across the two buses of a power system as well as other applications.
- The hardware implementation of the proposed method can be taken up as a future research work to examine the performance of the method under the working environment of a power system.

-
- [1] M. Y. Hassan, et al., "Electricity market models in restructured electricity supply industry", in *IEEE 2nd International Power and Energy Conference* (2008), pp. 1038-1042.
- [2] P. Asare, et al., "An overview of flexible AC transmission systems", (1994).
- [3] N. G. Hingorani, L. Gyugyi, "Understanding FACTS: Concepts and Technology of Flexible AC Transmission Systems", IEEE Press (2000).
- [4] S. Rahimzadeh, M. Tavakoli Bina, and A. Viki, "Simultaneous application of multi-type FACTS devices to the restructured environment: Achieving both optimal number and location", *IET Generation Transmission and Distribution* (2009), vol. 4, no. 3, pp. 349–362.
- [5] S. Gerbex, R. Cherkaoui, and A. J. Germond, "Optimal placement of multi-type FACTS devices in a power system by means of genetic algorithms", *IEEE Transaction on Power System* (2001), vol. 16, no. 3, pp. 537–544.
- [6] S. R. Najafi, M. Abedi, and S. H. Hosseinian, "A novel approach to optimal allocation of SVC using genetic algorithms and continuation power flow", in *Proceedings of the IEEE International conference on Power and Energy* (2006), pp. 202–206.
- [7] G. I. Rashed, H. I. Shaheen, and S. J. Cheng, "Optimal location and parameter setting of multiple TCSCs for increasing power system loadability based on GA and PSO techniques", in *Proceedings of the IEEE International conference on Natural Computation* (2007), vol. 4, pp. 335-344.
- [8] M. Saravanan, et al., "Application of PSO technique for optimal location of FACTS devices considering system loadability and cost of installation", in *Proceedings of the IEEE International Conference on Power Engineering* (2005), pp. 716-721.
- [9] S. T. J. Christa, P. Venkatesh, "Application of particle swarm optimization for optimal placement of unified power flow controllers in electrical systems with line outages", in *Proceedings of the IEEE International Conference on Computational Intelligence* (2007), vol. 1, pp. 119–124.
- [10] A. Kazemi, D. Arabkhabori, M. Yari, and J. Aghaei, "Optimal location of UPFC in power systems for increasing loadability by genetic algorithm", in *Proceedings of the IEEE International Conference on Power Engineering* (2006), vol. 2, pp. 774–779.

-
- [11] S. Gerbex, R. Cherkaoui, and A. J. Germond, “Optimal placement of FACTS devices to enhance power system security”, in *Proceedings of the IEEE Conference on Power Tech* (2003), vol. 3, pp. -6.
- [12] E. Ghahremani, I. Kamwa, “Optimal allocation of STATCOM with energy storage to improve power system performance’, in the *IEEE Conference and Exposition on PES T&D* (2014), pp. 1-5.
- [13] M. S. Luna and J. R. Cedeno-Maldonado, “Optimal placement of FACTS controllers in power systems via evolution strategies”, in *the IEEE Conference and Exposition on Transmission and Distribution* (2006), pp. 1-6.
- [14] R. P. Kalyani, M. L. Crow, and D. R. Tauritz, “Optimal placement and control of unified power flow control devices using evolutionary computing and sequential quadratic programming,” in the *Proceedings of the IEEE Conference and Exposition on Power Systems* (2006), pp. 959–964.
- [15] I. Marouani, et al., “Application of a multi-objective evolutionary algorithm for optimal location and parameters of FACTS devices considering the real power loss in transmission lines and voltage deviation buses”, in *the Proceedings of the IEEE conference on System, Signals and Devices* (2009), pp. 1-6.
- [16] H. I. Shaheen, G. I. Rashed, and S. J. Cheng, “Application of evolutionary optimization techniques for optimal location and parameters setting of multiple UPFC devices”, in *the Proceedings of the IEEE International conference on Natural Computation* (2007), vol. 4, pp. 688-697.
- [17] Z.Lu, et al., “Optimal location of FACTS devices by a bacterial swarming algorithm for reactive power planning”, in *the Proceedings of the IEEE conference on Evolutionary Computing* (2007), pp. 2344–2349.
- [18] Q. H.Wu, et al., “Optimal placement of FACTS devices by a group search optimizer with multiple producer”, in *the Proceedings of the IEEE conference on Evolutionary Computing* (2008), pp. 1033-1039.

-
- [19] A. Kazemi, A. Parizad, and H. R. Baghaee, "On the use of harmony search algorithm in optimal placement of FACTS devices to improve power system security", in *the Proceedings of the IEEE conference on EURO* (2009), pp. 540-576.
- [20] R. M. Idris, A. Kharuddin, and M. W. Mustafa, "Optimal choice of FACCTS devices for ATC enhancement using bees algorithm," in *the Proceedings of the IEEE conference on Power Engineering* (2009), pp. 1-6.
- [21] M.A. Abido, "Optimal power flow using particle swarm optimization", *International journal of Electrical Power and Energy Systems* (2002), vol. 24, no. 7, pp. 563-571.
- [22] S.Yuhui, C. E. Russell, "Empirical Study of Particle Swarm Optimization", in *the Proceedings of the IEEE Congress on Evolutionary Computation* (1999), pp. 1945-1950.
- [23] R. Eberhart, J. Kennedy, 'Particle swarm optimization', in *the Proceedings of the IEEE international conference on neural networks* (1995), pp. 1942-1948.
- [24] A. Q. Badar, B. S. Umre, A. S. Junghare, "Reactive power control using dynamic particle swarm optimization for real power loss minimization", *International Journal of Electrical Power & Energy Systems* (2012), vol.41, no.1, pp.133-136.
- [25] M. H. Moradi, M. Abedini, "A combination of genetic algorithm and particle swarm optimization for optimal DG location and sizing in distribution systems", *International Journal of Electrical Power & Energy Systems* (2012), vol. 34, no.1, pp. 66-74.
- [26] A. Z. Gamm and I. I. Gloub, "Determination of locations for FACTS and energy storage by the singular analysis", in *the Proceedings of the IEEE conference on Power System Technology* (1998), vol. 1, pp. 411-414.
- [27] A. D. Shakib and G. Balzer, "Optimal location and control of shunt FACTS for transmission of renewable energy in large power systems", in *the Proceedings of the IEEE conference on Mediterranean Electrotechnical* (2010), pp. 890–895.
- [28] S. N. Singh and A. K. David, "Optimal location of FACTS devices for congestion management", *Electric Power System Research* (2001), vol. 58, no. 2, pp. 71–79.
- [29] S. N. Singh and A. K. David, "Placement of FACTS device in open power market", in *the Proceedings of the IEEE conference on Power System Control, Operation and Management* (2000), vol. 1, pp. 173–177.

-
- [30] S. N. Singh and I. Erlich, "Locating unified power flow controller for enhancing power system loadability", in *the Proceedings of the IEEE International Conference on Future Power Systems* (2005), pp. 1–5.
- [31] K. S. Verma, S. N. Singh, and H. O. Gupta, "Location of unified power flow controller for congestion management" (2001), *Electric power systems research*, vol. 58, no. 2 pp. 89-96.
- [32] M. Saravanan, et al., "Application of particle swarm optimization technique for optimal location of FACTS devices considering cost of installation and system loadability", *Electric power systems research* (2007), vol. 77, no (3-4), pp.276-283.
- [33] L.J. Cai, I. Erlich, "Optimal choice and allocation of FACTS devices using genetic algorithms", in *the Proceedings of the conference on twelfth intelligent systems application to power systems* (2003), pp. 1-6.
- [34] L.J. Cai, I. Erlich, G. Stamtsis, "Optimal choice and allocation of FACTS devices in deregulated electricity market using genetic algorithms", *IEEE PES Conference and Exposition on Power Systems*, (2004), pp. 201-207.
- [35] J. Douglas, G. T. Heydt, "Power flow control and power flow studies for systems with FACTS devices", *IEEE Transactions on power systems* (1998), vol. 13, no. 1 pp. 60-65.
- [36] B. Roy, et al., "Impact of unified power flow controllers on power system reliability", *IEEE Transactions on Power Systems* (2000), vol. 15, no. 1, pp. 410-415.
- [37] T. Orfanogianni, and B. Rainer, "Steady-state optimization in power systems with series FACTS devices", *IEEE Transactions on Power Systems* 2003, vol. 18, no. 1, pp. 9-26.
- [38] S.K. Srivastava, L.N Giri, K.G Upadhyay, S.N Singh, "Analysis of internal operating limits of UPFC for power flow control" in *the proceedings of National conference on Power System* (2004).
- [39] L. Liming, et al., "Power-flow control performance analysis of a unified power-flow controller in a novel control scheme", *IEEE transactions on power delivery* (2007), vol. 22, no. 3, pp. 1613-1619.
- [40] M. Noroozian, L. Angquist, M. Ghandhari, G. Andersson, "Use of UPFC for optimal power flow control", *IEEE transactions on Power Delivery* (1997), vol. 12, no. 4, pp. 1629-1634.

-
- [41] V.G. Mathad, B.F. Ronad, S.H. Jangamshetti, "Review on comparison of FACTS controllers for power system stability enhancement", *International Journal of Scientific and Research Publications* (2013), vol. 3, no. 3, pp.1-4.
- [42] Rawat, Mahiraj Singh, and Shelly Vadhera, "Comparison of FACTS devices for transient stability enhancement of multi machine power system", in *the Proceedings of the IEEE, International Conference on Microelectronics, Computing and Communications* (2016), pp. 1-5.
- [43] R. Ghahnavieh Abbas, M. Fotuhi-Firuzabad, M. Othman, "Optimal unified power flow controller application to enhance total transfer capability", *IET Generation, Transmission & Distribution* (2015), vol. 9, no. 4, pp.358-368.
- [44] X.Ying, Y. H. Song, Y. Z. Sun. "Power flow control approach to power systems with embedded FACTS devices", *IEEE Transactions on power systems* (2002), vol. 17, no. 4, pp. 943-950.
- [45] M. A. Sayed, T. Takeshita, "Line Loss Minimization in Isolated Substations and Multiple Loop Distribution Systems Using the UPFC", *IEEE Transactions On Power Electronics* (2014), vol. 29, no. 11, pp.5813-5822.
- [46] M. Tripathy, S. Mishra, L.L. Lai, and Q.P. Zhang, "Transmission Loss Reduction Based on FACTS and Bacteria Foraging Algorithm" (2006), pp. 222 – 231, (Springer).
- [47] K.S.Smith, L. Ran, J. Penman, "Dynamic modelling of a unified power flow controller", in *IEE Proc Generation Transmission and Distribution* (1997), vol. 144, no. 1, pp. 7-12.
- [48] M.A. Sayed, T. Takeshita, "All nodes voltage regulation and line loss minimization in loop distribution systems using UPFC", *IEEE Transactions on Power Electronics* (2010), vol. 26, no. 6, pp.1694-1703.
- [49] F. Esquivel, C. R , E. Acha, "Unified power flow controller: a critical comparison of Newton–Raphson UPFC algorithms in power flow studies", *International journal of Generation, Transmission and Distribution* (1997), vol. 144 no. 5, pp. 437-444,.
- [50] D. Hazarika, B. Das, "Use of transmission line having SPFC for alleviation of line over load of transmission line of an interconnected power system", *International Journal of Electrical Power & Energy Systems* (2014), vol. 63, pp.722-729.

-
- [51] L. Gyugyi, C.D. Schauder, S.L. Williams, T.R. Rietman, D.R. Torgerson, A. Edris, "The unified power flow controller: a new approach to power transmission control", *IEEE Transactions on power delivery* (1995), vol. 10, no. 2, pp.1085-1097.
- [52] M. Kheradmandi, R. Feuillet "Using voltage control for reducing standing phase angle in power system restoration", *Electric Power Systems Research*, (2017), (Vol.146, pp. 9-16.
- [53] S. Wunderlich, M. M. Adibi, S. Fischi, C. O. D. Nwankpa, "An approach to standing phase angle reduction," *IEEE Transactions on Power Systems* (1994), vol. 9, no. 1, pp. 470-476.
- [54] D Hazarika, and A. K. Sinha, "Standing phase angle reduction for power system restoration", *IET Generation, Transmission, Distribution*, (1998), Vol.145 no. 1 pp. 82-88.
- [55] D Hazarika, and A. K. Sinha, "An algorithm for standing phase angle reduction for power system restoration" *IEEE Transactions on Power Systems* (1999), vol. 14, no. 4, pp. 1213-1218.
- [56] S. M. Shahidehpoura, and H. Y. Yamin, "A technique for the standing phase-angle reduction in power system restoration", *Electric Power Components and Systems* (2004), vol. 33, no. 3, pp. 277-286.
- [57] R.C. Leme, L.C.A. Ferreira, B.I.L. Lopes, A.C. Zambroni de Souza, "Using re-dispatch generators to reduce the standing phase angle during system restoration", *IET Generation, Transmission and Distribution* (2006), vol. 153, no. 5, pp. 531-539.
- [58] H. Ye, Y. Liu, "A new method for standing phase angle reduction in system restoration by incorporating load pickup as a control means", *International Journal of Electrical Power & Energy Systems* (2013), vol. 53, pp. 664-674.
- [59] R. Yuan, et al., "A genetic algorithm method for standing phase angle reduction in power system restoration", in *the IEEE Power and Energy Society General Meeting* (2010), pp. 25-29.
- [60] A. M. Ranjbar, M. R. Pishvaie, Morteza Sadegh, "Standing Phase Angle Reduction Based on a Wide Area Monitoring System Using Genetic Algorithm", *International Journal of Emerging Electric Power System* (2010), vol. 11, no. 3 pp. 1-14.

-
- [61] H. Ye, Y. Liu, “A new method for standing phase angle reduction in system restoration by incorporating load pickup as a control means”, *International Journal of Electrical Power & Energy Systems* (2013), vol. 53, pp. 664-674.
- [62] J. Quirós, T. Peter, W. V. Terzija, “Reducing excessive standing phase angle differences: A new approach based on OPF and wide area measurements”, *International Journal of Electric Power and Energy Systems* (2016), vol. 78, pp. 13-21,

A.1 Single line diagram and bus data and line data of IEEE 118 bus system

The single line diagram of IEEE 118 bus systems for the implementation of reduction of excessive SPA across the two end buses and system loss using FACTS devices such as UPFC and SPFC are presented in Figure A-1. The information of loads and generations for system is provided in Table A-1.

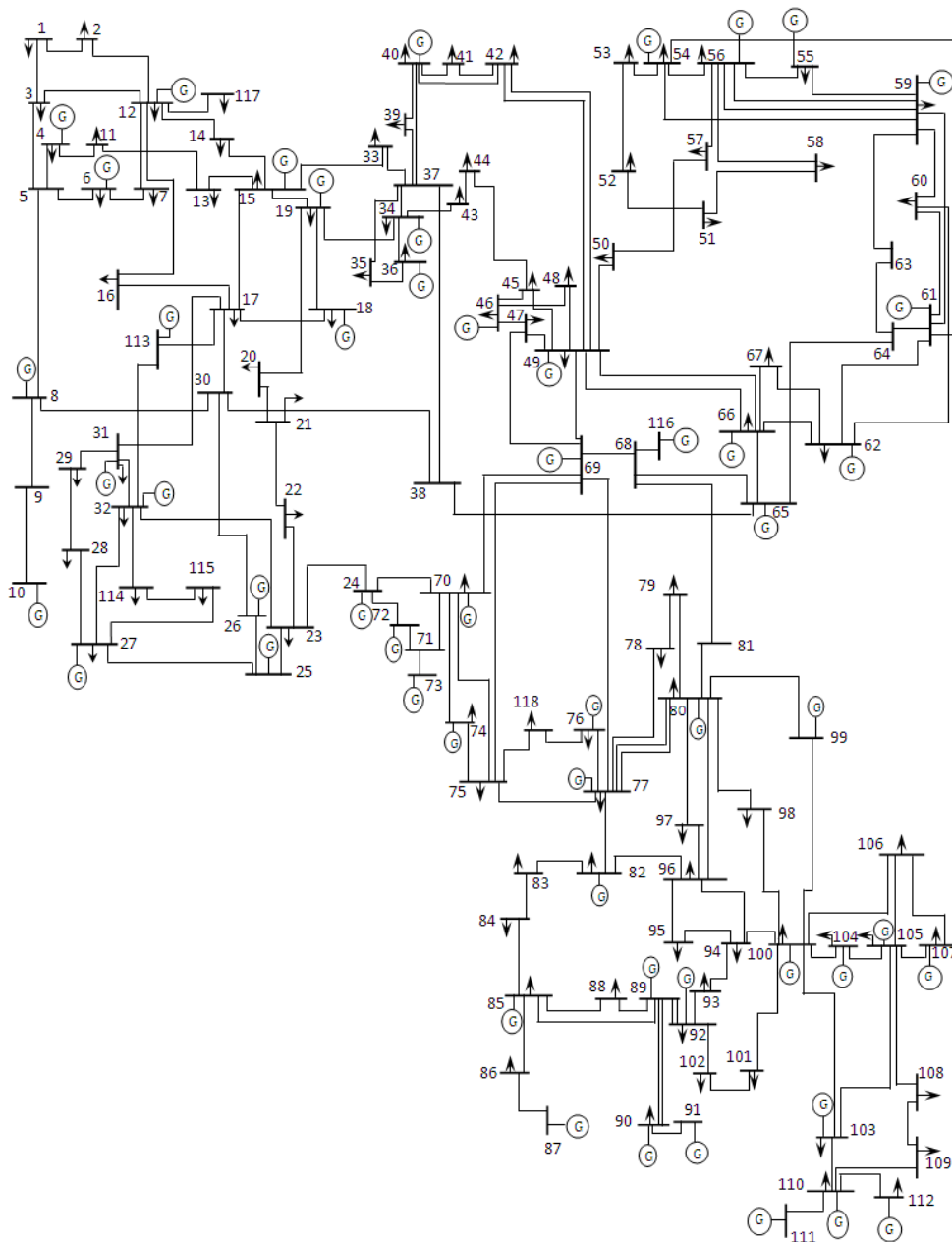


Fig. A-1 Single line diagram of IEEE 118 bus system

Table A-1.1 Generation and load data for IEEE 118 bus system

Bus No	Type	V_i p.u.	δ_i rad.	P_{Gi} MW	Q_{Gi} MVA	P_{Di} MW	Q_{Di} MVA	Q_{\min} MVA	Q_{\max} MVA
1	2	0.955	0	0	0	51	27	-5	15
2	3	0.971	0	0	0	20	9	0	0
3	3	0.968	0	0	0	39	10	0	0
4	2	0.998	0	0	0	39	12	-300	300
5	3	1.002	0	0	0	0	0	0	0
6	2	0.99	0	0	0	52	22	-13	50
7	3	0.989	0	0	0	19	2	0	0
8	2	1.015	0	0	0	28	0	-300	300
9	3	1.043	0	0	0	0	0	0	0
10	2	1.05	0	450	0	0	0	-147	200
11	3	0.985	0	0	0	70	23	0	0
12	2	0.99	0	85	0	47	10	-35	120
13	3	0.968	0	0	0	34	16	0	0
14	3	0.984	0	0	0	14	1	0	0
15	2	0.97	0	0	0	90	30	-10	30
16	3	0.984	0	0	0	25	10	0	0
17	3	0.995	0	0	0	11	3	0	0
18	2	0.973	0	0	0	60	34	-16	50
19	2	0.963	0	0	0	45	25	-8	24
20	3	0.958	0	0	0	18	3	0	0
21	3	0.959	0	0	0	14	8	0	0
22	3	0.97	0	0	0	10	5	0	0
23	3	1	0	0	0	7	3	0	0
24	2	0.992	0	0	0	13	0	-300	300
25	2	1.05	0	185	0	0	0	-47	140
26	2	1.015	0	313.9	0	0	0	-1000	1000
27	2	0.968	0	0	0	71	13	-300	300
28	3	0.962	0	0	0	17	7	0	0
29	3	0.963	0	0	0	24	4	0	0
30	3	0.968	0	0	0	0	0	0	0
31	2	0.967	0	7	0	43	27	-300	300
32	2	0.964	0	0	0	59	23	-14	42
33	3	0.972	0	0	0	23	9	0	0
34	2	0.986	0	0	0	59	26	-8	24
35	3	0.981	0	0	0	33	9	0	0
36	2	0.98	0	0	0	31	17	-8	24
37	3	0.992	0	0	0	0	0	0	0
38	3	0.962	0	0	0	0	0	0	0
39	3	0.97	0	0	0	27	11	0	0

40	2	0.97	0	0	0	66	23	-300	300
41	3	0.967	0	0	0	37	10	0	0
42	2	0.985	0	0	0	96	23	-300	300
43	3	0.978	0	0	0	18	7	0	0
44	3	0.985	0	0	0	16	8	0	0
45	3	0.987	0	0	0	53	22	0	0
46	2	1.005	0	19	0	28	10	-100	100
47	3	1.017	0	0	0	34	0	0	0
48	3	1.021	0	0	0	20	11	0	0
49	2	1.025	0	204	0	87	30	-85	210
50	3	1.001	0	0	0	17	4	0	0
51	3	0.967	0	0	0	17	8	0	0
52	3	0.957	0	0	0	18	5	0	0
53	3	0.946	0	0	0	23	11	0	0
54	2	0.955	0	48	0	113	32	-300	300
55	2	0.952	0	0	0	63	22	-8	23
56	2	0.954	0	0	0	84	18	-8	15
57	3	0.971	0	0	0	12	3	0	0
58	3	0.959	0	0	0	12	3	0	0
59	2	0.985	0	155	0	277	113	-60	180
60	3	0.993	0	0	0	78	3	0	0
61	2	0.995	0	160	0	0	0	-100	300
62	2	0.998	0	0	0	77	14	-20	20
63	3	0.969	0	0	0	0	0	0	0
64	3	0.984	0	0	0	0	0	0	0
65	2	1.005	0	391	0	0	0	-67	200
66	2	1.05	0	392	0	39	18	-67	200
67	3	1.02	0	0	0	28	7	0	0
68	3	1.003	0	0	0	0	0	0	0
69	1	1.035	0	516.4	0	0	0	-300	300
70	2	0.984	0	0	0	66	20	-10	32
71	3	0.987	0	0	0	0	0	0	0
72	2	0.98	0	0	0	12	0	-100	100
73	2	0.991	0	0	0	6	0	-100	100
74	2	0.958	0	0	0	68	27	-6	9
75	3	0.967	0	0	0	47	11	0	0
76	2	0.943	0	0	0	68	36	-8	23
77	2	1.006	0	0	0	61	28	-20	70
78	3	1.003	0	0	0	71	26	0	0
79	3	1.009	0	0	0	39	32	0	0
80	2	1.04	0	477	0	130	26	-165	280
81	3	0.997	0	0	0	0	0	0	0
82	3	0.989	0	0	0	54	27	0	0

83	3	0.985	0	0	0	20	10	0	0
84	3	0.98	0	0	0	11	7	0	0
85	2	0.985	0	0	0	24	15	-8	23
86	3	0.987	0	0	0	21	10	0	0
87	2	1.015	0	4	0	0	0	-100	1000
88	3	0.987	0	0	0	48	10	0	0
89	2	1.005	0	607	0	0	0	-210	300
90	2	0.985	0	0	0	163	48	-300	300
91	2	0.98	0	0	0	10	0	-100	100
92	2	0.993	0	0	0	65	10	-3	9
93	3	0.987	0	0	0	12	7	0	0
94	3	0.991	0	0	0	30	16	0	0
95	3	0.981	0	0	0	42	31	0	0
96	3	0.993	0	0	0	38	15	0	0
97	3	1.011	0	0	0	15	9	0	0
98	3	1.024	0	0	0	34	8	0	0
99	2	1.01	0	0	0	42	0	-100	100
100	2	1.017	0	252	0	37	18	-50	155
101	3	0.993	0	0	0	22	15	0	0
102	3	0.991	0	0	0	5	3	0	0
103	2	1.01	0	40	0	23	16	-15	40
104	2	0.971	0	0	0	38	25	-8	23
105	2	0.965	0	0	0	31	26	-8	23
106	3	0.962	0	0	0	43	16	0	0
107	2	0.952	0	0	0	50	12	-200	200
108	3	0.967	0	0	0	2	1	0	0
109	3	0.967	0	0	0	8	3	0	0
110	2	0.973	0	0	0	39	30	-8	23
111	2	0.98	0	36	0	0	0	-100	1000
112	2	0.975	0	0	0	68	13	-100	1000
113	2	0.993	0	0	0	6	0	-100	200
114	3	0.96	0	0	0	8	3	0	0
115	3	0.96	0	0	0	22	7	0	0
116	2	1.005	0	0	0	184	0	-1000	1000
117	3	0.974	0	0	0	20	8	0	0
118	3	0.949	0	0	0	300	528	0	0

Table A-1.2 Transmission line data for IEEE 118 bus system

Line No.	From Bus	To Bus	Circuit ID	R (p.u.)	X (p.u.)	B (p.u.)
1	1	2	1	0.0303	0.0999	0.0254
2	1	3	1	0.0129	0.0424	0.01082
3	4	5	1	0.00176	0.00798	0.0021
4	3	5	1	0.0241	0.108	0.0284
5	5	6	1	0.0119	0.054	0.01426
6	6	7	1	0.00459	0.0208	0.0055
7	8	9	1	0.00244	0.0305	1.162
8	9	10	1	0.00258	0.0322	1.23
9	4	11	1	0.0209	0.0688	0.01748
10	5	11	1	0.0203	0.0682	0.01738
11	11	12	1	0.00595	0.0196	0.00502
12	2	12	1	0.0187	0.0616	0.01572
13	3	12	1	0.0484	0.16	0.0406
14	7	12	1	0.00862	0.034	0.00874
15	11	13	1	0.02225	0.0731	0.01876
16	12	14	1	0.0215	0.0707	0.01816
17	13	15	1	0.0744	0.2444	0.06268
18	14	15	1	0.0595	0.195	0.0502
19	12	16	1	0.0212	0.0834	0.0214
20	15	17	1	0.0132	0.0437	0.0444
21	16	17	1	0.0454	0.1801	0.0466
22	17	18	1	0.0123	0.0505	0.01298
23	18	19	1	0.01119	0.0493	0.01142
24	19	20	1	0.0252	0.117	0.0298
25	15	19	1	0.012	0.0394	0.0101
26	20	21	1	0.0183	0.0849	0.0216
27	21	22	1	0.0209	0.097	0.0246
28	22	23	1	0.0342	0.159	0.0404
29	23	24	1	0.0135	0.0492	0.0498
30	23	25	1	0.0156	0.08	0.0864
31	25	27	1	0.0318	0.163	0.1764
32	27	28	1	0.01913	0.0855	0.0216
33	28	29	1	0.0237	0.0943	0.0238
34	8	30	1	0.00431	0.0504	0.514
35	26	30	1	0.00799	0.086	0.908
36	17	31	1	0.0474	0.1563	0.0399

37	29	31	1	0.0108	0.0331	0.0083
38	23	32	1	0.0317	0.1153	0.1173
39	31	32	1	0.0298	0.0985	0.0251
40	27	32	1	0.0229	0.0755	0.01926
41	15	33	1	0.038	0.1244	0.03194
42	19	34	1	0.0752	0.247	0.0632
43	35	36	1	0.00224	0.0102	0.00268
44	35	37	1	0.011	0.0497	0.01318
45	33	37	1	0.0415	0.142	0.0366
46	34	36	1	0.00871	0.0268	0.00568
47	34	37	1	0.00256	0.0094	0.00984
48	37	39	1	0.0321	0.106	0.027
49	37	40	1	0.0593	0.168	0.042
50	30	38	1	0.00464	0.054	0.422
51	39	40	1	0.0184	0.0605	0.01552
52	40	41	1	0.0145	0.0487	0.01222
53	40	42	1	0.0555	0.183	0.0466
54	41	42	1	0.041	0.135	0.0344
55	43	44	1	0.0608	0.2454	0.06068
56	34	43	1	0.0413	0.1681	0.04226
57	44	45	1	0.0224	0.0901	0.0224
58	45	46	1	0.04	0.1356	0.0332
59	46	47	1	0.038	0.127	0.0316
60	46	48	1	0.0601	0.189	0.0472
61	47	49	1	0.0191	0.0625	0.01604
62	42	49	1	0.0715	0.323	0.086
63	42	49	2	0.0715	0.323	0.086
64	45	49	1	0.0684	0.186	0.0444
65	48	49	1	0.0179	0.0505	0.01258
66	49	50	1	0.0267	0.0752	0.01874
67	49	51	1	0.0486	0.137	0.0342
68	51	52	1	0.0203	0.0588	0.01396
69	52	53	1	0.0405	0.1635	0.04058
70	53	54	1	0.0263	0.122	0.031
71	49	54	1	0.073	0.289	0.0738
72	49	54	2	0.0869	0.291	0.073
73	54	55	1	0.0169	0.0707	0.0202
74	54	56	1	0.00275	0.00955	0.00732

75	55	56	1	0.00488	0.0151	0.00374
76	56	57	1	0.0343	0.0966	0.0242
77	50	57	1	0.0474	0.134	0.0332
78	56	58	1	0.0343	0.0966	0.0242
79	51	58	1	0.0255	0.0719	0.01788
80	54	59	1	0.0503	0.2293	0.0598
81	56	59	1	0.0825	0.251	0.0569
82	56	59	2	0.0803	0.239	0.0536
83	55	59	1	0.04739	0.2158	0.05646
84	59	60	1	0.0317	0.145	0.0376
85	59	61	1	0.0328	0.15	0.0388
86	60	61	1	0.00264	0.0135	0.01456
87	60	62	1	0.0123	0.0561	0.01468
88	61	62	1	0.00824	0.0376	0.0098
89	63	64	1	0.00172	0.02	0.216
90	38	65	1	0.00901	0.0986	1.046
91	64	65	1	0.00269	0.0302	0.38
92	49	66	1	0.018	0.0919	0.0248
93	49	66	2	0.018	0.0919	0.0248
94	62	66	1	0.0482	0.218	0.0578
95	62	67	1	0.0258	0.117	0.031
96	66	67	1	0.0224	0.1015	0.02682
97	65	68	1	0.00138	0.016	0.638
98	47	69	1	0.0844	0.2778	0.07092
99	49	69	1	0.0985	0.324	0.0828
100	69	70	1	0.03	0.127	0.122
101	24	70	1	0.00221	0.4115	0.10198
102	70	71	1	0.00882	0.0355	0.00878
103	24	72	1	0.0488	0.196	0.0488
104	71	72	1	0.0446	0.18	0.04444
105	71	73	1	0.00866	0.0454	0.01178
106	70	74	1	0.0401	0.1323	0.03368
107	70	75	1	0.0428	0.141	0.036
108	69	75	1	0.0405	0.122	0.124
109	74	75	1	0.0123	0.0406	0.01034
110	76	77	1	0.0444	0.148	0.0368
111	69	77	1	0.0309	0.101	0.1038
112	75	77	1	0.0601	0.1999	0.04978

113	77	78	1	0.00376	0.0124	0.01264
114	78	79	1	0.00546	0.0244	0.00648
115	77	80	1	0.017	0.0485	0.0472
116	77	80	2	0.0294	0.105	0.0228
117	79	80	1	0.0156	0.0704	0.0187
118	68	81	1	0.00175	0.0202	0.808
119	77	82	1	0.0298	0.0853	0.08174
120	82	83	1	0.0112	0.03665	0.03796
121	83	84	1	0.0625	0.132	0.0258
122	83	85	1	0.043	0.148	0.0348
123	84	85	1	0.0302	0.0641	0.01234
124	85	86	1	0.035	0.123	0.0276
125	86	87	1	0.02828	0.2074	0.0445
126	85	88	1	0.02	0.102	0.0276
127	85	89	1	0.0239	0.173	0.047
128	88	89	1	0.0139	0.0712	0.01934
129	89	90	1	0.0518	0.188	0.0528
130	89	90	2	0.0238	0.0997	0.106
131	90	91	1	0.0254	0.0836	0.0214
132	89	92	1	0.0099	0.0505	0.0548
133	89	92	2	0.0393	0.1581	0.0414
134	91	92	1	0.0387	0.1272	0.03268
135	92	93	1	0.0258	0.0848	0.0218
136	92	94	1	0.0481	0.158	0.0406
137	93	94	1	0.0223	0.0732	0.01876
138	94	95	1	0.0132	0.0434	0.0111
139	80	96	1	0.0356	0.182	0.0494
140	82	96	1	0.0162	0.053	0.0544
141	94	96	1	0.0269	0.0869	0.023
142	80	97	1	0.0183	0.0934	0.0254
143	80	98	1	0.0238	0.108	0.0286
144	80	99	1	0.0454	0.206	0.0546
145	92	100	1	0.0648	0.295	0.0472
146	94	100	1	0.0178	0.058	0.0604
147	95	96	1	0.0171	0.0547	0.01474
148	96	97	1	0.0173	0.0885	0.024
149	98	100	1	0.0397	0.179	0.0476
150	99	100	1	0.018	0.0813	0.0216

151	100	101	1	0.0277	0.1262	0.0328
152	92	102	1	0.0123	0.0559	0.01464
153	101	102	1	0.0246	0.112	0.0294
154	100	103	1	0.016	0.0525	0.0536
155	100	104	1	0.0451	0.204	0.0541
156	103	104	1	0.0466	0.1584	0.0407
157	103	105	1	0.0535	0.1625	0.0408
158	100	106	1	0.0605	0.229	0.062
159	104	105	1	0.00994	0.0378	0.00986
160	105	106	1	0.014	0.0547	0.01434
161	105	107	1	0.053	0.183	0.0472
162	105	108	1	0.0261	0.0703	0.01844
163	106	107	1	0.053	0.183	0.0472
164	108	109	1	0.0105	0.0288	0.0076
165	103	110	1	0.03906	0.1813	0.0461
166	109	110	1	0.0278	0.0762	0.0202
167	110	111	1	0.022	0.0755	0.02
168	110	112	1	0.0247	0.064	0.062
169	17	113	1	0.00913	0.0301	0.00768
170	32	113	1	0.0615	0.203	0.0518
171	32	114	1	0.0135	0.0612	0.01628
172	27	115	1	0.0164	0.0741	0.01972
173	114	115	1	0.0023	0.0104	0.00276
174	68	116	1	0.00034	0.00405	0.164
175	12	117	1	0.0329	0.14	0.0358
176	75	118	1	0.0145	0.0481	0.01198
177	76	118	1	0.0164	0.0544	0.01356

Table A-1.3 Transformer tap changing data

Transformer No.	From Bus	To Bus	Circuit ID	Tap setting
1	8	5	1	0.985
2	26	25	1	0.96
3	30	17	1	0.96
4	38	37	1	0.935
5	63	59	1	0.96
6	64	61	1	0.985
7	65	66	1	0.935
8	68	69	1	0.935
9	81	80	1	0.935

Table A-1.4 Shunt data of IEEE 118 bus system

Bus No.	Shunt value in p.u.
5	-0.400
34	0.140
37	-0.250
44	0.100
45	0.100
46	0.100
48	0.150
74	0.120
79	0.200
82	0.200
83	0.100
105	0.200
107	0.060
110	0.060

The network transmission lines and transformer data for IEEE 118 bus system are presented in Table A-1.2 and Table A-1.3 respectively. The shunt parameters for IEEE 118 bus system is provided in Table A-1.4.